INFLUENZA A VIRUS:
HOST RESTRICTION OF THE VIRAL POLYMERASE AND A MECHANISM FOR vRNP NUCLEAR EXPORT

DUNCAN J. PATERSON

Sir William Dunn School of Pathology
and
Lincoln College

A thesis submitted for the degree of Doctor of Philosophy at the University of Oxford
Trinity Term 2015

Abstract

Most avian influenza viruses do not replicate efficiently in human cells. This is partly due to the low activity of the RNA polymerase of avian influenza viruses in mammalian cells. However, an E→K adaptive mutation at residue 627 of the PB2 subunit of the polymerase increases the activity of avian-derived virus polymerases in mammalian cells. In contrast, purified viral polymerases containing either PB2 627E or PB2 627K show comparable levels of activity in transcription assays that do not require ribonucleoprotein (RNP) assembly. To reconcile this conflict, a nucleoprotein(NP)-independent cell based transcription/replication assay was used to assess viral polymerase activity. This indicated that PB2 627E polymerase inhibition in mammalian cells is independent of NP expression, but is dependent on the length of the viral RNA template. In addition, restriction of PB2 627E polymerase could be overcome by mutations to the viral RNA template promoter sequence. Taken together, these results suggest that PB2 627 affects interaction between the viral RNA promoter and the viral polymerase in human cells. Due to influenza viruses replicating and transcribing their genomes within the nucleus of infected cells, progeny virus production is dependent on the nuclear export of genomic RNA, in the form of viral ribonucleoprotein complexes (vRNPs). This function is carried out by the viral nuclear export protein (NEP) but the mechanism whereby this process is regulated remains unclear. Experiments measuring NEP nuclear export demonstrate that phosphorylation of a highly conserved serine-rich motif

specifically up-regulates nuclear export of NEP in a manner that is conserved across viral genera. Further biophysical investigations revealed that modification of this site alters the backbone dynamics of NEP, shifting it towards an extended state that has the potential to be preferentially recognised by the cellular nuclear export machinery.

Declaration

I declare that this thesis is my own work, and except where otherwise acknowledged, describes my own research.

Duncan Paterson

Philadelphia, October 2015

Acknowledgements

Arriving in a cold, foreign country to start a four year DPhil project under the supervision of a scientist who I had only glimpsed briefly via a flickering Skype connection was a little harrowing. Nevertheless, it has been an amazing experience. Thank you Ervin for your steadfast support and sharing your enthusiasm for basic molecular biology – the best papers don't need colour. And to George Brownlee: Thank you for your insight and rigour – your presence at lab meetings was a joy. A large part of this work emanated from a collaboration with Jason Schnell and his post-doc Jolyon Claridge: Thank you for taking on a lowly microbiologist and teaching me the wonder that is NMR. Thank you, as well, to the rest of the Fodor lab, particularly Jane Sharps for occasionally valuing our survival more than we do. I am also much obliged to Lincoln College, The Polonsky Foundation, The IJC McNally Trust, South African National Research Foundation and the Society of General Microbiology for funding throughout this study.

To my friends in Oxford: I am so grateful for the comradeship we have shared – you have made winter nights bearable and cheap wine palatable; thank you. I am also massively indebted to my family: Mom, Dad and Rob, thank you for supporting my hare-brained schemes. And finally, to Hattie: You are the true wonder of my time in Oxford, thank you for your love and your grace.

Table of contents

Abbreviations

UNITS

In addition to SI units and derived units, the following additional units are used:

bp	Base pair
Ci	Curie; 1 Ci = 3.7 ×10^{10} becquerels
Da	Dalton
g	Standard gravity: 9.80665 $m.s^{-2}$
h	Hour(s)
kb	Kilobase
kDa	Kilodalton
min	Minute(s)
MOI	Multiplicity of infection
nt	nucleotide
PFU	Plaque-forming unit
pH	$-\log_{10} c$, where c is $[H^+]$ in mol/l
rpm	Revolutions per minute
s	Second(s)
U	Enzyme unit

OTHER ABBREVIATIONS

A	Adenine / Alanine
ATP	Adenosine-5′-triphoshate
BCE	Before the common era
C	Cysteine / Cytidine
cDNA	Complementary DNA
CSP	Chemical Shift Perturbation
cRNA	Complementary RNA
cRNP	Complementary ribonucleoprotein
CD	Circular Cichroism
CTD	C-terminal domain
D	Aspartic acid
dH_2O	Distilled water
DMEM	Dulbecco's modified Eagle's medium
DNA	Deoxyribonucleic acid
dNTP	Deoxynucleotide-5′-triphosphate
DTT	Dithiothreitol
E	Glutamic acid
EDTA	Ethylenediaminetetraacetic acid
F	Phenylalanine
FCS	Foetal calf serum

G Glycine / Guanine
GTP Guanosine-5′-triphoshate
H Histidine / Hygrogen
HA Haemagglutinin
HSQC Homonuclear Single Quantum Coherence Spectroscopy
IPTG Isopropyl β-D-1-thiogalactopyranoside
K Lysine
M1 Matrix protein 1
M2 Matrix protein 2
MEM Minimal Essential Medium
mRNA Messenger ribonucleic acid
MWCO Molecular weight cut-off
N Asparagine / Any nucleic acid base
NA Neuraminidase
NEP Nuclear export protein
NES Nuclear export signal
Ni Nickel
NLS Nuclear localisation signal
NMR Nuclear Magnetic Resonance
NOESY Nuclear Overhauser Effect Spectroscopy
NP Nucleoprotein
NS Non-structural
NS1 Non-structural protein 1
ORF Open reading frame
PA Polymerase acidic protein
PAGE Polyacrylamide gel electrophoresis
PB1 Polymerase basic protein 1
PB1-F2 PB1 reading frame 2
PB2 Polymerase basic protein 2
PBS Phosphate buffered saline
PCR Polymerase chain reaction
PDB Protein data bank
PMSF Phenylmethylsulfonyl fluoride
PNK T4 polynucleotide kinase
poly(A) Polyadenylic acid
poly(U) Polyuridylic acid
RMSD Root Mean Square Density
RNA Ribonucleic acid
RNP Ribonucleoprotein
S Serine
SD Standard deviation
SDS Sodium dodecyl sulfate
sem Standard error margin
ss Single-stranded
T Threonine
TAP Tandem affinity purification

TBE Tris-borate-EDTA
TEMED *N*,*N*,*N*',*N*'-Tetramethylethylenediamine
TEV Tobacco etch virus protease
TOCSY Total Correlation Spectroscopy
Tris Tris (hydroxymethyl) aminomethane
U Uracil
UTP Uridine-5'-triphosphate
UTR Untranslated region
vRNA Viral ribonucleic acid
vRNP Viral ribonucleoprotein
WHO World Health Organisation
WSN Influenza A/WSN/33 (Wilson-Smith Neurotropic)
WT Wild type
Y Tyrosine

1. Introduction

1.1 General introduction

Influenza viruses cause a highly contagious disease of the respiratory tract that is characterised by a range of common respiratory symptoms, as well as severe muscle ache and malaise. Although symptoms consistent with influenza infection were described in ancient Greece, influenza gained its current name in the 15th century from the Italian word for “influence”, which reflected a belief that these symptoms were influenced by the stars. Influenza viruses have probably existed in mammals and birds for millennia, however as human populations began to concentrate in urbanised settings the transfer of influenza viruses from animals to humans is likely to have followed. Throughout the ages influenza viruses have been responsible for a remarkable amount of illness and death caused by seasonal epidemics and occasional worldwide pandemics. Influenza epidemics generally occur in the winter months and are responsible for significant amounts of hospitalisation and death during this period. Indeed, the World Health Organisation (WHO) estimates that

annual influenza epidemics result in up to five million cases of severe illness and between 250 000 and 500 000 deaths worldwide. Occasional worldwide pandemics are usually the result of viral strains passing to humans from other animal species and are capable of increasing the annual influenza death rate by many times. During the last hundred years the world has experienced five influenza pandemics. The most serious of these was the Spanish influenza pandemic of 1918 which is the most severe disease outbreak to have been recorded in human history (Taubenberger & Kash 2010). The 1918 pandemic was caused by an H1N1 strain of influenza A virus of zoonotic origin and was estimated to have infected 500 million people across the globe, killing an estimated 50 to 100 million people, approximately 3–5% of the world's population at that time. More recently, in April 2009 another influenza pandemic, also caused by an H1N1 virus, infected up to 40% of the total population in some regions of the world — mainly in Africa and south-east Asia. This virus was also of zoonotic origin, resulting from the triple reassortment of avian, swine and human influenza viruses — thereby gaining the colloquial name "swine flu" (Neumann et al. 2009).

1.2 Influenza virus taxonomy and nomenclature

Influenza viruses belong to the *Orthomyxoviridae* family which is composed of single stranded, negative sense RNA viruses with segmented genomes. Within the *Orthomyxoviridae* influenza viruses form three distinct genera named influenza A, B and C viruses respectively. Due to the genomes of influenza viruses being segmented in nature, genetic reassortment between influenza viruses of the same genera is a

common occurrence, leading to exchange of genetic information. Influenza B viruses infect humans, seals and ferrets whilst influenza C viruses have isolated from humans, dogs and swine. In contrast to the narrow host range displayed by influenza B and C viruses, the host range of influenza A viruses is significantly broader. In this regard, aquatic birds represent the primary reservoir of influenza A viruses, however influenza A virus infection has been detected in a wide range of hosts including swine, horses, bats, seals, whales, poultry and humans (Neumann & Kawaoka 2015). Viruses within the influenza A genus can be further classified according to their serologic subtype, which is determined by the viral haemagglutinin (HA) and neuraminidase (NA) glycoproteins. There are currently 18 HA and 11 NA subtypes, although this almost certainly under-represents the true number due to sampling bias. Influenza virus isolates are named according to their genera, host species, geographical location of isolation, strain identification number, year of isolation and the HA and NA subtypes. For example: an influenza A virus isolated in 2009 from a Parisian ferret, with a strain number FR012 and a subtype of H1N1 would be named A/ferret/Paris/FR012/2009 (H1N1). If the influenza virus was isolated from a human then the species name is omitted (Lamb & Krug 2001).

1.3 Influenza virus virion

Influenza A virus particles typically range in diameter from 80–260 nm and are pleomorphic, but can be broadly assigned to spherical, bacilliform and filamentous morphologies (Lamb & Krug 2001). The viral exterior consists of a lipid envelope that is derived from the host cell membrane, out of which protrude the surface

glycoproteins, HA and NA. The M2 protein is embedded within the lipid envelope, bridging the exterior and interior of the virion. Lying directly beneath the lipid bilayer, the viral matrix protein M1 is the major structural component of the virus particle. The segmented viral genome resides within the matrix shell where it is packaged along with the viral nucleoprotein (NP) and the tripartite viral polymerase into viral ribonucleoprotein complexes. The genome of influenza viruses is relatively small and comprises a total of approximately 13.6 kilobases (kb), with the genome segments ranging in size from 0.9 to 2.3 kb. In addition to the structural proteins, influenza viruses encode several auxiliary proteins that fulfill diverse functions during infection. Two of these auxiliary proteins, non structural protein 1 (NS1) and nuclear export protein (NEP), have been found within influenza A virions, however it is not known if their presence is required (Hutchinson et al. 2014; Richardson and Akkina 1991). The roles of all known influenza virus proteins are outlined in Table 1.1 and their functions described in Table 1.2.

1.4 Influenza virus life cycle

Influenza A viruses primarily infect the epithelial cells of the respiratory and gastrointestinal tract. However, influenza A viruses have also been shown to infect alveolar macrophages and dendritic cells although it is unclear what role this plays during normal infection (Rodgers & Mims 1982). As is consistent with

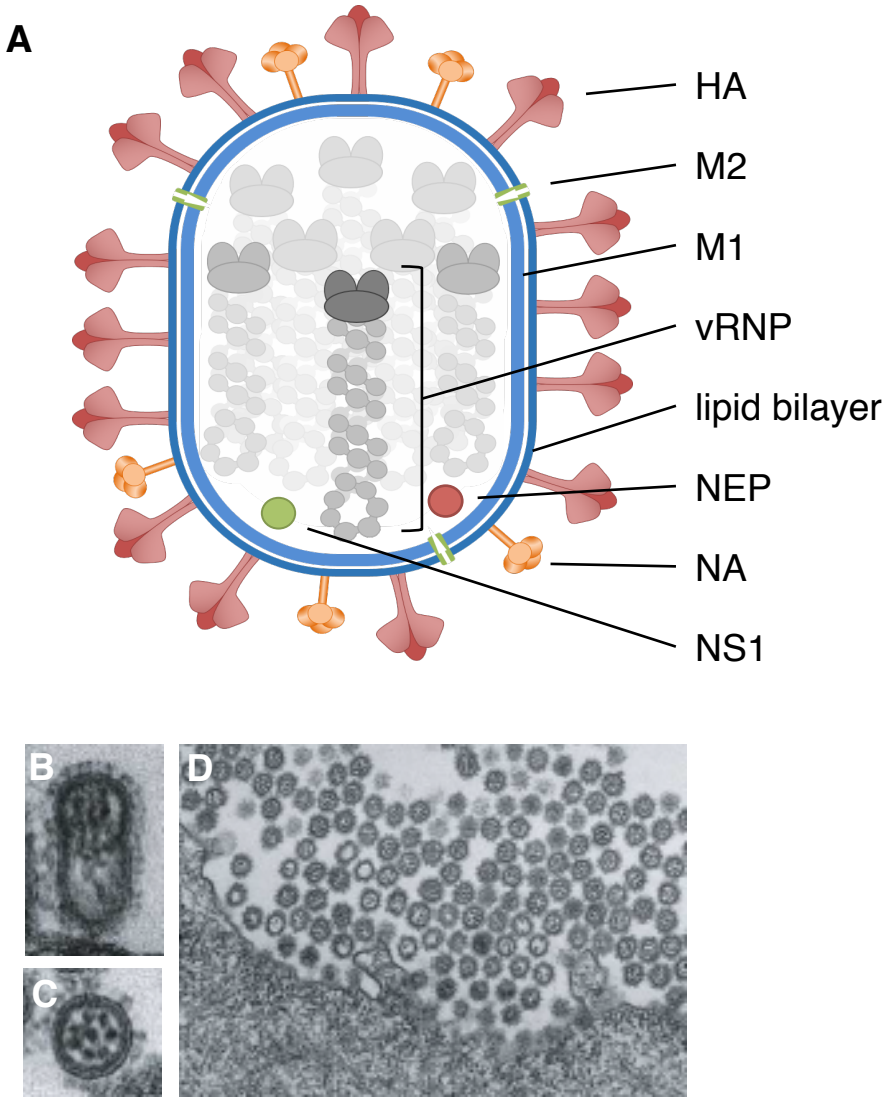

Figure 1.1 The influenza A virion. A. Schematic of the influenza A virions showing all structural proteins and vRNP complexes. B. Electron micrograph representing longitudinal section of an influenza virion. C. Electron micrograph of the transverse section of an influenza A virion. Genome segments are visible within the virion interior packaged in the 7+1 conformation. D. Virions budding from Madin-Darby Canine Kidney (MDCK) cells. Scale bars: 50 nm (B, C), 200 nm (D). Figures B, C and D were adapted from Noda et al. 2006.

Table 1.1 Summary of influenza A virus genome segments and gene products

Segment	Length (nt)	Protein product(s)	Length (amino acids)	Reference
1	2341	PB2	759	(Fields and Winter 1982)
2	2341	PB1	757	(Winter and Fields 1982)
		PB1-N40	718	(Wise et al. 2009)
		PB1-F2	87	(Chen et al. 2001)
3	2233	PA	716	(Fields and Winter 1982)
		PA-X	252	(Jagger et al. 2012)
		PA-N155	562	(Muramoto et al. 2013)
		PA-N182	535	(Muramoto et al. 2013)
4	1778	HA	566	(Winter et al. 1981)
5	1565	NP	498	(Winter and Fields 1981)
6	1413	NA	454	(Fields et al. 1981)
7	1027	M1	252	(Winter and Fields 1980)
		M2	97	(Winter and Fields 1980)
		M42	99	(Wise et al. 2012)
8	890	NS1	230	(Winter et al. 1981)
		NEP	121	(Winter et al. 1981)
		NS3	188	(Selman et al. 2012)

Table 1.2 Functions of influenza A virus gene products

Protein product	Function
PB2	Viral polymerase subunit responsible for cap-binding; innate immunity antagonist
PB1	Viral polymerase subunit harbouring the catalytic domain
PB1-N40	PB1 related protein; function unknown
PB1-F2	Apoptosis regulator and virulence factor
PA	Viral polymerase subunit responsible for endonucleolytic cap cleavage
PA-X	Modulates host response
PA-N155	PA-related; function unknown
PA-N182	PA-related; function unknown
HA	Transmembrane surface glycoprotein. Homotrimer binds sialic acid on host cell surface facilitating virus receptor binding; host range determinant; virulence factor
NP	The major constituent of RNP complexes encapsidating vRNA and cRNA; necessary for transcription and replication of viral RNA
NA	Transmembrane surface glycoprotein; homotetramer cleaves sialic acid on the cell surface facilitating viral release
M1	Major virion structural protein; involved in nuclear export of vRNPs
M2	Transmembrane protein; homotetrameric proton channel responsible for acidifying the virion and facilitating vRNP release; involved in viral budding and membrane scission
M42	M2-related protein; function unknown
NS1	Inteferon antagonist; binds dsRNA; inhibits cellular pre-mRNA polyadenylation; interacts with CPSF30 and PABP11
NEP	Mediates nuclear export of vRNPs; regulates viral RNA transcription and replication; minor virion component
NS3	NS1-related protein; potential role in host adaptation

other viruses causing acute infection, influenza A viruses have a relatively short replication cycle (8–10 hours in tissue culture).

1.4.1 Attachment and entry

In order to infect a host cell, viruses must first gain entry into the cell cytoplasm, a process that is usually initiated by attachment to a receptor on the surface of the host cell. Influenza A viruses accomplish this by way of the viral HA protein binding to sialic acid, a cellular receptor present on the surface of the cell membrane. Several types of sialic acid exist and can be identified by the sialic acid linkage to the penultimate galactose of an N-linked glycan chain on the receptor (Connor et al. 1994; Couceiro et al. 1993). Influenza A viruses have generally evolved to bind a single type of sialic acid specific to the viral host species. As such, sialic acid identity is a strong determinant of influenza virus host tropism. For example, the HA protein of avian influenza A viruses preferentially binds to sialic acid that is linked from their C2 to C3 of galactose (α–2,3-linked sialic acid) and is predominantly found in the gastrointestinal tract of birds as well as in the lower respiratory tract of mammals. In contrast, the HA protein of mammalian influenza A viruses preferentially bind to sialic acid that is linked by its C2 to the C6 of galactose (α–2,6-linked sialic acid) and is predominantly found in the upper respiratory tract of mammals. It is possible for epithelia to contain a mixed population of sialic acids, as is the case for swine. Consequently, swine have been

described as mixing vessels for the genetic re-assortment of avian and mammalian influenza viruses (Ito et al. 1998).

Upon binding by the virus to the sialic acid receptor, viruses are internalised into the host cell by receptor mediated endocytosis. Several methods of endocytosis have been proposed for influenza virus entry. The most widely accepted method uses the well-understood clathrin-mediated endocytosis pathway, however, caveolae-dependent, macropinocytosis-dependent, caveolae-independent and clathrin-independent pathways have also been described (Edinger et al. 2014; Mercer et al. 2010). Whether these differences repesent redundancy on the part of influenza A virus entry or the properties of different cell-types used to study this process remains unclear. Nevertheless, endocytosis ultimately leads to the internalisation of the virion within an early endosome, from which the virus genome and transcriptional machinery must escape to establish productive infection.

1.4.2 Fusion and nuclear import

Once within the endosome, the influenza A virion must fuse with the endosomal membranes, thereby releasing the vRNP complexes into the host cell cytoplasm. This process relies on an intriguing structural rearrangement of the viral HA protein that is triggered by decreasing pH within the maturing endosome (Hamilton et al. 2012). For fusion to occur, the HA protein must have been cleaved from the HA0 precursor into HA1 and HA2 subunits by host proteases

during the preceding round of viral replication (Boulay et al. 1987; Chen et al. 1998), or within the endosome (Zhirnov et al. 2002). The sites of proteolytic cleavage are surprisingly diverse in sequence across viral subtypes, but it is known that multi-basic cleavage sites, characteristic of highly pathogenic avian influenza viruses, can significantly enhance virulence due to a higher likelihood of cleavage site recognition in a wider variety of hosts (Taubenberger & Kash 2010). Nevertheless, the structural rearrangement of a cleaved HA protein brought about by a decrease in pH results in the exposure of a hydrophobic fusion peptide in HA2 that inserts into the endosomal membrane, causing it to fuse with the viral membrane (Bullough et al. 1994). During this process, the viral M2 ion channel pumps protons from the acidifying endosome into the virion interior (Pinto et al. 1992). This acts to disrupt the weak interactions between the viral matrix protein M1 and the vRNP, effectively freeing the vRNPs from what remains of the virion structure. Cumulatively, these processes result in the release of the vRNP complexes from the virion into the host cell cytoplasm.

The dissociation of M1 from the vRNP serves an additional purpose: to expose nuclear localisation signals (NLSs) on the vRNPs, thereby allowing the complex to be translocated across the nuclear membrane (Hutchinson & Fodor 2012). Although all protein constituents of the RNP contain at least one NLS, the nuclear import of the RNPs is dependent on the NLSs on NP, which interact with importins α–1 and α–5 to gain access to the cell nucleus. Once within the nucleus, the exact location of RNPs is not fully understood, however it is known that RNPs

show affinity for chromatin components as well as the insoluble nuclear matrix (Whittaker et al. 1996; Bui et al. 2000; Engelhardt & Fodor 2006; Chase et al. 2011).

1.4.3 Viral gene expression

Within the nucleus, the vRNPs undergo transcription to produce mRNA for the expression of viral proteins, as well as replication via a complementary RNA (cRNA) intermediate to produce more vRNPs for transcription and packaging into progeny virions (Fodor 2013). Both transcription and replication are carried out by the viral polymerase and occur within the context of a vRNP. A detailed description of these processes can be found in Section 1.5.

Viral gene expression is thought to be regulated as different proteins have been demonstrated to be expressed at differing times during infection (Enami et al. 1985; Hatada et al. 1989; Shapiro et al. 1987). Early in infection viral NS1 and NP proteins are expressed in high amounts concomitant with their roles in interferon inhibition and viral RNA synthesis (Shapiro et al. 1987; Smith & Hay 1982; Yángüez & Nieto 2011). In contrast, HA, NA and M1 which are expressed later during infection and associated with the nuclear export of genomic vRNPs and structural roles within progeny virions (Shapiro et al. 1987; Smith & Hay 1982; Yángüez & Nieto 2011). Although a global mechanism for the regulation of viral gene expression has yet to be elucidated, it has been proposed that expression of the viral polymerase genes (PA, PB1 and PB2) is regulated by a subtle difference

in the promoter sequence of the corresponding viral genomic segments (Lee & Seong 1998; Lee et al. 2003). To accomplish this, genomic segments coding for the viral polymerase subunits contain a C as the fourth residue from the 3′ end, whereas all other genomic segments generally have a U at this position. The presence of a C appears to up-regulate the replication of these segments at the expense of mRNA transcription (Lee et al. 2003). However, the assertion that the polymerase segments always contain a C at the fourth residue is often disputed due to the fact that the non-coding regions of the genomes of naturally-occurring influenza virus isolates rarely being sequenced.

1.4.4 Nuclear export of vRNP complexes

After vRNP complexes have been synthesised within the cell nucleus they must be transported through the nuclear membrane and to the periphery of the cell to be packaged into progeny virions. Two viral proteins are essential for transport through the nuclear membrane, M1 and NEP, which interact with the host cell nuclear export machinery to mediate this process. This process is described in detail in sections 1.5.2 and 1.5.3.

Subsequent to nuclear export, vRNPs accumulate at the perinuclear microtubule organising centre (MTOC), where they are proposed to interact with Rab11 via PB2. Rab11 then mediates transport of the vRNPs to the cell membrane by vesicular anterograde microtubule transport (Amorim et al. 2011; Bruce et al. 2010; Momose et al. 2011). Recent experiments relying on super resolution

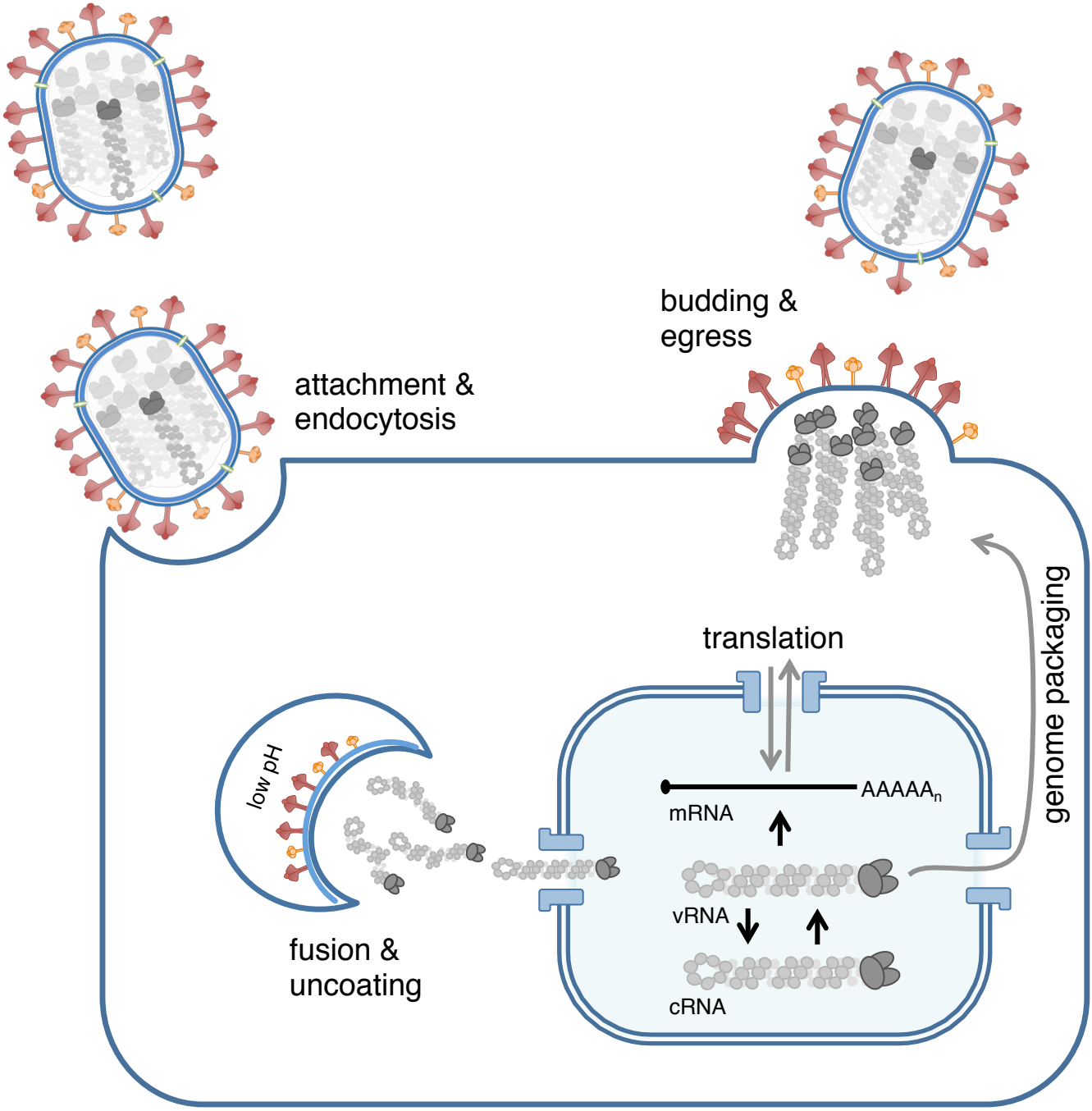

Figure 1.2 The influenza A virus replication cycle. Influenza A virus infection is initiated by the HA glycoprotein binding to sialic acid on the cell surface. Virions enter the cell by receptor-mediated endocytosis. Upon acidification of the maturing endosome, a conformational change in HA exposes a fusion peptide that facilitates fusion between the viral and endosomal membranes and releases the vRNP complexes into the cytoplasm. vRNP complexes are actively transported into the nucleus where the negative-sense RNA genome is transcribed and replicated by the viral polymerase. Viral transcription products are translated in the cytoplasm, yielding viral proteins. Replication of the vRNP takes place through a positive sense cRNA intermediate. The progeny vRNA complexes are exported form the nucleus to the periphery of the cell and packaged into nascent virions along with M1, M2, NS1, and NEP. Virions are released from the cell through budding.

.

microscopy techniques have suggested that vRNPs form subcomplexes within the cytoplasm, which further coalesce to form full viral genomic complements suitable for virion packaging (Lakdawala et al. 2014).

1.4.5 Genome packaging

Productive influenza virus infection relies on each virion receiving a full complement of viral genomic segments upon egress from the host cell. Accordingly, it is likely that the only way to achieve this is through selective packaging of the eight genomic segments, as opposed to a random packaging strategy. A selective packaging strategy is supported by microscopic and biochemical observations that the majority of influenza virions contain a single copy of each genomic segment (Gao et al. 2012; Smith & Hay 1982; Bergmann & Muster 1995). In order to accomplish this, full complements of viral genomic segments are proposed to assemble by way of RNA:RNA interactions between segments (Hutchinson et al. 2010). Indeed, tomographic reconstruction of budding influenza virions demonstrated that the relative positions of the eight genomic vRNPs is conserved, revealing a central vRNP surrounded by seven additional vRNPs (Fournier, Moules, Essere, Paillart, Sirbat, Isel, et al. 2012; Noda et al. 2012). In addition to the conserved positions, electron density proposed to correspond to RNA:RNA interactions was also observed. RNA:RNA interactions between viral genomic segments, otherwise known as packaging signals, have been narrowed down to locations predominantly corresponding to the 5′ and 3′ untranslated regions (UTRs) of each segment (Hutchinson et al. 2010).

Furthermore, interacting RNA sequences on separate genomic segments have been mapped using an *in vitro* RNA-binding assay (Fournier, Moules, Essere, Paillart, Sirbat, Cavalier, et al. 2012; Fournier, Moules, Essere, Paillart, Sirbat, Isel, et al. 2012), revealing interactions that, when disrupted, are incompatible with viral replication (Gavazzi et al. 2013).

1.4.6 Virion assembly and egress

To complete the cycle of viral replication, virions must ultimately leave the host cell. Influenza A virions accomplish this by budding from lipid raft domains on the apical surface of the cell membrane of polarised cells (Rodriguez Boulan & Sabatini 1978; Brown & Rose 1992; Scheiffele et al. 1999; Simons & Ikonen 1997). Prior to budding, the viral transmembrane proteins HA, NA and M2 are transported from their sites of synthesis at the endoplasmic reticulum via the Golgi apparatus to the apical membrane. The HA and NA glycoproteins are actively targeted to the lipid raft domains, resulting in broadening and coalescence of these domains (Chen et al. 2007; Leser & Lamb 2005; Takeda et al. 2003). This accumulation of HA and NA in lipid raft domains is proposed to result in membrane deformation and initiate budding (Chen et al. 2007). Once HA and NA are present at the cell membrane, M1 binds to their cytoplasmic tails and polymerises to form the interior matrix of the budding virion (Ali et al. 2000; Noton et al. 2007; Zhang et al. 2000). The M1 matrix acts as a platform for the incorporation of the viral genomic complexes, which are presumably packaged as a full complement of eight segments (Noda et al. 2006). In addition, M1 is thought

to recruit M2 (Chen et al. 2008; McCown & Pekosz 2006), which subsequently causes membrane curvature at the neck of the budding virion, resulting in membrane scission and release of the progeny virion into the extracellular environment (Rossman et al. 2010; Rossman & Lamb 2011). Once membrane scission has occurred, sialidase activity of the viral NA glycoprotein is required to hydrolyse sialic acid from the cell surface, thereby preventing re-attachment of the progeny virion and re-infection (Air & Laver 1989; Huang et al. 2008).

1.5 The viral ribonucleoprotein complex and its role in gene expression and replication

The early stages of influenza virus infection (fusion, uncoating and nuclear import) serve merely as a method for the delivery of the minimal functional unit of influenza virus infection — the viral ribonucleoprotein (vRNP). Each vRNP is composed of the tripartite viral polymerase, a single viral RNA genome segment and a nucleoprotein (NP) scaffold. The viral polymerase – composed of PA, PB1 and PB2 subunits – catalyses the replication and transcription of the viral genome and is bound to the conserved 5′ and 3′ ends of the viral RNA segments that form the vRNA promoter (Flick et al. 1996; Fodor et al. 1994). The rest of the vRNA is bound by multiple copies of the viral nucleoprotein (NP). vRNP complexes are the templates for transcription of mRNA for viral protein synthesis and replication of viral genomic segment for packaging into progeny virions, disparate processes that show distinct regulation. Viral transcription is dependent on a capped 10–15 nt long oligonucleotide that is cleaved from cellular pre-mRNA by the viral

polymerase and is used as a primer to transcribe each genome segment, producing an mRNA that contains a 5′ cap as well as a polyadenylated 3′ tail that results from stuttering of the viral polymerase. Replication of the vRNA genome does not require a primer and proceeds by first making a full-length positive sense copy of the vRNA genome segment known as complementary RNA (cRNA). The cRNA is subsequently used as a template to produce multiple copies of vRNA, thereby perpetuating multiple cycles of genomic amplification.

1.5.1 The vRNP

Each segment of the influenza virus genome exists as a single RNP complex that is composed of the genomic segments wound around multiple copies of the viral nucleoprotein which forms a double helical scaffold with a loop at one end and the viral RNA polymerase bound to the vRNA promoter at the other. The vRNP structure forms as a function of the polymerisation properties of NP, appearing as superhelical filaments on negative stain electron micrographs (Compans et al. 1972; Heggeness et al. 1982; Pons & Hirst 1969). Indeed, structures resembling RNPs can be reconstituted solely from NP *in vitro* (Ruigrok & Baudin 1995; Yamanaka et al. 1990). Within the vRNP, each NP monomer binds approximately 24 RNA nucleotides in a sequence-independent interaction between the RNA backbone and highly conserved basic patches on NP residues (Ortega et al. 2000).

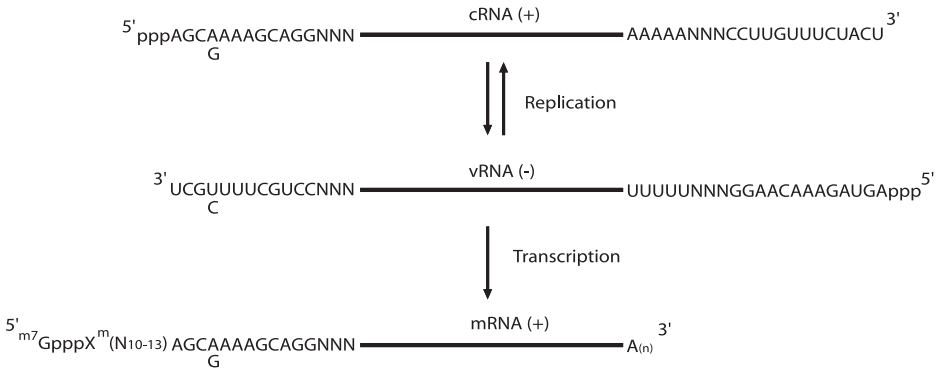

Figure 1.3 Influenza A viral RNA species synthesised during transcription and replication by the viral polymerase. The genomic negative sense vRNA is shown in the centre with conserved non-coding sequences at each terminus, which lie adjacent to segment-specific sequences (NNN). Polyadenylation of transcription products occurs by polymerase stuttering on the U stretch on the 5' end of the vRNA. Viral mRNA receives its cap along with 10-15 nucleotides from cellular pre-mRNAs. The vRNA genome is replicated via a cRNA intermediate which is the exact reverse complement of the genomic vRNA molecule. Nucleotide variation of the fourth nucleotide on the vRNA 3' end is illustrated.

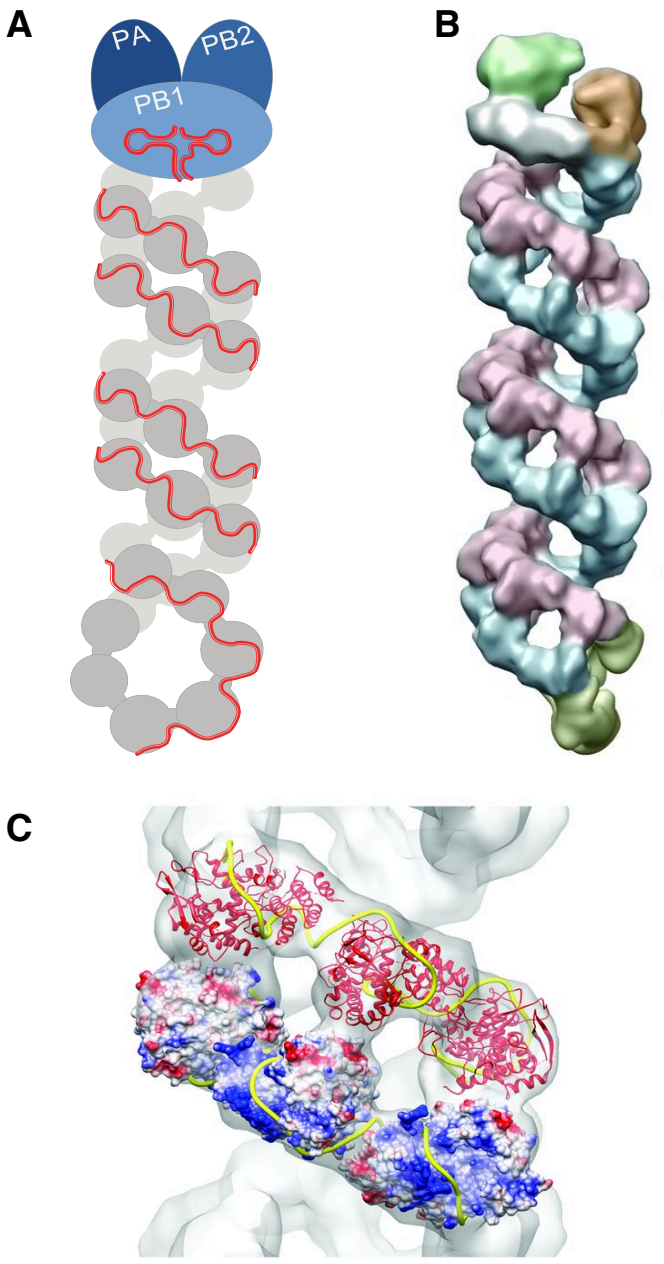

Figure 1.4 Structure of the influenza A virus vRNP complex. (A) Simplified diagram of a vRNP complex illustrating the trimeric polymerase complex bound to the viral RNA promoter shown here in the corkscrew conformation. The vRNA segment is wound around the helical NP scaffold. (B) Structural model of a vRNP derived from cryo-electron microscopic data (Arranz et al. 2012). (C) Model of vRNA wound around the NP scaffold (Arranz et al. 2012). The vRNA is proposed to follow a path around the continuous area of basic charge on the outside of the NP filament.

High resolution cryogenic electron microscopy (cryo-EM) of vRNPs has further elucidated the elegant structure of vRNP (Arranz et al. 2012; Moeller et al. 2012). These studies reveal that the central double-helical NP filament is formed by NP strands of opposite polarity and contains both a major and minor groove. To form the double helix, NP monomers interact with neighbouring monomers on the same strand (intra-strand interactions), as well as with NP monomers on the opposing strand (inter-strand interactions). The helical parameters of this arrangement show a rise of approximately 30Å per NP monomer and five to six NP monomers per helical turn. Electrostatic modelling of the NP double helix has revealed continuous positively charged pathway on the outer surface of the NP filament that is highly likely to bind the vRNA template. This RNA-binding arrangement would leave the RNA susceptible to digestion by ribonucleases, an observation that is consistent with early studies of ribonuclease susceptibility among segmented negative sense RNA viruses (Yamanaka et al. 1990; Pons et al. 1969). To form the antiparallel double-helix, the opposing NP strands form a loop at one end of the central filament that is composed of differing numbers of NP monomers, ranging from three to seven depending on the study. The opposite end of the filament contains the viral polymerase which is shown in one study to adopt two different conformations within the vRNP (Arranz et al. 2012). Specifically, a large domain within the polymerase was observed to move independently of the rest of the vRNP. Another study divided the polymerase into two separate domains: a small domain and a large flexible arm domain (Moeller et al. 2012). The flexible arm domain was proposed to correspond to the C-

terminal domain of the PA protein, with the authors speculating that this domain is responsible for feeding the RNA template into the polymerase active site. This observation is at odds with published structural data on the influenza virus polymerase, which has been described to form a more compact structure (Coloma et al. 2009; Area et al. 2004). The cRNP also contains NP and the viral polymerase forming a structure analogous to that of the vRNP (York et al. 2013).

1.5.1.1 The viral polymerase

The influenza virus polymerase is composed of three separate subunits — PB1, PB2 and PA — forming a stable complex with a molecular mass of 256 kDa. Biochemical studies have demonstrated that the C terminus of PA interacts with the N terminus of PB1, which in turn interacts with the N terminus of PB2 via its own C terminus, thereby forming a PA–PB1–PB2 linear arrangement of subunits (Ishihama, 1996). Cryo-electron microscopy has been used to demonstrate that the influenza RNA polymerase forms a compact globular structure, presumably with multiple contacts between subunits (Arranz et al. 2012; Coloma et al. 2009; Moeller et al. 2012). The PB1 subunit is the catalytic core of the RNA polymerase and contains and S–D–D motif within its central region that is likely to form the active site (Biswas & Nayak 1994). The PA subunit contains an endonuclease domain at its N-terminus which is responsible for cleaving cellular pre-mRNAs (Dias et al. 2009) which are immobilised by the mRNA cap-binding domain on the central region of PB2 (Guilligay et al. 2008).

1.5.1.1.1 Polymerase acid protein subunit (PA)

The PA subunit of the influenza virus polymerase mediates the cleavage of cellular pre-mRNAs, 10–15 nt downstream of the 7-methylguanosine cap structure, to produce 5′ capped RNA primers for viral transcription. The mechanism of this reaction was elucidated by crystallisation of an N-terminal fragment, revealing a domain with a fold similar to that of type II restriction endonucleases (Yuan et al. 2009; Dias et al. 2009). Endonucleolytic activity was determined to be dependent on bivalent cations, with RNA and DNA both able to act as substrates. The C-terminal domain of PA interacts with the N-terminal domain of PB1 and the structure of this interface has been resolved by crystallography (He et al. 2008; Obayashi et al. 2008), revealing the PA-CTD interacting with the first 15 residues of PB1.

1.5.1.1.2 Polymerase basic protein 1 subunit (PB1)

The PB1 protein represents the catalytic centre of the influenza RNA polymerase (Braam et al. 1983). The central region of PB1 contains the consensus S-D-D motif that is conserved in all nucleic acid polymerases and the mutation of which abolishes all polymerase activity (Biswas & Nayak 1994). Unsurprisingly, in addition to its role in RNA polymerisation, PB1 binds to both the vRNA and cRNA promoters, consisten with its role in catalysing both transcription and replication (González & Ortín 1999a; Li et al. 1998). In addition to the PA:PB1 interface, the PB1 C-terminus has been co-crystallised with the first 37 residues of PB2 which form three helices (Sugiyama et al. 2009).

1.5.1.1.3 Polymerase basic 2 subunit (PB2)

During transcription of the influenza virus genome PB2 is responsible for immobilising the 5′ 7-methyguanosine cap of cellular pre-mRNAs prior to cleavage by the PA endonuclease (Blaas et al. 1982; Guilligay et al. 2008). In addition to its role in transcription, the N-terminus of PB2 contains residues critical for viral RNA replication (Gastaminza et al. 2003).

PB2 interacts with PB1 through three N-terminal α-helices (Sugiyama et al. 2009). The central region of PB2 is responsible for cap-binding which occurs through an aromatic sandwich mechanism, mediated by H357 and F404, similar to that observed for cellular cap-binding proteins (Guilligay et al. 2008). The C-terminal portion of PB2 is composed of the 627 domain which is important for host adaptation, as well as a nuclear localisation domain. The 627 domain is named for amino acid 627 which is predominantly lysine in mammalian influenza viruses but glutamic acid in avian viruses and is the canonical host-range determinant for the influenza virus polymerase (Subbarao et al. 1993). The structure of this domain has been determined, revealing a basic patch with residue 627 at the centre (Tarendeau et al. 2008). The nuclear localistion domain of PB2 contains a classical bipartite NLS, the structure of which has been solved in complex with importin α–5 (Tarendeau et al. 2007).

1.5.1.1.4 Structure of the polymerase trimer

Recently the structures of influenza A and B virus polymerases were solved at atomic resolution (Reich et al. 2014; Pflug et al. 2014). The structures reveal a U-

like structure with the cap-binding (PB2) and endonuclease (PA) domains projecting out from the large polymerase core that is formed by a range of complex interactions involving all three subunits. In this respect, the cap-binding and endonuclease domains face each other, allowing *in situ* cleavage of bound pre-mRNAs to a length that appears to be defined by the distance between the two domains. The viral RNA promoter binding site is distal to the cap-snatching apparatus, positioning the 3′ promoter strand in close proximity to the polymerase active site. The structure of the viral polymerase core is largely analogous to other viral polymerases, with channels for template entry and exit, product exit and nucleotide entry.

1.5.1.2 The viral promoter

Each influenza virus vRNA segment is composed of at least one open reading frame that is flanked by non-coding regions (NCRs) at the 5′ and 3′ termini (Robertson 1979; Skehel & Hay 1978). A portion of each NCR sequence is segment specific, however the terminal sequences are conserved for all the viral vRNA segments — comprising 13 nt at the 5′ end and 12 nt at the 3′ end. Both the 5′ and 3′ terminal sequences are necessary for viral polymerase activity (Fodor et al. 1994; Tiley et al. 1994), forming a promoter structure for recognition by the viral polymerase. Several models have been proposed for the structure of the vRNA promoter, all of which seek to explain the partial inverted complementarity of the 5′ and 3′ terminal sequences (Desselberger et al. 1980). Initially it was thought that this partial complementarity led to the formation of a panhandle

structure due to Watson-Crick basepairing between the termini (Hsu et al. 1987) . This model is supported by data from cross-linking experiments demonstrating that vRNA segments adopt a circular configuration, as well as structural studies of the unbound promoter using nuclear magnetic resonance (NMR) spectroscopy (Bae et al. 2001; Hsu et al. 1987). In addition to the panhandle promoter structure, an RNA fork model has been proposed where the extreme termini of the viral promoter remain single-stranded (Fodor et al. 1994; Kim et al. 1997). However, the currently favoured model predicts that the vRNA promoter forms a corkscrew-like structure where the extreme 5′ and 3′ termini form secondary structures (Flick et al. 1996; Flick & Hobom 1999). The predominant features of this corkscrew secondary structure are two short stem loop structures, each containing a stem of two basepairs and a four nucleotide loop. Formation of the corkscrew structure appears to be important for endonuclease activity (M. B. Leahy et al. 2001; Michael B. Leahy et al. 2001) and polyadenylation of viral mRNA (Pritlove et al. 1998). It is possible that the vRNA promoter exists as a panhandle in its unbound state and upon binding to the viral polymerase adopts a corkscrew conformation, as observed in single molecule FRET experiments (Tomescu et al. 2014). Indeed, binding of the vRNA promoter has been demonstrated to stabilise the viral polymerase (Brownlee & Sharps 2002), suggesting that the promoter may function in a structural capacity, as well as a sequence for molecular recognition of viral vRNA. The recent publication of the viral polymerase structure containing bound promoter RNA (Reich et al. 2014; Pflug et al. 2014) has validated the existence of a 5′ stem loop that is tightly

bound to a distinct site near the template entry channel. The 3′ promoter strand, however, does not appear as a stem loop in published structures, but rather as a dynamic single-stranded element forming a number of different conformations in or near the template entry channel (Reich et al. 2014; Pflug et al. 2014) .

The cRNA promoter is complementary to the vRNA promoter and is generally thought to adopt a structure analogous to that of the vRNA promoter. Accordingly, basepairing within both the 5′ and 3′ stemloops is required for vRNA synthesis in cell culture (Azzeh et al. 2001; Crow et al. 2004).

1.5.1.3 The viral nucleoprotein

NP molecules compose most of the mass of the vRNP complex, forming a structural scaffold around which the vRNA template is wound. This structural role is proposed to make NP essential for replication and transcription of full-length vRNA templates (Huang et al. 1990), but is entirely dispensable for replication and transcription of short vRNA-like templates in vitro and in cell culture (Resa-Infante et al. 2010; Turrell et al. 2013; Lee et al. 2002). Although, NP has previously been proposed to play a role in the regulation of transcription and replication of vRNA templates, the ability of the viral polymerase to both transcribe and replicate in the absence of NP suggests that its role, if any, in this regard is more subtle.

Crystallographic analysis of NP identified three major structural domains: a head, body and tail-loop (Ye et al. 2006; Ng et al. 2008). The positively charged area

between the head and body domains is proposed to bind the viral template, the binding of which can be abolished by the introduction of negatively charged residues to this area (Ng et al. 2008; Turrell et al. 2013). Oligomerisation of NP relies on the tail-loop domain of one NP molecule docking into a basic groove proximal to the RNA binding residues of another NP molecule. Within a vRNP, NP must also bind to the promoter-bound polymerase. This is accomplished through interactions with the PB1 and PB2 polymerase subunits (Poole et al. 2004; Biswas et al. 1998). In addition to interactions with other vRNP components, NP also interacts with numerous host-factors including UAP56 and TatSF1 which have been proposed to act as chaperones during vRNP formation (Momose et al. 2001; Naito et al. 2007).

1.5.2 Viral RNA transcription, processing and transport

1.5.2.1 Transcription

Influenza viruses do not encode an mRNA capping enzyme and as such viral mRNA synthesis relies on a 5′ prime capped primer that is snatched from cellular pre-mRNA produced by the cellular RNA polymerase II complex (Engelhardt & Fodor 2006). Viral transcription requires that all three subunits of the viral polymerase work in concert, beginning with the PB2 subunit which is responsible for binding the 5′ cap of a pre-mRNA (Cianci et al. 1995; Li et al. 1998). Once immobilised by PB2, the pre-mRNA is endonucleolytically cleaved by the PA subunit, creating a 10–15 nt 5′ capped primer (Beaton & Krug 1981; Dias et al. 2009; Plotch et al. 1981; Yuan et al. 2009). This primer is then fed into the active

site of the viral polymerase located on the PB1 subunit, where it presumably aligns with the 3′ end of the viral promoter. Transcription is initiated by the addition of a G residue, which is templated by the penultimate C residue on the 3′ vRNA promoter (Beaton & Krug 1981). It has also been demonstrated that the first nucleotide to be incorporated can be templated by the G residue third from the vRNA 3′ end, resulting in the addition of a C residue to the 5′ capped primer (Fodor et al. 1995). mRNA synthesis proceeds along the vRNA template until the viral polymerase encounters a stretch of U residues approximately 16nt from the 5′ end of the vRNA template that result in the synthesis of a poly(A) tail.

1.5.2.2 Polyadenylation

Cellular mRNA transcripts are polyadenylated through a complex set of interactions between RNA polymerase II, template and a range of auxilliary proteins (Papantonis & Cook 2013). In contrast, the influenza virus polymerase gets round these requirements by using an elegant stuttering mechanism. All vRNA templates contain a stretch of 5–7 U residues approximately 16nt from the vRNA 5′ terminus that are used as a template for polyadenylation (Robertson et al. 1981). It is proposed that polyadenylation occurs while the vRNA 5′ promoter is still bound to the viral polymerase, resulting in steric hinderance of the vRNA template and thereby causing the viral polymerase to stutter on the poly-U stretch, which then generates a poly(A) tail (Fodor et al. 1994). Indeed, replacement of the 5–7 U residues with A residues results in the polyuridylation of viral transcripts (Poon et al. 2000; Poon et al. 1999).

1.5.2.3 Splicing

The two shortest segments of the influenza A virus genome can produce both spliced and unspliced transcripts. In this regard, transcription of segment 7 produces an unspliced transcript encoding the M1 protein. However, alternate splicing of this transcript can give rise to multiple species of transcripts, the most important of which encodes the M2 protein (Lamb & Choppin 1981; Lamb et al. 1981). Likewise, segment 8 expresses the NS1 protein from an unspliced transcript and NEP from a spliced variant (Lamb & Lai 1980). Splicing of viral transcripts is performed by the cellular spliceosome, using the canonical donor and acceptor sequences (Lamb & Horvath 1991). Nevertheless, the exact mechanism used by the spliceosome to splice viral transcripts has yet to be elucidated. Splicing of viral transcripts appears to be tightly controlled by several cellular and viral factors, resulting in ~10% of viral transcripts being spliced (Lamb & Lai 1980; Lamb et al. 1981). To this end, the NS1 protein has been proposed to regulate the splicing of NS1 transcripts by an interesting feedback loop (Garaigorta & Ortín 2007). However, this finding has been challenged by conflicting data suggesting that NS1 expression does not affect NS1 transcript splicing (Robb et al. 2010). Interestingly, regulation of NS1 transcript splicing by way of a sub-optimal splice site has been proposed to coordinate the timing of infection by controlling the gradual accumulation of NEP during viral infection, in effect working as a molecular clock (Chua et al. 2013).

1.5.2.4 Nuclear export

Delivery of a translatable message to ribosomes in the cytoplasm for viral protein synthesis is the end goal of viral transcription. To accomplish this, viral transcripts must be exported from the nucleus which requires that they bind to a variety of host mRNA binding proteins. Indeed, there is strong evidence that influenza viruses commandeer cellular mRNA-binding proteins and export pathways for this purpose (Bier et al. 2011). The result of several biochemical studies have demonstrated that viral mRNPs are exported from the nucleus using the NXF1-p15 pathway (Read & Digard 2010; Hao et al. 2008) through direct interaction with viral transcripts (Wang et al. 2008) .

1.5.3 Viral RNA replication

Replication of the influenza virus genome is necessary in order to produce templates for transcription, as well as the production of genomic vRNA for incorporation into progeny virions. This process proceeds in two distinct stages. During the first stage, negative-sense vRNA is used as a template to synthesise a full-length positive-sense cRNA. During the second stage the cRNA is used as a template to synthesise vRNA. Neither vRNA or cRNA possess a 5′ cap or 3′ poly(A) tail and as such initiation and termination of replication is distinct from transcription. Initiation of replication is proposed to occur in a de novo primer-independent mechanism due to the fact that the 5′ terminus of both vRNA and cRNA contain a triphosphate moiety (Smith & Hay 1982; Honda et al. 1998; Lee et al. 2002). For the synthesis of cRNA from a vRNA template, initiation occurs by

incorporation of the GTP through base-pairing to the penultimate C residue on the 3′ terminus of the vRNA. This GTP residue is then used as the substrate for the formation of a 5′ phosphodiester bond with ATP, which in turn basepairs with the terminal U residue, resulting in a pppApG dinucleotide (Vreede et al. 2008). The pppApG dinucleotide is subsequently extended by the viral polymerase. In an alternative model cRNA synthesis starts with the addition of a non-templated residue to the 3′ end of the vRNA template by a cellular ribonucleotidyltransferase, followed by initiation on what is now the penultimate nucleotide of the vRNA 3′ end (Zhang et al. 2010). The nascent cRNA strand is hypothesised to be bound by a free viral polymerase via its 5′ promoter sequence and to associate with NP (Jorba et al. 2009), ultimately forming a cRNP capable of synthesising multiple copies of vRNA.

Initiation of vRNA synthesis from a cRNA template is proposed to occur by a mechanism distinct from cRNA synthesis. In this regard, vRNA synthesis is proposed to initiate via synthesis of a pppApG dinucleotide that is templated by the fourth and fifth nucleotides on the 3′ end of the cRNA molecule (Deng et al. 2006). This dinucleotide then realigns with the terminal two nucleotides on the cRNA template, followed by elongation by the viral polymerase (Deng et al. 2006). The reasons for the differences in initiation of vRNA and cRNA synthesis remain unresolved, however it has been proposed that the observed differences stem from the promoter structures and their affinity for the viral polymerase (Azzeh et al. 2001; González & Ortín 1999b). In addition to differences during the initiation

of RNA replication, vRNA and cRNA synthesis appear to employ different strategies. Synthesis of cRNA from a vRNA template has been demonstrated to be catalysed by the viral polymerase that is resident on the vRNP, i.e. in *cis* (Jorba et al. 2009; Vreede & Brownlee 2007). In contrast biochemical analyses have shown that vRNA synthesis from a cRNA template requires a second viral polymerase, i.e. in *trans* (Jorba et al. 2009). This originally led to the suggestion that the trans-acting polymerase was responsible for vRNA synthesis (Jorba et al. 2009). Intriguingly however, trans-acting polymerase does not need to be catalytically active to result in vRNA synthesis (York et al. 2013). Consequently, it is proposed that vRNA synthesis from a cRNA template requires a second polymerase to activate the polymerase resident on the cRNP which then catalyses vRNA synthesis (York et al. 2013).

1.6 Influenza A virus host adaptation and the viral polymerase

Influenza A viruses predominantly infect wild waterfowl, which act as a natural reservoir, and rarely infect mammals. While viruses from wild waterfowl can infect some mammals, including humans, this usually results in sporadic dead-end infections. However, in rare cases zoonoses can lead to sustained epidemics in the human population. For this to occur, avian viruses must adapt to interact with mammalian-specific factors and thereby replicate more efficiently in their new hosts.

The most obvious sites of adaptation are understandably the HA and NA proteins which must contend with viral entry and egress in an entirely different cell type. However, as the minimal replicative units, viral RNPs must undergo adaptation to an intracellular environment that is equally foreign. Indeed, it is well known that viral polymerases from avian influenza A viruses display restricted activity in mammalian cells. Nevertheless, this restricted activity can be overcome by adaptive mutations — the presence of which are a prerequisite for viral spread in mammalian hosts. Accordingly, host-specific genetic residues have been described for all viral polymerase subunits.

1.6.1 Host adaptation and the PB2 polymerase subunit

The PB2 polymerase subunit has long been known to be the dominant determinant of influenza A virus polymerase host range, having originally been implicated in the restriction of fowl plague virus in mammalian cells (Almond 1977). This restricted phenotype was later demonstrated to be overcome by a single mutation (Subbarao et al. 1993) — PB2 E627K — thereby identifying what is still considered the canonical viral polymerase host range determinant.

1.6.1.1 PB2 627 — the canonical polymerase host range determinant

The adaptive mutation best known for increasing avian viral polymerase activity in mammalian cells occurs at residue 627 of the PB2 polymerase subunit (Subbarao et al. 1993). Avian viral isolates predominantly encode glutamic acid at

PB2 627 (627E), whereas this residue is almost exclusively a lysine (627K) in influenza viruses isolated from mammals, with the notable exception of the 2009 pandemic H1N1 viruses (Chen et al. 2006; Mehle & Doudna 2009).

The PB2 627 E→K mutation is strongly selected for in human infections of zoonotic origin. Indeed, this mutation is proposed to have arisen early in the 1918 influenza pandemic that was caused by a virus with an avian origin PB2 segment (Taubenberger et al. 2005). Likewise, PB2 627K is present in viruses from the two subsequent influenza virus pandemics in 1957 and 1968, which retained the PB2 genome segment from the 1918 pandemic virus (Scholtissek et al. 1978). Moreover, isolated human infections from avian-borne H5N1, H7N7 and H7N9 viruses often select for the PB2 627 E→K mutation (Hatta et al. 2001; Fouchier et al. 2004; Gao et al. 1999; Kageyama et al. 2013). Furthermore, PB2 627K arises quickly upon passage of avian viruses in mammalian models, increasing viral replication and pathogenicity, as well as facilitating increased viral transmission between animals (Hatta et al. 2001; Steel et al. 2009; Herfst et al. 2012). The physical effect of substituting a negatively charged glutamic acid residue with a positively charged lysine is to form a basic patch on the 627 domain of PB2 which is otherwise disrupted by the presence of glutamic acid (Tarendeau et al. 2008).

Although selection of the PB2 627 E→K mutation is generally accepted as necessary for increasing avian viral polymerase activity in mammalian cells, the mechanism by which this increase in activity occurs remains unclear. Temperature was one of the first factors to be implicated in PB2 627K selection.

In this regard, mammalian and avian influenza viruses replicate at different temperatures due to physiological differences in the site of infection. Mammalian viruses infect the upper respiratory tract, which at 33°C is far cooler than the 41°C encountered by avian viruses in the intestines of birds. Investigations into the effect of this temperature difference have demonstrated that avian virus replication is disproportionately attenuated at 33°C in mammalian cells when compared to human virus replication (Hatta et al. 2007; Ayora-Talavera et al. 2009; Massin et al. 2001). This attenuation could be somewhat ameliorated by the PB2 627 E→K mutation. Similarly, reconstitution of viral RNPs in mammalian and avian cells confirmed that PB2 627E polymerases were comparatively cold-sensitive and that this sensitivity could be overcome by introducing PB2 627K.

The effect of temperature on viral polymerase activity was further studied on viral polymerases that had been expressed in insect cells and purified to homogeneity. In contrast to cell-based findings, purified PB2 627E polymerases did not exhibit restricted activity at lower temperatures when subjected to in *vitro* activity assays (Aggarwal et al. 2011). More intriguingly however, purified polymerases encoding either K or E at PB2 627 showed near identical activity in RNA replication and transcription assays. This finding led to the suggestion that the restricted activity displayed by PB2 627E polymerase was not due to an inherent defect in PB2 627E polymerases but could potentially be explained by failure of these polymerases to effectively form RNPs. Indeed, the interaction between PB2 and NP in the context of an RNP complex has previously been

implicated in the necessity for PB2 627K in mammalian cells. In this regard, the PB2 627 E→K mutation was shown to be required to stabilise the interaction between PB2 and NP (Labadie et al. 2007; Ng et al. 2012; Rameix-Welti et al. 2009; Mehle & Doudna 2008). Accordingly, it has been proposed that there may be a requirement for co-selection of the PB2 and NP segments during viral adaptation to mammalian hosts (Ng et al. 2012; Bogs et al. 2011). However, in more recent experiments, mammalian adaptive PB2 mutations including PB2 627 E→K have been conclusively demonstrated not to enhance the stability of PB2:NP binding (Cauldwell et al. 2012).

It is clear that there are several distinct differences between influenza virus infection in birds and mammals, not least the cell type infected. In this regard, it seems sensible to suggest that one or more host factors necessary for efficient functioning of the viral RNP would differ between host species. Host-specific protein interactions have been implicated in the restriction of PB2 627 viral polymerases in mammalian cells. The results of these studies however, are less clear. Using a polymerase activity assay in heterokaryons of human and avian cells, the restricted activity of PB2 627E viral polymerases was ascribed to an inhibitory factor within mammalian cells (Mehle & Doudna 2008). In contrast, another study using nearly identical methods ascribed the restricted PB2 627E mammalian phenotype to the lack of an activating factor present in the avian cell nucleus (Moncorgé et al. 2010). Contradictory as these results appear, it is well known that the viral polymerase interacts with myriad cellular proteins

(Watanabe et al. 2014; York et al. 2014) and it is conceivable that there may be a dynamic interplay between activating and inhibitory factors within the nucleus of an infected cell.

Although neither of the aforementioned studies suggests cellular proteins likely to function as activators or inhibitors, another study attempted to catalogue the PB2 627-dependent host protein binding profiles of influenza virus polymerases (Bortz et al. 2011). This study used a functional genomics approach to identify proteins that differentially regulate viral polymerase activity depending on the identity of the PB2 627 residue. This approach led to the identification of the DEAD box RNA helicase 17 protein (DDX17), the knockdown of which inhibited PB2 627K polymerases but increased the activity of PB2 627E polymerases in mammalian cells. DDX17 was also required for efficient avian and mammalian influenza virus infection in avian cells. Although there is clearly a role for DDX17 in influenza virus infection, the mechanism of this role is yet to be defined. In addition, it should be noted that the effect of DDX17 on viral polymerase function observed in this study appears to be relatively minor, indicating that DDX17 is unlikely to be the sole determinant for PB2 627K selection in mammalian cells.

While DDX17 would likely affect RNA replication and transcription by the viral RNA polymerase once the complex is present in the host cell nucleus, several studies have proposed that restriction of PB2 627E viral polymerases may occur prior to this during nuclear import. To this end, it has been demonstrated that avian influenza viruses undergo a switch in α-importin dependency upon

adaptation to mammalian cells. In this regard, avian viruses appear to require importin α-3 whereas mammalian adaptation requires a switch to importin α-7 (Gabriel et al. 2011; Gabriel et al. 2008; Hudjetz & Gabriel 2012). The identity of PB2 627 has been directly implicated in this change in importin preference with the finding that transient knockdown of importin α-1 and 7 reduced the activity of polymerases encoding PB2 627K but not PB2 627E (Hudjetz & Gabriel 2012). Moreover, transgenic mice lacking importin α-7 displayed reduced susceptibility to a PB2 627K virus but not a PB2 627E virus. These findings are not as surprising as they may first seem as the PB2 nuclear localisation signal (NLS) was found to pack against the 627 domain in structural studies (Tarendeau et al. 2008). Accordingly, two mechanisms have been proposed for the role of α-importin isoforms in viral polymerase host adaptations (Hudjetz & Gabriel 2012). Firstly, selection for binding of specific importins could increase nuclear import of the vRNP or newly synthesised viral polymerase. Indeed, in a single study avian viral polymerase that had been expressed from transfected plasmids was shown to diffuse more slowly within mammalian nuclei compared to a PB2 627K polymerase (Foeglein et al. 2011). However it is unclear whether the observed impairment in diffusion is dependent on PB2 nuclear import (which occurs independently of PA and PB1), polymerase assembly, or another factor. In this respect, viral polymerase assembly does not seem to be affected by the identity of PB2 627 (Mehle & Doudna 2008). Secondly, α-importin isoform dependency may indicate that α-importin serves as a cofactor to enhance vRNP activity. Intriguingly, complementation of PB2 nuclear import with an SV40 NLS does not

affect nuclear accumulation of PB2 or polymerase assembly but severely inhibits polymerase activity indicating a potential role during viral RNA replication and transcription (Resa-Infante et al. 2008).

1.6.1.2 Other PB2 mutations implicated in host adaptation

Despite PB2 627 E→K being the prototypical host adaptation mutation on the viral polymerase, mutations at several other positions in PB2 can likewise overcome the host range restriction of avian polymerases. The 2009 pH1N1 virus encodes PB2 627E in keeping with the avian lineage of its PB2 segment, however this virus replicated very efficiently in cell culture and mouse models (Herfst et al. 2010; Jagger et al. 2010; Zhu et al. 2010). Moreover, genetically engineering a lysine at PB2 627 led to attenuation of viral replication and pathogenicity (Jagger et al. 2010). In order to overcome the restricted phenotype, the pH1N1 virus contains two mutations, PB2 590 G→S and 591 Q→R, that appear adjacent to PB2 627 on crystalised 627 domains (Mehle & Doudna 2009). These mutations are proposed to mimic PB2 627K by masking the negative charge caused by the presence of PB2 627E on the protein surface (Yamada et al. 2010).

The identity of PB2 701 has also been demonstrated to affect the ability of avian viral polymerases to replicate and transcribe viral RNA in mammalian cells. In this regard, the PB2 701 D→N mutation was originally identified when an avian H7 virus was serially passaged in mice, leading to increased viral replication and pathogenicity (Gabriel et al. 2008; Gabriel et al. 2005). In addition to H7 viruses, PB2 701N has been demonstrated to cause a similar increase in H5N1 virus

replication and transmission in mammalian animal models (de Jong et al. 2006; Li et al. 2005; Zhou et al. 2013). In addition, it was found that PB2 701N can compensate for the lack of the canonical PB2 mammalian host range determinant: PB2 627K (Gao et al. 1999; Steel et al. 2009). PB2 701 resides on a domain that has been co-crystallised with importin α–7 (Tarendeau et al. 2007), potentially implicating it in PB2 nuclear localisation. However, little is known about the stimulatory mechanism of PB2 701N and it remains unclear whether host adaptive mutations at this residue are complementary or compensatory to mutations at PB2 627.

Most host adaptive mutations cluster to the C-terminus of PB2, potentially implicating a shared mechanism of action. Nevertheless two PB2 mutations to the N-terminal region of PB2 have been implicated in host adaptation. Specifically, PB2 271 T→A and 158 E→G have been demonstrated to increase avian viral polymerase activity in mammalian cells (Cauldwell et al. 2012; Bussey et al. 2011; Foeglein et al. 2011). In addition, both mutations have been demonstrated to increase morbidity and mortality in mammalian animal models (Zhang et al. 2012; Zhou et al. 2013). However, the mechanisms by which these mutations affect host adaptation are unknown.

1.6.2 Host adaptation and the PA polymerase subunit

The role of PA in host adaptation is not as well characterised as PB2, however a number of studies have implicated PA in overcoming viral host restriction.

Although these studies have generally sought to identify mutations in mammalian adapted PA proteins that confer benefits to viral polymerase activity and viral replication, only one study has investigated the effect of these mutations in avian and human cells. In this regard, mutations to a variety of residues on the C-terminus of a human-adapted PA (P400L, M423I, V476A, T552S and V630E) increased viral polymerase activity in human cells but not in avian cells, suggesting that these could represent bonafide adaptive mutations (Mehle et al. 2012). Of these mutations, 552 T→S was demonstrated to markedly increase viral polymerase activity, as well as viral replication in mammalian cells when introduced into an avian virus. In addition to biochemical data, 552 T→S has been identified in large bioinformatic analyses as a potential host range determinant (Chen et al. 2006).

The prevailing logic behind adaptive mutations to the influenza virus polymerase is that they act to increase viral polymerase activity in mammalian cells and thereby increase viral replication. However, some proposed adaptive mutations to PA seem to challenge this idea. Two independent studies have identified diverse PA mutations, that appear upon viral adaptation to mammalian hosts, which increase viral polymerase activity but do not increase viral replication or indeed virulence in mice (Bussey et al. 2011; Gabriel et al. 2005). This suggests that adaptive mutations to PA probably act in a more subtle manner than the classical PB2 adaptive mutations. Moreover, PA mutations appear along the length of the protein, indicating that several independent mechanisms for

adaptation may be selected for on PA, each of which incrementally aids in adaptation to a new host species.

1.6.3 Host adaptation and the PB1 polymerase subunit

Of all the RNP constituents, PB1 appears to harbour the least potential for host adaptive changes. Only one residue, PB1 375, has so far been demonstrated to confer an adaptive benefit to avian viruses infecting mammalian cells. In this regard, asparagine is found preferentially at PB1 375 in avian viruses whilst mammalian viruses code for a serine at this position (Taubenberger et al. 2005; Kawaoka et al. 1989). However, the effect of PB1 375 on viral polymerase activity or indeed its role during viral infection is currently unknown.

1.7 The multifunctional NEP protein

In addition to NS1, viral segment 8 encodes a 121 amino acid polypeptide from a spliced form of the segment mRNA transcript (Lamb & Lai 1980). This small protein was originally thought to have no structural function within the virion, leading to its designation as non-structural protein 2 (NS2) (Takeda et al. 2003; Inglis et al. 1979). Subsequently, it was noted that small amounts of NS2 protein were present in virions where it may interact with the viral matrix protein M1 (Richardson & Akkina 1991; Ward et al. 1995; Yasuda et al. 1993). NS2 was later implicated in mediating the export of vRNPs from the host cell nucleus, thereby ensuring that the viral genomic segments are available for packaging into

daughter virions on the cellular periphery (O'Neill et al. 1998). This led to the proposal that NS2 protein be renamed as the nuclear export protein (NEP).

Recent studies have suggested that NEP may have more than one function during the influenza virus replication cycle. In addition to nuclear export of vRNPs, it has been demonstrated that NEP contributes to the viral budding process through interaction with a cellular ATPase (Gorai et al. 2012). Furthermore, studies have demonstrated that NEP is capable of regulating the accumulation of viral RNA species, potentially leading to a switch from viral transcription during early viral replication to favour the production of genomic vRNPs (Robb et al. 2009; Mänz et al. 2012). In this regard, there is substantial evidence that mutations in NEP capable of increasing viral RNA replication are able to confer a significant replicative advantage during mammalian adaptation of a highly pathogenic avian influenza virus (Mänz et al. 2012). Consequently, NEP appears to perform several distinct, biologically important functions during influenza virus replication.

1.7.1 NEP organisation and structure

NEP can be divided into a protease-sensitive N-terminal domain (amino acids 1–53) and a protease-resistant C-terminal domain (amino acids 54–121), the crystal structure of which has been solved (Akarsu et al. 2003) (Fig. 1.5A). Although there is as yet no structural information available for the N-terminal domain, there is considerable evidence for two nuclear export sequences (NESs) located between residues 12–21 (O'Neill et al. 1998; Iwatsuki-Horimoto et al. 2004) and

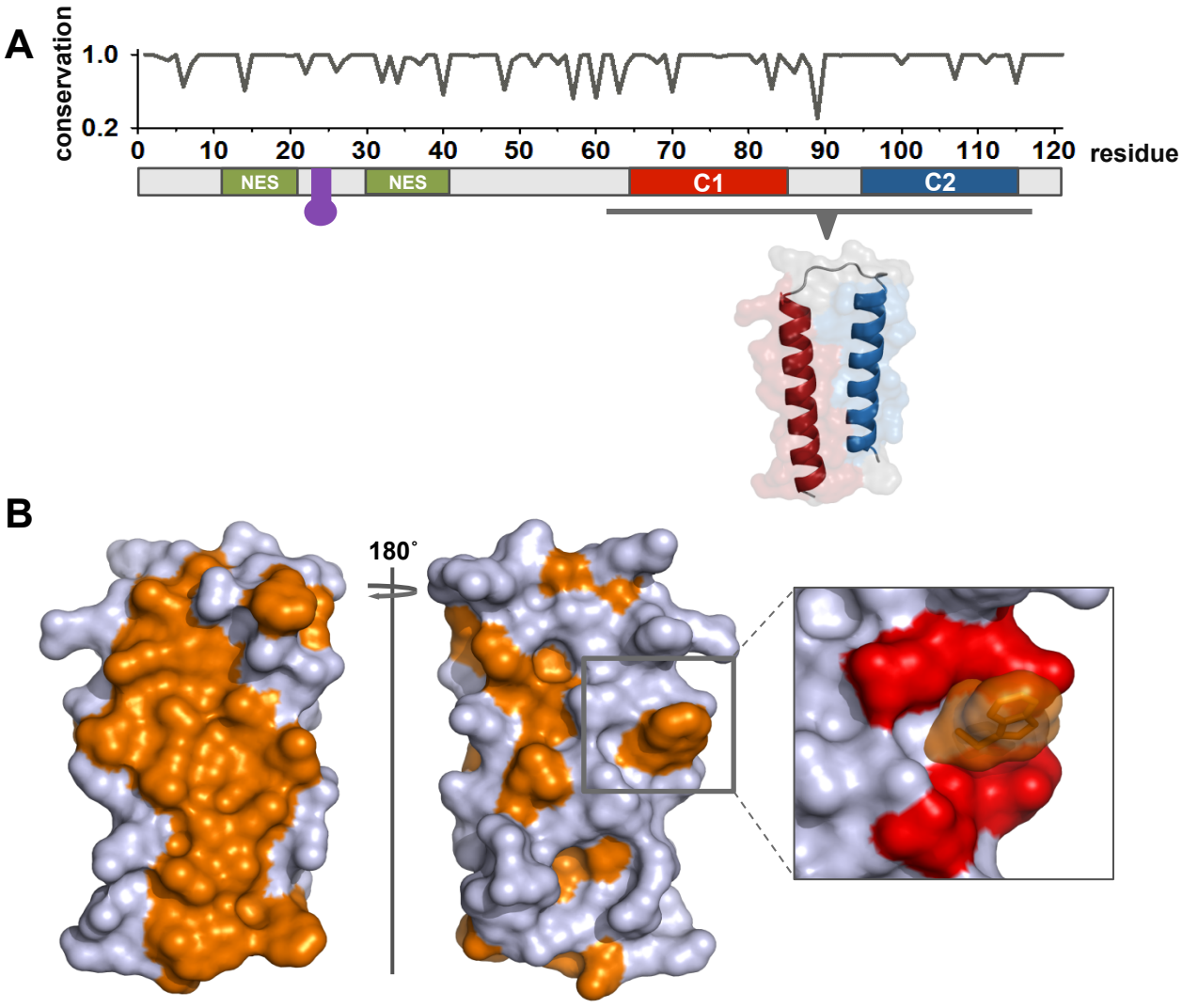

Figure 1.5 Organisation and structure of influenza A virus NEP. (A) A schematic representation of NEP including amino acid conservation at each position marked graphically above. Conservation at each amino acid position was calculated using Bioedit (Ibis Biosciences) from alignments of 16065 full-length influenza A NEP sequences obtained from http://www.fludb.org (accessed 14-03-2012). The N-terminal nuclear export signals (NES) enable binding of NEP to the cellular β-importin Crm1. A highly conserved serine-rich motif at positions 23-25 (purple) is phosphorylated during virus infection and is found in the modified form within virions. The C-terminal α-helices interact along their lengths to form an almost perfectly anti-parallel hairpin, the structure of which has been solved (PDB:1pd3). (B) Hydrophobic residues on the NEP C-terminal domain are depicted in orange. The opposing hydrophobic and hydrophilic faces result in the NEP C-terminal domain forming an amphipathic molecule. In full-length NEP the N-terminal domain is proposed to pack against the hydrophobic face, effectively burying it. The putative M1-binding tryptophan residue (W78, orange) projects prominently from within a ring of glutamate residues (red) on the hydrophilic face of the NEP C-terminal domain.

31–40 (Huang et al. 2013). These NESs are proposed to interact with the cellular nuclear export protein Crm1, and are unusual in the sense that several of the critical hydrophobic residues are methionines or phenylalanines rather than the canonical leucine (Iwatsuki-Horimoto et al. 2004; Neumann et al. 2000). Although the functional importance is as yet unknown, NEP is phosphorylated during the influenza replication cycle (Hutchinson et al. 2012). Indeed, the phosphorylation of a highly conserved serine-rich motif (S23, S24 and S25) proximal to the NES has recently been demonstrated in virion-associated NEP, with S24 proposed to be the modified residue (Hutchinson et al. 2012). In addition to phosphorylation, NEP has been identified as a target for in vitro sumoylation, however it is unclear whether NEP is sumoylated during virus replication or indeed what function this could serve (Pal et al. 2011).

The highly-structured C-terminal domain consists of two α-helices C1 (amino acids 64–85) and C2 (amino acids 94–115) that are connected by a short inter-helical turn. The two α-helices are comparable in length and interact extensively, forming an almost perfectly anti-parallel hairpin (Fig. 1.5A). The hairpin conformation results in the C-terminal domain being amphipathic in character, with the opposing external faces predominantly displaying hydrophobic and hydrophilic functional groups respectively (Fig. 1.5B). It is not known if the N-terminal domain interacts with the C- terminal α-helices, however it has been postulated that the N-terminal domain effectively buries the hydrophobic face of the C-terminal hairpin (Akarsu et al. 2003). In contrast, the opposing hydrophilic

face of NEP appears to be surface-exposed and displays a prominent hydrophobic tryptophan residue (W78) in the centre of a glutamate cluster (Fig. 1.5B). It has been demonstrated that W78 is required for binding to the viral M1 protein in an interaction that is proposed to be important for vRNP nuclear export (Akarsu et al. 2003). As a whole NEP amino acid identity is highly conserved across all sequenced influenza A strains (93.4%) (Fig. 1.5).

1.7.2 Role of NEP in vRNP export

During influenza virus infection, incorporation of newly synthesised vRNPs into progeny virions is dependent on the export of vRNPs from the host cell nucleus. In this regard, nuclear export of vRNPs appears to be predominantly dependent on the cellular β-importin protein Crm1, which along with its cofactor RanGTP recognises a structurally conserved hydrophobic NES (Elton et al. 2001; Ma et al. 2001; Dong et al. 2009; Güttler et al. 2010). Accordingly, influenza virus-infected cells treated with leptomycin B, a potent inhibitor of the Crm1 pathway, show intranuclear retention of vRNPs (Elton et al. 2001; Ma et al. 2001; Watanabe et al. 2001). Crm1-mediated nuclear export of viral nucleoprotein complexes has been extensively studied in HIV–1 infection where unspliced viral mRNA is exported from the nucleus bound to the Crm1 export complex by way of the NES-containing viral mRNA-binding protein Rev (Meyer & Malim 1994; Fischer et al. 1995; Askjaer et al. 1998). Interestingly, the HIV–1 mRNA nuclear export pathway can be reconstituted when the Rev NES is replaced with the influenza virus NEP NES (O'Neill et al. 1998). Moreover, the introduction of anti-NEP

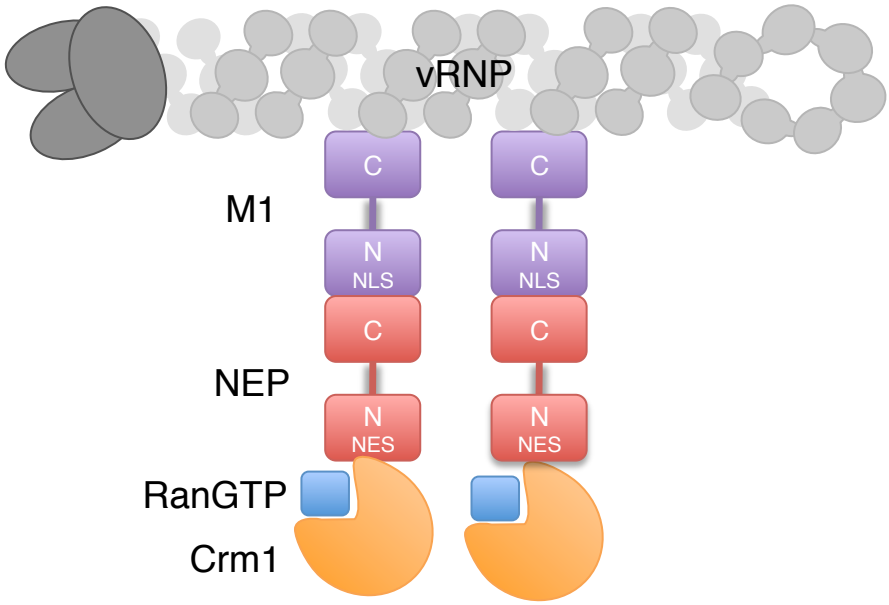

Figure 1.6 The daisy chain model for NEP-mediated nuclear export of influenza virus vRNPs. The β-importin Crm1 mediates export of the vRNP complex by binding to the N-terminal domain of NEP, as well as to its cofactor, the small GTPase Ran. The C-terminus of NEP binds to the nuclear localisation signal (NLS) on the N-terminal domain of the viral matrix protein M1. The C-terminus of M1 in turn binds to the vRNP through interaction with NP (grey).

antibodies into influenza virus-infected cells was shown to block vRNP export (O'Neill et al. 1998), a phenotype that is shared with non-viable recombinant viruses that do not encode NEP (Neumann et al. 2000). These findings, along with the observation that nuclear localisation of NEP is essential for productive infection (Martin & Helenius 1991; Whittaker et al. 1996; Bui et al. 2000), implicate NEP as a key mediator in vRNP nuclear export.

This evidence suggests that NEP serves a similar function to the HIV–1 Rev protein by acting as an adapter between vRNPs and the Crm1 export machinery. In this model for vRNP nuclear export (Fig. 1.6), Crm1 recognises the NES on the N-terminus of NEP but binds with RanGTP to an unknown site distinct from the NES (Neumann et al. 2000) – although this study was published before the discovery of a second NES (Huang et al. 2013), potentially representing the true site of Crm1 binding. The C-terminal hairpin of NEP in turn associates with the N-terminal nuclear localisation signal (NLS) of the viral matrix protein M1 (Ward et al. 1995; Yasuda et al. 1993; Akarsu et al. 2003; Shimizu et al. 2011) and the M1 protein binds to the vRNP through a C-terminal interaction with NP (Baudin et al. 2001). However, it should be noted that the N-terminus and the N-terminal domain of M1 have also been implicated in NP binding (Ye et al. 1999; Noton et al. 2007). These interactions have led to the description of the vRNP nuclear export complex as a daisy chain consisting of Crm1, NEP, M1 and vRNP. A recent study has alluded to a further function for NEP after the vRNP-nuclear export complex has exited the nucleus. In this regard, it was demonstrated that the NEP-binding

cellular ATPase F1Fo localises at the bottom edge of budding virions and is critical for efficient influenza virus egress (Gorai et al. 2012). Although the role of NEP in this process is unclear it is conceivable that F1Fo is recruited by vRNP-bound NEP in the cytoplasm prior to viral genome packaging.

Although a plausible model for vRNP nuclear export has been demonstrated, several studies have called into question the role of NEP as the principal arbiter in this process. In this respect, it has been repeatedly noted that NEP and M1 do not colocalise with vRNPs, as would be expected if this was the sole mechanism for exporting viral genome segments from the nucleus (Elton et al. 2001; Ma et al. 2001). In addition, disruption of the Crm1 pathway following treatment with leptomycin B does not alter the localisation of M1 or NEP, but does cause accumulation of NP at the nuclear periphery (Elton et al. 2001). Similarly, overexpression of Crm1 shows no effect on the localisation of NEP (Elton et al. 2001). It is important to note that these studies rely heavily on fluorescence microscopy and it is possible that small differences in NEP and M1 localisation have gone undetected. However, a potential role for NP in vRNP nuclear export should not be dismissed. NP has been shown to actively accumulate in lipid rafts at the apical cell membrane in the absence of other viral proteins, a role that has been proposed to govern the polarity of viral budding (Carrasco et al. 2004). Indeed, NP is a structural component of vRNPs and has been shown to contain three functional nuclear export signals, one of which is Crm1-dependent (Akarsu et al. 2003; Elton et al. 2001; Yu et al. 2012). Interestingly, the interaction

between NP and Crm1 has been proposed to facilitate wild-type levels of vRNP nuclear export in cells infected with a mutant virus that expresses greatly reduced levels of NEP (Elton et al. 2001; Wolstenholme et al. 1980). In a similar manner, nuclear retention of vRNPs could be overcome by exogenously expressed M1 in cells blocked for the expression of late viral proteins including NEP (Bui et al. 2000). In agreement with this finding, M1 has recently been shown to contain an NES capable of mediating Crm1-independent nuclear export, the mutagenesis of which results in a significant decrease in viral titre (Cao et al. 2012)

In addition to the extensively studied roles of influenza virus-encoded proteins in vRNP nuclear export, several cellular factors have been proposed to contribute to this process. Perhaps the most interesting of findings is that inhibition of the (mitogen-activated protein kinase) MAPK signalling cascade leads to impaired nuclear export of vRNPs by interfering directly with NEP-mediated export (Pleschka et al. 2001). Further studies present evidence that MAPK signalling is activated by protein kinase Cα (PKCα) late in influenza virus infection as a result of HA accumulation on lipid rafts at the cell membrane (Marjuki et al. 2006). This suggests that membrane accumulation of HA has the potential to act as a switch that activates MAPK signalling, thereby directing the nuclear export of vRNPs to the cell membrane for packaging into progeny virions. It is, however, unclear how vRNP nuclear export would be triggered as NEP is not a direct target of MAPK signalling (Pleschka et al. 2001) (i.e. activation of the MAPK cascade does not result in NEP phosphorylation). Another cellular factor that has been

demonstrated to influence vRNP nuclear export is the apoptotic regulator caspase 3 (Wurzer et al. 2003). In this regard, it has been observed that inhibition of caspase 3 leads to a phenotype similar to that of MAPK signalling inhibition or treatment with leptomycin B, characterised by the nuclear retention of vRNPs. As a result, caspase 3 is proposed to play a role in vRNP nuclear export by increasing the diffusion limit of nuclear pores in a manner that is independent of MAPK signalling and Crm1 (Wurzer et al. 2003).

These observations indicate that there is the potential for considerable interplay between viral proteins and several distinct cellular factors during the nuclear export of vRNPs. Consequently, there appears to be significant redundancy in the influenza virus nuclear export pathway.

1.7.3 Emerging role for NEP during transcription and replication

In addition to the much-studied role of NS2/NEP in vRNP export, several studies have alluded to a novel role for NEP during influenza virus replication. Although a biochemical mechanism has yet to be described, NEP appears to play a significant role in regulating the accumulation of influenza virus mRNA, cRNA and vRNA. Moreover, this function of NEP has been demonstrated to play a critical role in the adaptation of some avian H5N1 influenza viruses to efficient replication in mammalian cells (Mänz et al. 2012).

The first study to conclude that NEP could influence events other than the export of vRNPs demonstrated that a single point mutation, I32T, results in highly efficient production of defective interfering (DI) particles lacking an intact PA gene (Odagiri & Tobita 1990; Odagiri et al. 1994). In viruses containing the mutated NEP, replication of the full-length PA segment vRNA was shown to be suppressed during cRNA synthesis, whereas replication of the DI vRNA was enhanced (Odagiri & Tobita 1990). While the evidence for the formation of DI particles during natural infection is controversial (Bean et al. 1985; Chambers & Webster 1991), it is evident that NEP could play a role during vRNA genome replication and mutations affecting this function may lead to the replication of short, subgenomic RNA species.

Although the role of NEP in the production of aberrant genomic replication products is intriguing, it sheds little light on the role of NEP during virus replication. Subsequently however, NEP was demonstrated to inhibit reporter gene expression in a dose-dependent manner using an influenza virus mini-replicon system (Bullido et al. 2001). Moreover, it was demonstrated that the NEP concentrations required to significantly inhibit reporter gene expression could physiologically be reached within an infected cell, indicating that this is unlikely to be an artefact of NEP over-expression (Bullido et al. 2001). Further experiments conducted using intracellular vRNP reconstitution assays have corroborated the evidence that higher levels of NEP expression inhibit the transcription and replication of all viral RNA species (Mänz et al. 2012).

Recent studies have shown that, in addition to inhibiting viral genomic replication and transcription, low concentrations of NEP can stimulate the accumulation of influenza virus vRNA and cRNA (Robb et al. 2009; Mänz et al. 2012). Consequently, it was proposed that NEP plays a critical role in determining the viral mRNA:cRNA ratio within infected cells. Moreover, regulation by NEP occurred independently of viral M1 protein expression and did not require the presence of the terminal NEP NES (Robb et al. 2009). This has led to the proposal that the regulatory role of NEP is mechanistically distinct from the vRNP nuclear export pathway. Interestingly, as is the case for interaction with M1 during nuclear export, NEP regulation requires the C-terminal α-helices, although mutation of the putative M1-binding residue (W78) showed no effect on regulatory activity (Robb et al. 2009). Furthermore, the ability of NEP to regulate RNP accumulation was conserved between influenza type A and B viruses in a type-specific manner, further alluding to the critical role of NEP-regulated viral RNA transcription during influenza virus replication (Robb et al. 2009; Bullido et al. 2001).

Until recently, the biological significance of NEP-mediated regulation of viral RNA accumulation was unknown. However, a recent study has demonstrated that a mutation within NEP was responsible for the adaptation of a highly pathogenic avian influenza virus, thereby enabling increased replication in mammalian cells (Mänz et al. 2012). This is of biological importance as most avian influenza viruses do not replicate efficiently in mammalian cells (Reperant et al. 2012). One

of the factors that leads to this host-range restriction is the reduced activity of avian viral polymerases in mammalian cells (Subbarao et al. 1993; Cauldwell et al. 2014). The reduction in polymerase activity has been ascribed to impaired cRNP synthesis by avian influenza polymerases in mammalian cells (Mänz et al. 2012). However, restricted avian influenza virus polymerase activity could be overcome by a number of ostensibly non-related compensatory point-mutations in NEP, causing an increase in the accumulation of cRNPs (Mänz et al. 2012). It is interesting to note that compensatory mutations occurred in both the N- and C-terminal domains of NEP, and that NEP has previously been implicated in phylogenetic studies on host-range adaptation (Chen et al. 2006; Miotto et al. 2010). Intriguingly, the compensatory function of NEP may hint towards a potential mechanism for NEP regulation of viral RNA accumulation. The C-terminal α-helices of NEP were demonstrated to interact directly with the two basic polymerase subunits, PB1 and PB2 (Mänz et al. 2012). Both PB1 and PB2 have been implicated in promoter binding (Fodor et al. 1993; Perales et al. 1996; Jung & Brownlee 2006; González & Ortín 1999a; González & Ortín 1999b; Li et al. 1998) and it is therefore tempting to speculate that NEP binds to the polymerase and acts as a co-factor to stimulate viral genomic replication. Taken together, this and previous studies suggest that NEP may function in switching the role of the viral polymerase from transcription early in infection, to the production of genomic vRNPs by up-regulating cRNP synthesis (Mänz et al. 2012; Robb et al. 2009).

In a recent study, a novel species of virally encoded RNA was implicated in regulating the switch from viral transcription to replication (Perez et al. 2010). These short single-stranded molecules, dubbed small viral RNAs (svRNAs), are 22–27 nucleotides in length and correspond to the 5′ end of each of the eight vRNA segments (Perez et al. 2010; Umbach et al. 2010). During the late stages of viral infection, svRNAs are proposed to regulate vRNA replication, favouring the synthesis of the cRNA replication intermediate over mRNA transcription. It is suggested that svRNA-mediated regulation of vRNA replication is conferred through binding to the viral polymerase, thereby serving as a segment-specific guide capable of augmenting the vRNA promoter so as to favour the synthesis of full-length cRNA over prematurely terminated and polyadenylated mRNA transcripts. Interestingly, expression of only the polymerase subunits, nucleoprotein and negative-sense template is not sufficient for the generation of svRNAs; however, the addition of NEP to the RNP reconstitution assay leads to svRNA accumulation (Perez et al. 2010). Nonetheless, it remains unclear whether the requirement for NEP alludes to a prospective role during an svRNA-mediated switch from transcription to replication, or if the stimulatory activity of NEP on viral genomic replication results in the detectable accumulation of short aborted viral transcripts produced during normal transcription by the influenza virus polymerase.

Although the mechanism for NEP-mediated regulation of transcription and replication requires further elucidation, these studies all suggest a role for NEP

during influenza virus infection that is independent of vRNP export. In this respect, it is salient to consider that other negative-sense viruses encode proteins, other than the nucleocapsid components, capable of regulating transcription and replication of their respective viral genomes. In particular, the NS1, NS2 and M2–2 proteins of human respiratory syncytial virus down-regulate viral RNA transcription and replication (Atreya et al. 1998; Collins et al. 1995; Cheng et al. 2005) and the C protein of Sendai virus specifically inhibits RNA synthesis from the genomic promoter (Cadd et al. 1996). Likewise, the P protein of parainfluenza virus, which does not possess enzymatic activity but is an essential co-factor for viral polymerase activity, regulates viral mRNA synthesis in a phosphorylation-dependent manner (Sun et al. 2011). Accordingly, it is conceivable that influenza virus NEP may share functional similarities with these viral regulatory proteins.

1.8 Thesis objectives and outline

Influenza A viruses predominantly infect waterfowl and as such have evolved to replicate in the intracellular environment of avian hosts. Occasionally however these viruses spread to mammalian hosts and encounter an intracellular environment subtly different to that in which they evolved. One of the major obstacles that avian influenza viruses must overcome when infecting mammalian cells is the low activity of the avian viral polymerase in mammalian cells. A single mutation – PB2 627 E→K – is capable of overcoming this restriction and is consequently strongly selected for during mammalian host adaptation. Several hypotheses have been proposed for the mechanism of polymerase restriction by

PB2 627E and the subsequent increase in polymerase activity observed when mutated to PB2 627K, however none of these studies have conclusively answered this question. To address this, a cell-based assay that does not rely on the incorporation of NP for RNP activity was used to probe several prospective determinants of viral polymerase restriction by PB2 627E (Chapter 3).

The second part of this thesis involves investigations into a phosphorylation site described on the viral mediator of vRNP nuclear export. NEP is a multifunctional viral protein that, among other roles in the host cell nucleus, is responsible for mediating vRNP nuclear by forming an interface between the cellular nuclear export machinery and viral proteins attached to vRNPs. Although nuclear export of vRNPs is an essential step during influenza virus infection, little is known about how this process is regulated. In this regard, a study was conducted to understand the role of phosphorylation in NEP function, revealing that phosphorylation increased NEP nuclear export in a manner that was conserved amongst viral genera (Chapter 4). As structural information on NEP is sparse, an NMR-based approach was used to determine the secondary structure of NEP, as well as predict a molecular model (Chapter 5). Using this new information, the mechanism by which phosphorylation of NEP increased nuclear export was studied using NMR-based relaxation experiments. This led to the finding that phosphorylation causes a conformational shift in NEP that potentially provides the cellular nuclear export machinery better access to two N-terminal NESs (Chapter 6).

2. Materials and methods

2.1 Materials

2.1.1 General reagents

All chemical reagents used for general molecular biology procedures were AnalaR grade and purchased from GE Healthcare Life Sciences, New England Biolabs, Roche, Invitrogen Life Technologies, Millipore, VWR International, Geneflow, Agilent Technologies, Thermo Scientific, Sigma-Aldrich, QIAGEN, Bio-Rad and Promega. Reagents used for more specialised techniques are indicated separately.

2.1.2 Enzymes

Restriction endonucleases were purchased from New England Biolabs, Roche and Thermo Scientific. T4 Polynucleotide Kinase (PNK) was purchased from Thermo Scientific; Pfu Turbo DNA polymerase from Stratagene, Tobacco Etch Virus (AcTEV) protease from Invitrogen, Ligation High from Toyobo Life Sciences,

RNasin ribonuclease inhibitor from Promega, Phusion DNA polymerase from New England Biolabs, Thrombin from Sigma-Aldrich and Prescission 3C protease from Pierce

2.1.3 Radiochemicals

Radiochemicals were obtained from PerkinElmer at the following specific activities:

[α–32P]GTP ~3000 Ci/mmol (10mCi/ml)

[γ–32P]ATP ~3000 Ci/mmol (10mCi/ml)

2.1.4 Synthetic DNA and RNA

Synthetic oligodeoxyribonuleotides were purchased from Sigma-Aldrich and Invitrogen, synthetic oligoribonucleotides were purchased from Dharmacon. The open reading frame of A/WSN/33 (H1N1) NEP was codon optimised for translation in bacteria and synthesised as a linear DNA molecule by Geneart Gene Synthesis.

2.1.5 Antibodies

Anti-NP antibodies were kind gifts from Otto Haller (University of Freiburg, Germany) and Paul Digard (University of Edinburgh, UK). Anti-PB2 antibody was a kind gift from Simon Carr (Sir William Dunn School of Pathology, University of Oxford). Anti-NEP antibody was a kind gift from Rob Ruigrok (EMBL Grenoble,

France). Anti-RanBP5 was purchased from Santa Cruz Biotechnology. Anti-Actin antibody (A2066) was purchased from Sigma-Aldrich.

2.1.6 Bacteria and bacterial culture media

Escherichia coli DH5a and *E.coli* BL21(DE3) were purchased from Invitrogen and New England Biolabs respectively. Luria-Bertani (LB) broth bacterial media (10 g bacto-tryptone, 5 g yeast extract and 10 g NaCl per litre) and LB agar plates supplemented with ampicillin or kanamycin were supplied by the Sir William Dunn School of Pathology. Ampicillin (100 µl/ml) or kanamycin (50 µl/ml) were added to LB broth as required.

2.1.7 Mammalian cell culture media

Minimal Essential Medium (MEM) and Dulbecco's Modified Eagle Medium (DMEM), Foetal Calf Serum (FCS) and Phosphate Buffered Saline (PBS) were purchased from Sigma-Aldrich. TrypLE Express dissociation reagent and L-glutamine were purchased from Invitrogen.

2.1.8 Cell lines

Human Embryonic Kidney 293T (HEK 293T) cells, Madin-Darby Bovine Kidney epithelial (MDBK) cells and chicken embryo firoblast (DF–1) cells were obtained from the cell bank of the Sir William Dunn School of Pathology, University of Oxford.

2.1.9 Viruses

Influenza A/WSN/33 (H1N1) virus stocks were a gift from Peter Palese (Icahn School of Medicine at Mount Sinai, New York, USA).

2.1.10 Plasmids

Protein expression plasmids pcDNA-PB1, pcDNA-PB2, pcDNA-PA, pcDNA-NP, pcDNA-NEP and pcDNA–3A have been described previously (Robb et al. 2009), as has pPolI-NA (Fodor et al. 1999). A mutated version of pcDNA-PB2, pcDNA-PB2 627E, was a kind gift from Pang-Chui Shaw (Chinese University of Hong Kong, China). The pPolI-NP plasmid used for primer extension assays and as a template for mutagenesis contains has a deleted start-codon and an introduced downstream stop-codon, rendering it incapable of producing NP protein, as previously described (Turrell et al. 2013). Plasmids used for influenza A/WSN/33 (H1N1) virus reverse genetics (pHW2000 vectors) have been described previously (Hoffmann et al. 2000) and were a kind gift from Gulsah Gabriel (University of Hamburg, Germany). The influenza virus reverse genetics plasmid containing separate NS1 and NEP coding sequences separated by a FMDV–2A cleavage site was a kind gift from Chris Basler (Basler et al. 2001). The pCMV-Rev and Luc-RRE plasmids were a kind gift from Stuart Wilson (Williams et al. 2005).

2.2 Plasmid construction and mutagenesis

2.2.1 cDNA amplification

Viral cDNA was PCR amplified using 1 ng of template plasmid , 25 pmol of each primer, 200 µM of each dNTP and 1.25 U Phusion polymerase in 1×Phusion HF reaction buffer. The reaction mixture was incubated in a thermocycler at 95°C for 10 s denaturing, 50°C for 20 s annealing and 68°C for 30 s elongation for a total of 25 cycles. Amplification products were analysed by agarose gel electrophoresis, purified by precipitation with 2 volumes of absolute ethanol and 0.1 volumes of 4.2 M ammonium acetate, washed twice with 70% ethanol and resuspended in dH_20.

2.2.2 PCR Mutagenesis

Mutations were introduced into viral cDNA sequences within pcDNA-NEP, pPolI-NA and pPolI-NP (see section 2.1.10) by PCR mutagenesis with primers shown in Table 2.1. The PCR reaction was carried out using 25 ng of template plasmid, 25 pmol of each primer, 200 µM of each dNTP, 3% DMSO and Pfu Turbo DNA polymerase in 1×Pfu Turbo reaction buffer. The reaction mixture was incubated in a thermocycler at 95°C for 30 s denaturing, 55°C for 60 s annealing and 68°C for 16 min elongation for a total of 18 cycles. The PCR product was digested with DpnI, column purified and transformed into *E. coli* DH5α.

2.2.3 Cloning

To construct the pRev$_N$ plasmid, cDNA corresponding to the first 69 N-terminal amino acids of the HIV–1 Rev protein was PCR amplified from pCMV-Rev with primers encoding KpnI and EcoRI restriction sites respectively (Table 2.1). The PCR product and pcDNA–3A were digested with EcoRI and KpnI, column purified, ligated and transformed into *E. coli* DH5α. To construct pRev-NEP, the NEP open reading frame was PCR amplified from pcDNA-NEP using primers encoding EcoRI and NotI respectively (Table 2.1). The PCR product and pRev were digested with EcoRI and NotI, column purified, ligated and transformed into *E. coli* DH5α.

For construction of the pET-M14-NEP bacterial protein expression plasmid, cDNA corresponding to the NEP gene from A/WSN/33 (H1N1) was PCR amplified with primers that added NcoI and NotI restriction sequences to the 5' and 3' ends of NEP respectively. The PCR product and pET-M14 were digested with NcoI and NotI, column purified, ligated and transformed into *E. coli* DH5α.

All ligations were performed using Ligation High according to the manufacturer's instructions.

2.2.4 Plasmid preparation and sequencing

For initial plasmid preparations, bacterial colonies containing the plasmid of interest were used to inoculate 2 ml of LB broth supplemented with either 100 μg/ml ampicillin or 50 μg/ml kanamycin and incubated overnight at 37°C whilst

shaking at 180 rpm. Cells were pelleted from the overnight culture and plasmid DNA was extracted using a QIAprep spin miniprep kit (QIAGEN) according to the manufacturer's specifications. Plasmid DNA was eluted in 30 µl of ddH_2O.

For large scale plasmid DNA preparations, transformed bacterial colonies were used to inoculate 100 ml of LB broth supplemented with either 100 µg/ml ampicillin or 50 µg/ml kanamycin and incubated overnight at 37°C whilst shaking at 180 rpm. Cells were pelleted and plasmid DNA was extracted using a QIAfilter maxiprep kit (QIAGEN) according to the manufacturer's specifications. Extracted plasmid DNA was dissolved in ddH_2O to a final concentration of 1 mg/ml.

All plasmids used in this study were sequenced by Source Bioscience LifeSciences (Oxford) using Sanger's method. Sequence analysis was conducted using BioEdit Software (Ibis Biosciences).

2.3 Mammalian cell culture

HEK 293T cells were maintained in in DMEM supplemented with 10% FCS. MDBK cells were maintained in MEM supplemented with 2 mM L-glutamine and 10% FCS. All cells were maintained in 75 cm^2 flasks and incubated at 37°C and 5% CO_2. For passaging, mammalian cell monolayers were removed from the flask surface with TrypLE Express and diluted 1:10 in the requisite cell culture media.

2.4 Virus culture

2.4.1 Reverse genetics

Wild-type and recombinant influenza A/WSN/33 (H1N1) viruses were rescued using the eight plasmid reverse genetics system (Hoffmann et al. 2000). HEK 293T cells were grown in 35 mm dishes and transfected with 1 μg of each bidirectional plasmid using Lipofectamine–2000 transfection reagent (Invitrogen) according to the manufacturer's specifications. Transfected cells were incubated at 37°C, 5% CO_2 in DMEM (10% FCS) for 24h and then rinsed with PBS and the medium replaced with low-serum DMEM (0.5% FCS), followed by incubation for another 48 h. The rescued viruses were then amplified by applying 200 μl of the virus-containing supernatant to 80% confluent MDBK cell monolayers in 25 cm^2 flasks and incubating cells for 72 h. Media from these flasks were harvested and centrifuged briefly at 4000*g* to remove cellular debris. The viral titre of the supernatants was then assessed by plaque assay, followed by storage at –80°C.

2.4.2 Plaque Assay

Cell culture supernatants containing influenza A virus were serially diluted in MEM supplemented with 0.5% FCS and 2 mM L-glutamine. Recently confluent monolayers of MDBK cells in 6-well plates were rinsed with PBS and each well infected with 200 μl of serially diluted virus for 1 h at room temperature. After infection, the inoculum was aspirated and 2 ml of agarose solution (2% agarose

dissolved in PBS diluted 1:1 in MEM supplemented with 0.5% FCS and 2 mM L-glutamine) was added to the cell monolayer and allowed to polymerise. The plates were then incubated at 37°C, 5% CO_2 for 72 h, followed by removal of the agarose and staining of the plaques with 2 ml 0.2% Coomassie Brilliant Blue dissolved in 7.5% glacial acetic acid and 50% methanol.

2.4.3 Growth Curve

Growth curve analyses were performed by infecting recently confluent 6-well plates of MDBK cells at an MOI of 0.0008 with influenza A viruses and harvesting the supernatants at 6, 24, 36 and 60h post infection. Viral titres were determined by plaque assay.

2.5 RNA analyses

2.5.1 RNP reconstitution

RNP reconstitutions were conducted by transfecting approximately 1×10^6 HEK 293T or DF–1 cells in 35 mm dishes with 1 µg of each of the relevant plasmids using Lipofectamine 2000 (Invitrogen) according to the manufacturer's specifications. Cells were incubated in at 37°C and 5% CO_2 and harvested 48 h post-transfection.

2.5.2 RNA extraction

Total RNA was extracted from cells using TRIzol reagent (Invitrogen) according to the manufacturer's specifications. Typically, cells from a 35 mm dish were lysed in 500 µl of TRIzol reagent. After 10 min incubation at room temperature, 0.2 volumes of chloroform (100 µl) was added to the sample, followed by 10 s of agitation and subsequent centrifugation at 17 000*g* for 20 min. The clear aqueous phase was then transferred to a new microcentrifuge tube and an equal volume of isopropanol added, followed by centrifugation at 17 000*g* for 20 min. The resulting RNA pellet was washed in 70% ethanol, dissolved in 50 µl of ddH_2O and stored at –20°C.

2.5.3 Primer extension analysis

2.5.3.1 Primers

Viral RNA species, as well as cellular 5S rRNA were detected by segment-specific oligodeoxyribonucleotides shown in Table 2.2.

2.5.3.2 Radiolabelling of primers

Primers were labelled in a 10 µl reaction containing 1 pmol of primer, 10 µCi [γ–32P] ATP and 2.5 U of PNK in 1× kinase buffer A. The reaction was incubated for 1 h at 37°C. Primers were purified away from excess [γ–32P] ATP and reaction constituents using a nucleotide removal kit (QIAGEN) according to the manufacturer's specifications. Radiolabelled primers were eluted in 30 µl of ddH_2O and stored at –20°C.

Table 2.1. Sequences of primers used in this study

Primer	Sequence (5'-3')
Cloning	
EcoRI-NEP	GTGCTGGAATTCATAATGGATCCAAACACTGTG
NEP-NotI	ATCATCGCGGCCGCTTAGTTTCTGTTTTGGAGTGAGTGG
NcoI-NEP	CATCATCCATGGATCCGAATA
KpnI-Rev	CATCATGGTACCGCCACCATGGCAGGAAGAAGCGG
Rev-EcoRI	CATCATGAATTCCTCTGCAGATCGTCCCAG
Mutagenesis	
NEP S24E F	CAAAAATGCAGTTGGGGTCCGAATCGGAGGACTTGAATGG
NEP S24E R	CCATTCAAGTCCTCCGATTCGGACCCCAACTGCATTTTTG
NEP S24A F	CAAAAATGCAGTTGGGGTCCGCATCGGAGGACTTGAATGG
NEP S24A R	CCATTCAAGTCCTCCGATGCGGACCCCAACTGCATTTTTG
NP 3p 3A/8U F	GGGACCATGCCGGCCAGTAAAAACAGGGTAGATAATCACTCACAG
NP 3p 3A/8U R	CTGTGAGTGATTATCTACCCTGTTTTTACTGGCCGGCATGGTCCC
NP76 3p 3A/8U F	CAGGGTAGATAATCACTCACAGA
NP76 3p 3A/8U R	TGACTTCGATGTCACTCTGTGAG
NP 3p 3U/8A F	GGGACCATGCCGGCCAGAAAAATCAGGGTAGATAATCACTCACAG
NP 3p 3U/8A R	CTGTGAGTGATTATCTACCCTGATTTTTCTGGCCGGCATGGTCCC
NP 5p 3C/8G F	GGAGTACGACAATTAAAGAAAAATACCCTTGCTTCTGCTAATAACCCGGCGGCCC
NP 5p 3C/8G R	GGGCCGCCGGGTTATTAGCAGAAGCAAGGGTATTTTTCTTTAATTGTCGTACTCC
Primer extensions	
NA +	TCCAGTATGGTTTTGATTTCCG
NA -	TGGACTAGTGGGAGCATCAT
NA47 +	CATTT AAACTCCTGCTTTCGC
NA47 -	GTTCAAAAAACTCCTTG TTTC
NP +	TGATTTCAGTGGCATTCTGG
NP -	TGGAAAGTGCAAGACCAGAA
NP37 +	GGTACTAGTCTACCCTGCTTTTGC
NP37 -	GCAAAAGCAGGGTAGACTAGTACC
NP47 +	TTACTAGTCTACCCTGCTTTTGC
NP47 -	TTACTAGTCTACCCTGCTTTTGC
NP76 +	TGATTTCGATGTCACTCTGTGAG
NP76 –	GCAGGGTAGATAATCACTCACAGA
NP101 +	TGATTTCGATGTCACTCTGTGAG
NP101 -	GCAGGGTAGATAATCACTCACAGA
5S rRNA	TCCCAGGCGGTCTCCCATCC

2.5.3.3 Primer extension assay

Primer extension assays were conducted as has been described previously (Robb et al. 2009). Briefly, RNA was mixed with an excess of radiolabelled primers complementary to the positive and negative senses of the viral segment of interest and a primer complementary to 5S rRNA which was used as an internal cellular control. This mixture was denatured by heating at 95°C for 3 min followed by immediate cooling to 0°C. An equal volume of transcription mix (2×First Strand buffer [Invitrogen], 20 mM dithiothreitol [DTT], 1mM dNTP mix [Thermo Scientific] and 50 U Superscript III [Invitrogen]) was added to the sample, followed by heating to 50°C and incubation for 1 h. The reaction was stopped by the addition of RNA loading buffer (90% formamide, 10 mM EDTA, 0.001% bromophenol blue and xylene cyanol) and heating to 95°C for 5 min.

2.5.3.4 Recombinant polymerase transcription assay

The purified polymerase was used in ApG or β-globin mRNA-primed in vitro transcription assays, as described previously (Brownlee & Sharps, 2002). Briefly, 1.5 µl of purified polymerase and 15 pmol of each of 5' end (15 nt [AGUAGAAACAAGGCC]) and 3' end (14 nt [GGCCUGCUUUUGCU) promoter templates were incubated in a 3 µl reaction mixture for 2 hours at 30°C with 1 mM ATP, 0.5 mM CTP, 0.5 mM UTP and 0.1 µM [α-^{32}P]GTP, 0.5 mM ApG, 5 mM $MgCl_2$, 2 mM DTT and 5 U RNasin. After 2 hours, 10 µl formamide was added (90% formamide, 10 mM EDTA, 0.001% bromophenol blue and 0.001% xylene cyanol) and heated to 95°C for 3 min and cooling directly on ice. Transcription

products were analyzed by 20% PAGE containing 7 M urea in Tris-borate-EDTA (TBE) buffer and quantified by phosphorimage analysis using AIDA software (Raytest).

2.5.3.5 Polyacrylamide gel electrophoresis (PAGE)

DNA products from primer extension assays or RNA products from in vitro transcription assays were analysed on polyacrylamide gels in 7M urea and 1×TBE(90 mM Tris, 90 mM orthoboric acid and 2.5 mM EDTA), respectively. Polymerisation of gels was accomplished by the addition of ammonium persulphate (APS) to 0.2% and TEMED to 0.02%. The gels were run at 1200 V in 1×TBE buffer. Transcription products were detected by autoradiography and quantitated using phosphor Fujifilm imaging plates and a Fujifilm FLA–5000 fluorescent image analyser. Autoradiography data was analysed using Aida software (Raytest).

2.6 Protein purification and analyses

2.6.1 Purification of recombinant influenza A polymerase

Recombinant influenza A/WSN/33 virus polymerase was prepared by transiently transfecting HEK 293T cells with each of the viral polymerase expression plasmids (pcDNA-PA-TAP, pcDNA- PB1 and pcDNA-PB2 627E or 627K) using Lipofectamine-2000 (Invitrogen) according to the manufacturer's instructions. Cells were incubated for 48 h post-transfection and then harvested by

centrifugation at 200 × g for 5 min at 4°C. Cells were then washed with ice cold PBS and lysed in 2 ml of Tris lysis buffer (50 mM Tris-HCl [pH 8.0], 200 mM NaCl, 33% glycerol, 0.5% Igepal CA-630, 1 mM DTT, 1× complete EDTA-free protease inhibitor cocktail) by rotation for 1 h at 4°C. The soluble and insoluble fractions were separated by centrifugation at 17,000 × g for 5 min at 4°C and the soluble fraction was diluted 1:5 with binding buffer (20 mM Tris-HCl [pH 8.0], 150 mM NaCl,) and incubated with of IgG Sepharose (GE Healthcare Life Sciences) for 2 h whilst rotating at 4°C. After this initial incubation, IgG Sepharose was washed extensively with wash buffer (20 mM Tris-HCl [pH 8.0], 150 mM NaCl, 0.1% Igepal CA-630, 10% glycerol and 1× PMSF) and the bound protein was released by cleavage overnight at 4°C with 20 U of AcTEV (Invitrogen) in cleavage buffer (10 mM Tris-HCl [pH 8.0], 150 mM NaCl, 0.1% Igepal CA-630, 10% glycerol, 1 mM DTT). Cleaved viral polymerase was then purified away from the IgG Sepharose by centrifugation and stored at -20°C until needed. Purified polymerase was analyzed by SDS-PAGE, and PB2 levels were assessed using AIDA software (Raytest).

2.6.2 Protein gel electrophoresis and immunoblotting

2.6.2.1 SDS-PAGE analysis of proteins

Protein samples were mixed with all volume of 2×protein solvent buffer. The samples were heated for five minutes at 98°C prior to gel loading. Proteins samples were subsequently resolved by electrophoresis on a discontinuous gel system as described by Laemmli (Laemmli 1970). Separating gels contained 8–

16% acrylamide in 375 mM Tris–HCl (pH 8.8) and 0.1% SDS and the stacking gel contained 3.2% acrylamide in 120 mM Tris-HCl (pH 6.8) and 0.1% SDS. Gel polymerisation was achieved by the addition of 0.2% APS and 0.02% TEMED. Samples were loaded onto the gel and run at 120 V in SDS running buffer(20 mM Tris, 250 mM glycine and 0.1% SDS) at room temperature. A pre-stained protein marker was run in parallel for molecular weight determination.

2.6.2.2 Immunoblotting

Proteins were transferred from SDS-PAGE gels onto nitrocellulose membrane (GE Healthcare Life Sciences) in transfer buffer(30 mM Tris, 20 mM glycine, 10% methanol), at 100V and 4°C. The immunoblot membrane was then blocked in 2.5% non-fat milk in 1×PBS for 1h at room temperature. The membrane was then incubated with the indicated antibodies diluted in 2.5% non-fat milk in 1×PBS for 1h at room temperature on a rotating wheel. Membranes were washed four times in 1×PBS (0.1% Tween–20)(5 min washes), then incubated for one hour with the appropriate secondary antibody conjugated to horseradish peroxidase. The membrane was then washed four times in 1×PBS(0.1% Tween–20)(5 min washes). The blots were then developed by chemiluminescence using Amersham ECL Western blotting reagents (Amersham Biosciences). After treatment with chemiluminescence substrate, membranes were exposed to X-ray film (Super RX Fuji Medical X-ray film, Kodak). Where necessary, films were analysed by densitometry using Aida software (Raytest).

2.6.2.3 Staining of protein gels

Gels were silver stained using the SilverXpress kit (Invitrogen) according to the manufacturer's specifications. Briefly, SDS-PAGE gels were transferred to a plastic dish and fixed in a solution of 50% methanol and 10% acetic acid for 10 minutes; fixed gels were then sensitised in 50% methanol and 2.5% sensitizer prior to washing in dH_20 three times. Gels were stained and developed according to manufacturer's instructions. For Coomassie staining, the Coomasie brilliant blue staining kit (Invitrogen) was used according to the manufacturer's instructions.

2.6.3 NEP nuclear export assays

Cell-based nuclear export essays were conducted essentially as described previously (Williams et al. 2005). HEK–293T cells were transfected with pLuc–RRE and pcDNA–Rev–NEP or mutated variants thereof using Lipofectamine 2000 reagent (Invitrogen). Transfected cells were incubated at 37°C for 24 hours. Luciferase signal was detected using the Promega luciferase assay system according to the manufacturer's instructions. Essentially, cell monolayers were resuspended in Promega lysis buffer and incubated for 15 minutes whilst shaking to ensure lysis. Luciferase substrate was then added to aliquots of lysed samples and analysed using a Spectramax M5 luminometer with 1000 ms accumulation time. Each experiment was conducted in duplicate with five biological repeats. Luciferase activity was normalised to NEP protein expression as determined by immunoblotting

2.6.4 Expression and purification of NEP

2.6.4.1 Bacterial expression of NEP

Expression plasmids encoding his-tagged NEP or mutated variants thereof were transformed into *E.coli* BL21 (DE3) using standard techniques. Overnight culture of transformed *E.coli* (50 ml) was used to inoculate 2 litres of LB media and grown to an OD_{600} = 0.8. On reaching OD_{600} = 0.8, bacteria were pelleted at 4000*g*, washed in 1×PBS and resuspended in 500 ml of M9 minimal growth media (Marley et al. 2001). For preparation of protein for NMR experiments, M9 minimal growth media was made with $^{15}NH_4Cl$, ^{13}C glucose or D_2O, depending on the experiment as described previously (Marley et al. 2001). The resuspended culture was then incubated at 37°C for 45 min before being induced with 0.1 mM IPTG and incubated for a further 4 h at 37°C. Thereafter, the cells harvested by centrifugation at 4000*g* for 20 min and the pellets were frozen at –20°C until needed.

2.6.4.2 Purification of NEP

2.6.4.2.1 Lysis and solubilisation of inclusion bodies

NEP was predominantly expressed as inclusion bodies within bacterial cells. To isolate inclusion bodies, frozen cell pellets were resuspended in 1×PBS and passed 10–12 times through an Emulsiflex-C5 homogeniser (Avestin). Inclusion bodies were isolated from homogenised lysates by centrifugation 48,000*g* for 20 min at 4°C. Inclusion bodies were rinsed once with 1×PBS and then resuspended in solubilisation buffer (50 mM Tris, 200 mM NaCl, 6 M guanidine-HCl, 2 mM β-

mercaptoethanol, 2 mM imidazole, 10% glycerol, pH 8.0). In order to solubilise inclusion bodies, samples were subjected to shaking at 270 rpm for 4 h at 30°C, during which the sample was pulled through an 18-gauge needle three times. Solubilised material was clarified by centrifugation at 48,000*g* for 30 minutes at 4°C. Typically this technique resulted in the solubilisation of 70% of inclusion body material.

2.6.4.2.2 Affinity purification and refolding of bacterially-expressed NEP

Solubilised protein was loaded onto a 1 ml Ni-NTA column (Amersham) using a syringe at a flow rate of approximately 1 ml/min. The column was then attached to an AKTA pure (GE Healthcare) and any residual unbound protein was removed by washing the column with solubilization buffer. Column-bound NEP was refolded in a gradient of 6 M to 0 M urea (50 mM Tris, 200 mM NaCl, 2 mM β-mercaptoethanol, 2 mM imidazole, 10% glycerol, pH 8.0) over the course of 35 ml at a flow-rate of 0.5 ml per minute. Following refolding, bound protein was eluted from the column by the addition of elution buffer (50 mM Tris, 200 mM NaCl, 2 mM β-mercaptoethanol, 300 mM imidazole, 10% glycerol, pH 8.0) and collected in 1 ml fractions. Fractions corresponding to the eluted protein (as determined by absorbance at 280 nm) were pooled and the N-terminal His-tag was removed by overnight cleavage at RT with 3C protease, leaving a two amino acid (Gly-Pro) extension. The identities of elution peak fractions and protease cleavage products were confirmed by SDS-PAGE.

2.6.4.2.3 Size exclusion gel chromatography

NEP was purified away from the proteolytic cleaved N-terminal his-tag by size exclusion gel chromatography. The proteolytic cleavage reaction was concentrated down to 1ml using a centrifugal concentrator with a 3 kDa molecular weight cut-off and loaded onto a Superdex 75 column (Amersham) connected to an AKTA pure (GE Life Sciences) that had been equilibrated in NMR buffer (20 mM Tris, 100 mM NaCl, pH 7). The sample was run through the column at 0.5 ml/min, resolving a symmetrical peak, the identity and purity of which was confirmed by SDS-PAGE. Peak fractions were pooled and stored at 16°C until needed.

2.6.4.2.4 Quantification of protein sample concentration

Protein sample concentration was determined by measuring absorbace at 280 nm on a NanoDrop 2000 UV spectrometer (Thermo). For determination of NEP concentration an extinction coefficient of 12490 was used.

2.7 Circular Dichroism

CD spectra were collected on a Jasco J-815 circular dichroism spectropolarimeter by collecting spectra from 200–280 nm with 10 accumulations per experiment and 3 independent replicates. CD experiments were carried out at 20°C on protein samples (58 μM) in buffer containing 20 mM Tris, 100 mM NaCl, at pH 7. The resultant CD spectra were smoothed using five point moving average. Melting curves were generated from CD spectra (single accumulations) collected between

20°C and 80°C in 2°C increments. Melting curves were then plotted from mean residue ellipticity values at 222 nm and fitted to a Boltzmann sigmoid curve using Graphpad Prism 6 (Graphpad).

2.8 Nuclear magnetic resonance experiments

NMR experiments were conducted in collaboration with Jason Schnell and Jolyon Claridge at the Department of Biochemistry, University of Oxford. Jolyon Claridge was responsible for all NMR experimental setup. All sample preparation and data analysis was conducted by the author.

2.8.1 ^{1}H, ^{15}N HSQC

Two dimensional ^{1}H, ^{15}N HSQC experiments were conducted on a Bruker 600 MHz spectrometer at 30°C. Protein samples in NMR buffer (20 mM Tris, 100 mM NaCl, pH 7) were concentrated to between 0.4 and 0.6 mM and placed into a Shigemi NMR tube. Spectra were obtained with 16 scans over 1024 points in the direct dimension and 128 points in the indirect dimension. The proton sweep width was set at 14 ppm and the nitrogen at 34 ppm. Data were processed using NMRPipe (Delaglio et al. 1995) and analysed using CCPN analysis (Vranken et al. 2005). Chemical shift perturbations were calculated for assigned ^{1}H, ^{15}N HSQC peaks using the Follow Shift Changes Module in CCPN Analysis. Weightings of 1.00 and 0.15 were used for ^{1}H and ^{15}N respectively.

2.8.2 Triple resonance experiments

All triple resonance experiments were performed at 30°C on a Bruker Avance II 600 MHz spectrometer equipped with a triple resonance cryogenic probe. Standard versions of HNCA, HNCACB, HN(CO)CA, CBCA(CO)NH, HNCO and HN(CA)CO experiments were conducted (Hyberts et al. 2010) on ^{2}H, ^{13}C, ^{15}N - labelled protein sample that had been concentrated to 0.5mM in NMR buffer (20 mM Tris, 100 mM NaCl, pH 7) at 30°C. All experiments were conducted using Poisson gap sampling schedules with 10% of points (shown in Table 2.3) being collected. The resultant spectra were processed in NMRPipe (Delaglio et al. 1995) and reconstructed with iterative soft thresholding using hmsIST software (Hyberts et al. 2012), followed by analysis using CCPN Analysis (Vranken et al. 2005).

Table 2.2. Experimental parameters for backbone assignment spectra

Experiment	Data Points			Sweep Width		
	^{1}H	^{15}N	^{13}C	^{1}H	^{15}N	^{13}C
HNCA	2048	32	128	14	34	30
HNCACB	2048	48	128	14	34	64
HN(CO)CA	2048	32	128	14	34	30
CBCACONH	2048	32	128	14	32	75
HNCO	2048	32	128	14	32	22
HN(CA)CO	2048	32	128	14	32	22

2.8.3 Relaxation experiments

Standard ^{1}H, ^{15}N HSQC-based T_1 and T_2 experiments (Farrow et al. 1995) were conducted at 600MHz with conditions as described in Section 2.8.1, processed using NMRPipe and analysed using the Follow Intensity Changes Module in CCPN

Analysis. To this end, T_1 spectra were collected in duplicate at delays of 100 ms, 300 ms and 800 ms and T_2 spectra were collected in duplicate at delays of 8 ms, 16 ms and 48 ms. Both T_1 and T_2 experiments were collected with 1024 points in the direct dimension and 128 points in the indirect dimension over 24 scans. Once analysed in CCPN analysis, relaxation rates were plotted for residues across the length of the protein with values for any residues with overlapping peaks excluded. Rotational correlation times (τc) were calculated using the equation:

$$\tau_c \approx \frac{1}{4\pi\nu_N}\sqrt{6\frac{T_1}{T_2} - 7}$$

T_1 and T_2 values were calculated by taking the 30% trimmed mean of values across all residues.

3. Host restriction of PB2 627E is diminished on short templates in a nucleoprotein-independent manner

3.1 Introduction

A major obstacle blocking the efficient replication of avian influenza viruses in humans is the low activity of avian influenza virus polymerases in human cells (Imai et al. 2013). Accordingly, in order to function efficiently in human cells, avian-derived influenza virus polymerases are known to undergo adaptive changes. The viral polymerase — composed of three subunits: polymerase acidic (PA) and polymerase basic one and two (PB1, PB2) — catalyses the replication and transcription of the viral genome, composed of eight single-stranded, negative-sense RNA segments. In order to accomplish this, the viral polymerase binds to the 5′ and 3′ ends of a viral RNA segments that form the vRNA promoter (Flick et al. 1996; Fodor et al. 1994). The rest of the vRNA is bound by multiple copies of the viral nucleoprotein (NP) to form viral ribonucleoprotein complexes

(vRNPs). vRNPs are transcribed by the viral polymerase, which produces mRNA and positive-sense cRNA replication intermediate, that is in turn used as a template for vRNA synthesis (Fodor 2013; Resa-Infante et al. 2011).

The archetypal adaptive mutation known to confer increased activity to viral polymerases of avian origin in mammalian cells occurs at residue 627 of the PB2 polymerase subunit (Subbarao et al. 1993). Avian viral isolates predominantly encode glutamic acid at PB2 627 (627E), whereas this residue is almost exclusively a lysine (627K) in influenza viruses isolated from humans, with the exception of the 2009 pandemic H1N1 viruses (Mehle & Doudna 2009). The presence of lysine at this position results in increased viral replication in mammalian models (Hatta et al. 2001; Steel et al. 2009; Herfst et al. 2012). In addition, the PB2 627 E→K mutation has been associated with lethality in humans infected with H5N1, H7N7 and H7N9 avian viruses (Hatta et al. 2001; Fouchier et al. 2004; Gao et al. 1999; Kageyama et al. 2013).

Several studies have sought to elucidate the molecular basis for the increase in viral polymerase activity in human cells associated with the PB2 627 E→K mutation. In this regard, it has been demonstrated that PB2 627K allows avian-derived viral polymerases to evade a cellular inhibitor in human cells (Mehle & Doudna 2008)). In contrast, a similar study proposed that human cells are deficient in an activating factor that acts selectively on polymerases containing PB2 627E (Moncorgé et al. 2010). Moreover, it has been suggested that PB2 627E has a decreased affinity for NP, thereby inhibiting the formation of

transcriptionally active viral RNPs (Mehle & Doudna 2008; Labadie et al. 2007; Ng et al. 2012; Rameix-Welti et al. 2009). Furthermore, recent studies have implicated the cytoplasmic innate immune sensor RIG-I in PB2 627E restriction, proposing that PB2 627E polymerases on incoming vRNPs are unable to shield the 5′ promoter strand from RIG-I (Weber 2015). In this study, we use a recently developed cell-based replication assay to study the viral determinants of PB2 627E polymerase restriction. Using this approach, we demonstrate that restriction of viral polymerases containing PB2 627E occurs independently of the interaction between PB2 and NP. In addition, we show that PB2 627E polymerase activity can be rescued on short vRNA-like templates or by introducing mutations to the vRNA promoter sequence.

3.2 Results

3.2.1 PB2 627E restricts polymerase activity in human cells but not in vitro

In order to address the role of adaptive mutations associated with PB2 627, plasmids encoding PB2 genes derived from A/WSN/33 (H1N1) with either 627K or 627E were transfected into human (HEK–293T) or avian (DF1) cells along with plasmids encoding PA, PB1, NP and a segment 5 vRNA template. Transcription and replication of the vRNA template by reconstituted vRNPs were measured 48 h after transfection by primer extension analysis of viral steady-state RNA levels. In agreement with previous studies (Mehle & Doudna 2008; Massin et al. 2001), the PB2 627 K→E mutation resulted in a dramatic decrease in RNA replication

and transcription by the viral polymerase in human cells, but showed no effect when vRNP reconstitutions were conducted in avian cells (Fig. 3.1A). To determine whether the reduction in viral polymerase activity in human cells was due to a defect in viral polymerase assembly, polymerases containing either PB2 627K or PB2 627E were purified from HEK–293T cells using a TAP-tag on the C-terminus of the PB1 polymerase subunit (Deng et al. 2005). SDS-PAGE analysis of the purified polymerases indicated that all three viral polymerase subunits were expressed efficiently in human cells and co-purified with similar efficiency as a trimeric complex irrespective of the identity of PB2 627 (Fig. 3.1B). To determine if the purified viral polymerases were able to function outside the cellular context, both polymerases were incubated for 1 h at 37˚C with a short double-stranded viral promoter and NTPs including [α–32P]GTP. The PB2 627E viral polymerase that exhibited restricted activity in the vRNP reconstitution assay was able to catalyse ApG-primed and cap-dependent transcription as efficiently as the mammalian-adapted PB2 627K polymerase (Fig. 3.1), in agreement with previous studies (Aggarwal et al. 2011).

3.2.2 PB2 627E restriction is independent of NP

In contrast to the vRNP reconstitution assay, *in vitro* transcription of a short vRNA promoter does not require the formation of a canonical vRNP, or indeed the presence of NP. In agreement with this, reduced interaction between PB2 and NP has been proposed to account for the decreased activity associated with avian viral polymerases in mammalian cells (Mehle & Doudna 2008; Labadie et al.

2007; Ng et al. 2012; Rameix-Welti et al. 2009). To investigate the contribution of the interaction between PB2 and NP to the restricted phenotype of the PB2 627E polymerase we made use of a recently developed NP-independent cell-based replication assay (Turrell et al. 2013; Resa-Infante et al. 2010). This system takes advantage of the observation that viral RNA transcription and replication can take place in the absence of NP on templates up to 76 nucleotides in length. Accordingly, replication assays were conducted in the presence and absence of NP on vRNA templates between 37 and 101 nucleotides in length that were derived from a segment 6 vRNA template (Fig. 3.2A and B respectively). Omission of NP did not alter the accumulation of RNA products from templates that do not require NP for replication and transcription (37–76nt templates) (compare Fig. 3.2A, B). This indicates that PB2 627E restricts polymerase activity in a manner that is independent of NP and consequently independent of canonical RNP formation. This is in agreement with the recent suggestion that the previously reported decrease in the affinity of PB2 627E for NP stems from a decrease in viral RNA replication (Cauldwell et al. 2012). Surprisingly, on the shortest template assayed (37nt), transcription and replication by the PB2 627E polymerase approach levels observed for the mammalian-adapted PB2 627K polymerase (Fig. 3.2). However, the level of RNA transcription and replication by the PB2 627E polymerase on longer templates (47 to 101 nt-long) appears to decrease in a manner that is proportional to template length (Fig. 3.2). The experiment was repeated using segment 6 derived short vRNA templates, producing comparable results (Fig. 3.3A). To ascertain whether NP-independent

replication and transcription of viral RNA was possible in avian cells, and if so, whether there were any appreciable differences in the accumulation of RNA products in avian and mammalian systems, experiments with the 37nt vRNA template were conducted in DF1 cells. As expected, replication and transcription of the short vRNA template by PB2 627K and 627E polymerases was comparable in avian cells (Fig 3.3B).

3.2.3 Mutation of viral RNA promoter residues abrogates PB2 627E restriction

The intriguing finding that a restricted polymerase with PB2 627E is active on short vRNA templates in the context of a cell suggests that the restriction could occur at the level of template binding or elongation. In fact, the template, or more specifically promoter stability, has been implicated previously in the mechanism of restriction of avian influenza virus polymerases in mammalian cells (Crescenzo-Chaigne et al. 2002). In order to test the effect of promoter stability on PB2 627E polymerase activity, a range of mutations were introduced into the promoter of a full-length non-coding segment 5 template. Mutations were designed not to disrupt intra-strand base-pairing between nucleotides proposed to interact in the corkscrew model (Flick et al. 1996), but rather to stabilise the formation of a panhandle structure. When compared to the activity of a vRNA template with a wild-type promoter, mutations in the 3′ promoter strand that are proposed to stabilise the panhandle structure, led to increased replication and

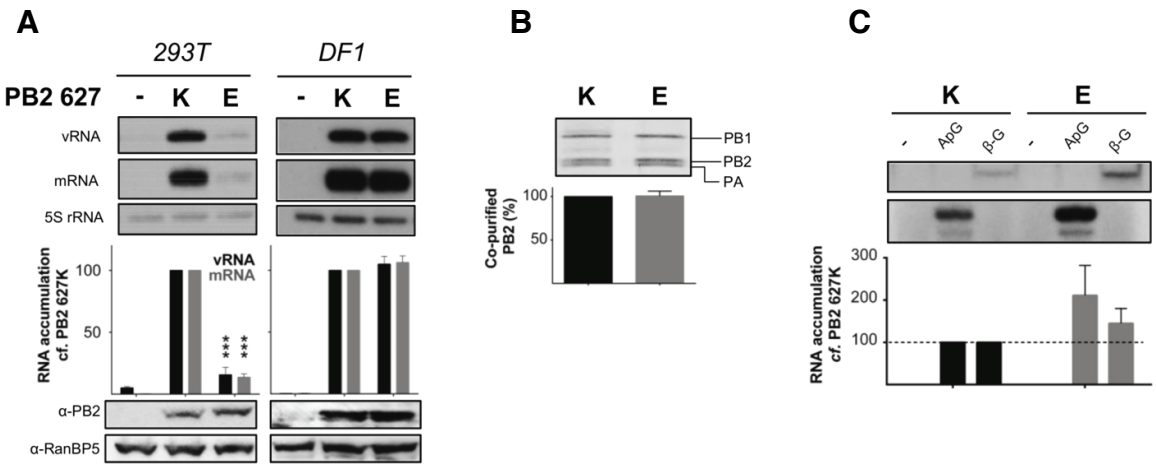

Figure 3.1. Effects of PB2 K627E mutation on polymerase assembly and activity in cultured cells and *in vitro*. (A) HEK 293T (human) or DF1 (chicken) cells were co-transfected with plasmids expressing PA, PB1, PB2 627K or 627E, NP and a segment 5 vRNA containing mutations to prevent expression of NP. Accumulation of mRNA and vRNA was assessed by primer extension 48 hours post-transfection. RNA levels detected for the E627K polymerase were set to 100. Error bars indicate s.e.m. of 3 independent experiments, and the asterisks indicate a significant difference from 100 (one sample t test; **P*<0.001). Expression of PB2 was analysed by Western blotting with RanBP5 serving as a loading control. (B) HEK–293T cells were co-transfected with plasmids expressing PA, PB1-TAP and PB2 627K or 627E and polymerase was purified using IgG Sepharose chromatography 48 hours post-transfection. Purified polymerase was analysed by SDS-PAGE, silver stained and PB2 levels assessed using Aida software (Raytest). PB2 627K levels were set to 100. The error bar indicates s.e.m. of three experiments. (C) Activity of purified polymerase from panel (B) was assessed in an *in vitro* transcription assay using ApG primer or -globin mRNA as cap donor. RNA levels detected for the E627K polymerase were set to 100. Error bars indicate s.e.m of three experiments.

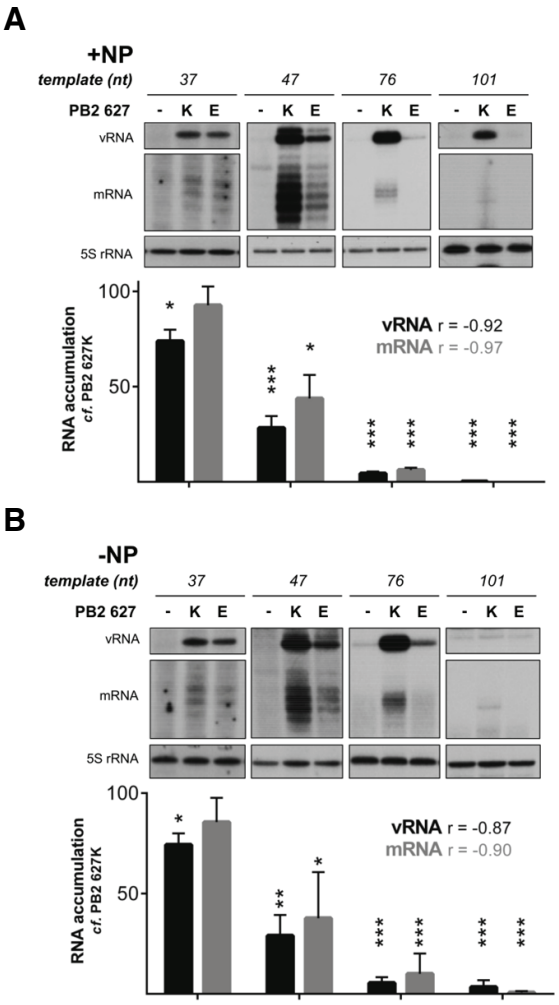

Figure 3.2. Transcription and replication of short vRNA templates in the presence or absence of NP by influenza virus RNA polymerase containing PB2 627K or 627E in a cell-based replication assay. HEK 293T cells were co-transfected with plasmids expressing short segment 5-based vRNA-like templates of the indicated length, PA, PB1, PB2 627K or 627E and (A) a plasmid expressing NP or (B) empty vector. Accumulation of vRNA and mRNA was assessed by primer extension 48 hours post-transfection. The level of vRNA template produced by cellular transcription was determined by the omission of the PB2 subunit of the viral polymerase and set to zero. RNA levels detected for the 627K polymerase were set to 100 for each template length. Error bars indicate s.e.m. of three experiments, and the asterisks indicate a significant difference from 100 (one sample t test; *$P<0.05$, **$P<0.01$, ***$P<0.001$). Pearson's correlation coefficient was calculated for the PB2 627E polymerase activities, producing the r-values shown.

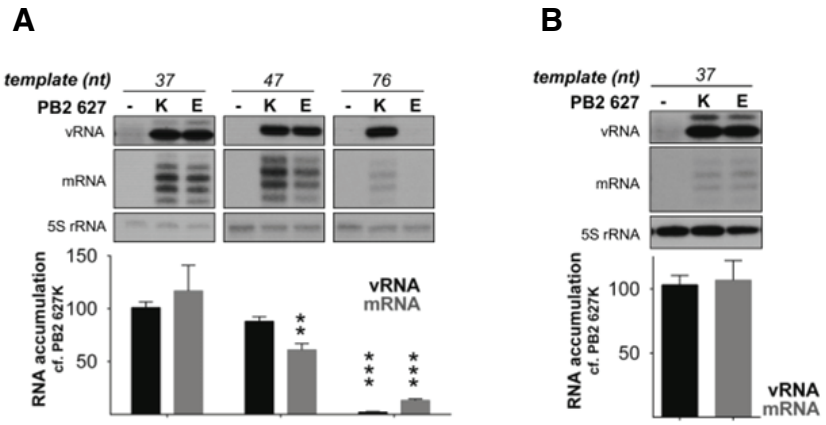

Figure 3.3. Transcription and replication of short NA segment vRNA templates by PB2 627K or 627E in human and avian cells. (A) HEK 293T or (B) DF1 cells were co-transfected with plasmids expressing short segment 6-based vRNA-like templates of the indicated length, as well as PA, PB1, PB2 627K or 627E. Accumulation of vRNA and mRNA was assessed by primer extension 48 hours post-transfection. The level of vRNA template produced by cellular transcription was determined by the omission of the PB2 subunit of the viral polymerase and set to zero. RNA levels detected for the 627K polymerase were set to 100 for each template length. Error bars indicate s.e.m. of three experiments, and the asterisks indicate a significant difference from 100 (one sample t test; $^{**}P<0.01$, $^{***}P<0.001$).

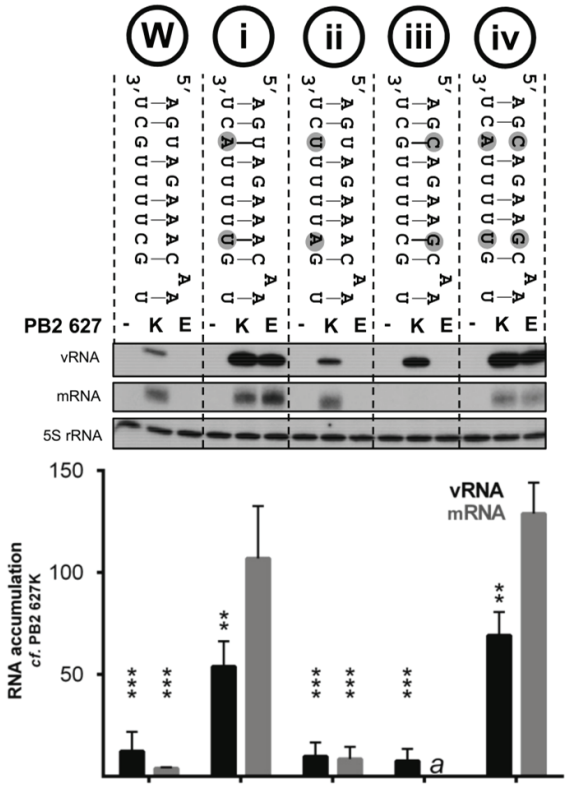

Figure 3.4. Effects of vRNA promoter mutations on transcription and replication by viral polymerase with PB2 627K or 627E. Schematic representation of wild-type (W) and mutant (i–iv) influenza virus vRNA promoter structures according to the panhandle model. Mutated residues are shown in italics and are indicated by a circle. HEK–293T cells were co-transfected with plasmids expressing PA, PB1, PB2 627K or 627E, NP and segment 5 vRNA with the indicated promoter mutations and mutations to prevent expression of NP. Accumulation of mRNA and vRNA was assessed by primer extension 48 hours post-transfection. The level of vRNA template produced by cellular transcription was determined by the omission of the PB2 subunit of the viral polymerase and set to zero. RNA levels detected for the 627K polymerase were set to 100. Error bars indicate s.e.m. of three experiments, and the asterisks indicate a significant difference from 100 (one sample t test; *P<0.001). _a No mRNA signal was detected above background levels for either PB2 627K or PB2 627E polymerases when template (iii) was used.

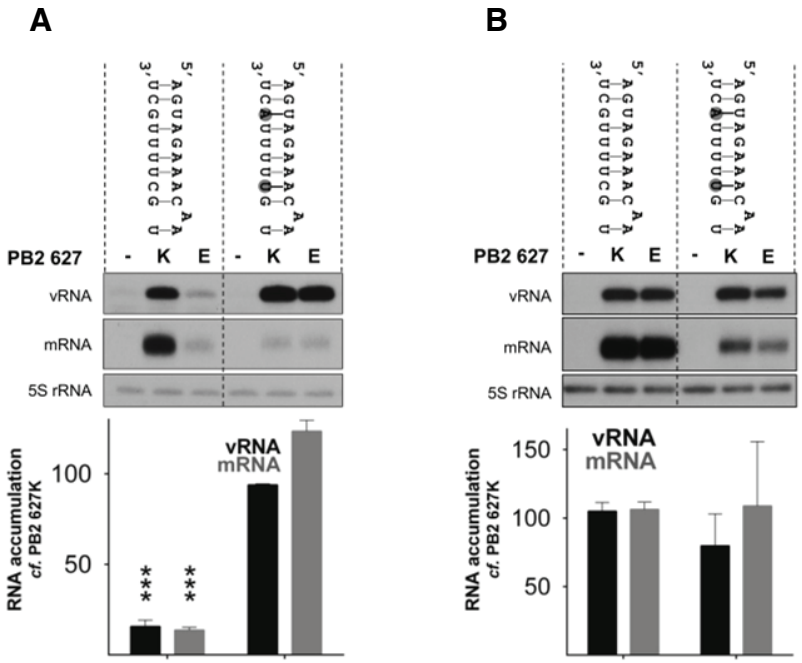

Figure 3.5. Effect of the vRNA promoter mutations on PB2 627K or 627E polymerase activity in human and avian cells. (A) HEK 293T or (B) DF1 cells were co-transfected with plasmids expressing full-length segment 6 containing the indicated mutations, as well as PA, PB1, PB2 627K or 627E. Accumulation of vRNA and mRNA was assessed by primer extension 48 hours post-transfection. The level of vRNA template produced by cellular transcription was determined by the omission of the PB2 subunit of the viral polymerase and set to zero. RNA levels detected for the 627K polymerase were set to 100 for each template length. Error bars indicate s.e.m. of three experiments, and the asterisks indicate a significant difference from 100 (one sample t test; *P<0.001).

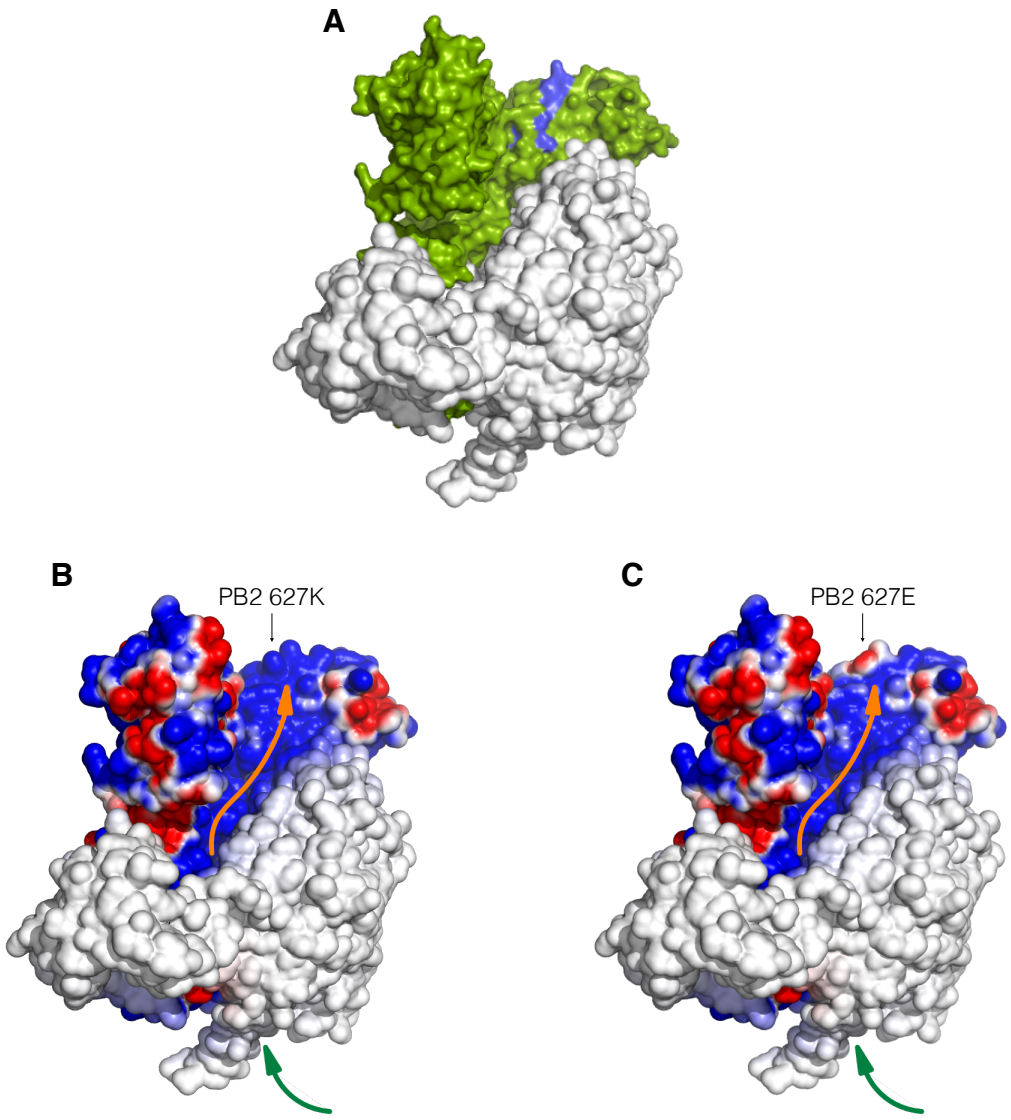

Figure 3.6. PB2 627E disrupts a basic cuff near the RNA product exit channel of the viral polymerase. (A) Structure of the influenza A polymerase (PDB: 4WSB) showing the positions of residues on the PB2 627 domain that have been demonstrated to be influenced by RNA binding (Lim et al. 2014) PB2 is shown in green and the affected residues in blue. Structures of the influenza A polymerase were modified by mutating PB2 627 to either (B) K or (C) E in pymol (the influenza A polymerase crystal structure was solved for a bat strain which encodes PB2 627S). The electrostatics of the PB2 subunit were calculated using APBS with blue indicating basic surfaces and red indicating acidic surfaces. The PA and PB1 subunits are depicted in white. Green arrows represent the path of template RNA and orange arrows represent the proposed path of the RNA product emanating from the polymerase exit channel.

transcription by the PB2 627E polymerase (Fig. 3.4i). Replication and transcription by a PB2 627E polymerase returned to the level observed for the wild-type promoter when the nucleotides stabilising the panhandle conformation were substituted for nucleotides not capable of pairing with the opposing 5′ promoter strand (Fig. 3.4ii). In contrast, panhandle-stabilising mutations introduced into the 5′ strand of the vRNA promoter resulted in restricted activity of the PB2 627E polymerase (Fig. 3.4iii). Surprisingly, this template could be replicated by the PB2 627K polymerase but could not be transcribed. However, destabilisation of the panhandle by introducing mutations into the 3′ promoter strand resulted in increased transcription and replication by both PB2 627K and E polymerases relative to the wild-type promoter (Fig. 3.4iv). When stimulatory mutations were introduced into the 3′ promoter strand of a segment 6 vRNA template a comparable increase in PB2 627E polymerase activity was observed, thereby confirming that this effect is not segment-specific (Fig. 3.5A). In addition, viral polymerases containing PB2 627K and 627E retained similar activity when an identical experiment was conducted in avian cells (Fig 3.5B).

3.3 Discussion

Infection of humans by avian influenza viruses requires that the viral polymerase overcomes restricted activity in human cells. However, the molecular determinants of avian viral polymerase restriction remain elusive. Using a cell-based replication and transcription assay that does not rely on the formation of canonical RNPs, we show here that restriction of PB2 627E polymerase occurs

independently of NP. However, this restriction is dependent on the length of short templates with the increased activity observed for the 37nt template decreasing as a function of template length. In addition to the use of a 37 nt template, PB2 627E restriction of viral polymerase activity could also be overcome when mutations were introduced to the 3′ vRNA promoter strand. The mechanism by which these mutations increase PB2 627E polymerase activity is unclear, although it is interesting to note that mutation of these residues changes the relative amounts of RNA replication and transcription products. It is tempting to speculate that the preferential synthesis of replication products is the result of making the promoter sequence more similar to that of the cRNA promoter which is incapable of serving as a template for transcription products due to cRNA-bound polymerases being incapable of cap-snatching (Leahy et al. 2002).

Intra-strand 3′ promoter basepairing proposed "cork-screw" model was not tested in this study, however it is known that disruption of these proposed basepairs ablates viral polymerase binding (Flick et al. 1996; Flick & Hobom 1999). Despite this, promoter mutations that stimulate the PB2 627E polymerase do not appear to require stabilisation of the panhandle promoter conformation but rather have sequence specific effects on the 3′ strand (Fig. 3.4ii, iv). Indeed structural studies published after the completion of this work suggest that the 3′ vRNA promoter strand does not form a stable secondary structure upon polymerase binding, unlike the 5′ strand which forms the proposed corkscrew structure (Pflug et al. 2014). This could imply that any changes to secondary

structure brought about by stimulatory promoter mutations may be acting on the 5′ promoter strand of the cRNA product. The new structural data suggest that this could indeed be the method of action for these mutations as the PB2 627 domain is distal to the promoter binding site of the viral polymerase, adjacent to the RNA product exit channel. As such, the PB2 627 domain appears to form a basic cuff over which the RNA product must pass before exiting the polymerase. Indeed, residues that have been demonstrated to influence RNA binding by the isolated PB2 627 domain (Lim et al. 2014) cluster around this site (Fig. 3.6A). In addition, introduction of PB2 627E disrupts the basic charge of this area, as has been observed in structural characterisation of the isolated 627 domain (Kuzuhara et al. 2009; Tarendeau et al. 2008; Yamada et al. 2010). Moreover, by modelling PB2 627E into the full polymerase structure, it is apparent that introduction of glutamic acid disrupts the basic cuff over which RNA is most likely to pass (Fig. 3.6A, B). This leads to the obvious hypothesis that disruption of this surface could lead to the RNA product being less occluded due to charge repulsion. This, in turn, could result in the RNA product being more accessible to the nuclear milieu, including host restriction factors such as nucleases and antiviral helicases.

The suggestion that the nascent RNA product is the site of PB2 627E restriction is consistent with the previous observation that an RNP containing a PB2 627E polymerase can replicate vRNA→cRNA but that these cRNA templates are somehow defective and cannot be used for vRNA synthesis (Mänz et al. 2012).

Accordingly, it is possible that the PB2 627 domain acts to protect the nascent cRNA promoter strand from mammalian host-restriction factors prior to encapsidation by a second viral polymerase, which would have high affinity for the nascent 5′ RNA promoter (Pritlove et al. 1995). Indeed, mutations in the vRNA 3′ promoter strand which abrogate PB2 627 restriction would result in an altered 5′ promoter sequence in the cRNA product. As a result, it is tempting to speculate that alterations to the 5′ cRNA promoter could preclude the binding of a host factor but not binding by the viral polymerase. By this logic, introduction of mutations into the vRNA 3′ promoter would result in decreased recognition of the nucleic acid termini by antiviral host factors, resulting in increased viral RNA replication.

Although the identity of the 627-specific host restriction factor(s) remains unclear, it is prescient to note that other viruses protect the ends of their genomes during viral RNA replication by variety of means. Intriguingly, Hepatitis C virus is dependant on host microRNA miR–122 to shield the 5′ end of its RNA genome from degradation by the 5′ exoribonucleases Xrn1 and Xrn2 (Sedano & Sarnow 2014; Li et al. 2015). Consequently, it is conceivable that influenza viruses may similarly protect their genomes against host nucleases, and that these nucleases may not be conserved between mammalian and avian hosts. Indeed a helicase, DDX17, that shows limited conservation between humans and birds has previously been proposed to influence PB2 627 restriction (Bortz et al.

2011), however the mechanism and magnitude of its action remain to be confirmed.

Infection of humans by avian influenza viruses requires that the viral polymerase overcomes restricted activity in human cells. However, the molecular determinants of avian viral polymerase restriction remain elusive. Using a cell-based replication and transcription assay that does not rely on the formation of canonical RNPs, we show here that restriction of PB2 627E polymerase occurs independently of NP. In addition, we observed that a viral polymerase containing PB2 627E shows unrestricted activity in human cells when provided with a 37nt vRNA template containing a wild-type promoter. This activity however, declined steeply as the template length increased. Nevertheless, PB2 627E polymerases do not appear to be defective during RNA elongation as full-length templates with mutated 3′ ends could be efficiently replicated and transcribed. Taken together, these findings along with recent structural data, indicate that restriction of avian viral polymerases may result from insufficient protection of the nascent RNA product due to disruption of a basic surface on the terminal region of the viral polymerase.

4. Phosphorylation of NEP 24S increases nuclear export

4.1 Introduction

Posttranslational modification of proteins by phosphorylation is a ubiquitous regulatory mechanism that is present in all domains of life. In eukaryotic cells, phosphorylation of serine, threonine and occasionally tyrosine represent a common reversible protein modification that can have a wide range of effects on protein structure and function. The importance of phosphorylation is emphasised by the fact that the human genome contains 518 protein kinase domains, representing the third most popular protein domain (Johnson 2009). Accordingly, it is unsurprising that viruses have evolved to make use of phosphorylation. Influenza A viruses are no different with all major viral gene products containing at least one site of phosphorylation (Hutchinson et al. 2012).

Influenza A virus NEP mediates the nuclear export of vRNPs and has been shown to be phosphorylated during viral infection (Richardson & Akkina 1991; O'Neill et al. 1998). Subsequently, a large proteomic screen identified NEP 24S as the phosphorylated residue (Hutchinson et al. 2012). NEP 24S falls within a highly conserved serine-rich motif located between two NESs that are responsible for interacting with the cellular nuclear export machinery to facilitate vRNP nuclear export. Although the main protein constituents in vRNP nuclear export have been identified it is still unclear what factors govern the formation of the viral nuclear export complex. In addition to nuclear export, NEP stimulates viral RNA replication via a C-terminal interaction with the viral polymerase (Mänz et al. 2012; Robb et al. 2009). In this regard, the N-terminal domain of NEP has been proposed to regulate the stimulatory function of NEP. However, the mechanism by which NEP stimulates viral RNA replication or how it is regulated remains unknown. Nevertheless, this process has been demonstrated to be an important determinant in the adaptation of avian influenza viruses to replicate in human hosts (Mänz et al. 2012).

In order to study the effect of phosphorylation on NEP function, NEP 24S was mutated to either alanine or a glutamic acid, representing non-phosphorylatable and phosphomimetic forms of NEP respectively. These NEP phosphomutants were then tested with regard to their ability to sustain viral replication and stimulate viral RNA replication, as well as the effect of these mutations on nuclear export.

4.2 Results

4.2.1 Generation of influenza A viruses containing mutations at NEP 24S

NEP is encoded by a short spliced transcript generated from segment 8 of the viral genome, which also encodes the viral interferon antagonist NS1. Although NEP and NS1 are translated from different open reading frames (ORFs), the nucleotide sequence encoding the N-terminus of NEP overlaps the sequence encoding the C-terminus of NS1. As such, it is impossible to engineer mutations into the N-terminal domain of NEP without making changes to the NS1 ORF. To overcome this problem, viruses were produced using a segment 8 construct that contained in-frame coding sequences of both NS1 and NEP separated by a picornaviral 2A sequence (Fig. 4.1A) (Basler et al. 2001). During translation, the 2A sequence causes ribosomal stalling resulting in the release of the upstream NS1 before resuming translation of the downstream NEP sequence (Luke et al. 2008). Accordingly, this technique allows for manipulation of the NEP coding sequence without affecting the NS1 coding region.

Influenza A viruses encoding NEP 24S (wildtype), 24E and 24A were generated using the eight plasmid reverse genetics system (Hoffmann et al. 2000). The replication kinetics of the wildtype and mutant viruses were subsequently examined, revealing that both viruses containing mutations at NEP 24 displayed severely attenuated replication (Fig. 4.1B). In addition to attenuated growth kinetics, mutant viruses produced very small plaques, further indicating

replication abnormalities (Fig. 4.1C). Accordingly, these experiments suggest that neither the non-phosphorylatable (NEP 24A) nor the phosphomimetic (NEP 24E) forms of NEP are compatible with normal viral replication. Consequently, it is possible that post-translational modification of NEP 24S may be required to regulate between two different states of NEP, each of which plays an essential role during viral infection.

4.2.2 Mutation of NEP 24 does not affect stimulation of viral RNA replication

One of the functions proposed for NEP during infection relates to the switch from transcription of the viral genome during early infection to viral RNA replication for the production of genomic vRNPs during late infection (Robb et al. 2009). This stimulatory activity is mediated by binding of the NEP C-terminus to the PB2 subunit of the viral polymerase in an interaction that is thought to be regulated by the N-terminal domain of NEP (Reuther et al. 2014). In order to determine if phosphorylation of NEP 24S affected stimulation of viral RNA replication, mutated variants of NEP were transiently expressed in HEK 293T cells along with vRNP components. The viral RNA replication and transcription products from transfected cells were compared by primer extension analysis and quantitated by phosphorimaging. As has been described previously (Robb et al. 2009; Mänz et al. 2012), co-expression of wild-type NEP in vRNP reconstitution assays resulted in the increase of viral RNA replication products (vRNA and cRNA) with a concomitant decrease in viral RNA transcription (Fig 4.2). The introduction of

non-phosphorylatable and phosphomimetic NEP mutants stimulated viral RNA replication in a manner consistent with that seen for wild-type NEP. As such, it appears unlikely that phosphorylation of NEP 24S plays a role in the stimulation of viral RNA replication observed late in viral infection.

4.2.3 A phosphomimetic mutant of NEP displays increased nuclear export

NEP mediates vRNP nuclear export by acting as an adapter between the vRNP and the cellular nuclear export protein Crm1. To accomplish this, NEP interacts with Crm1 through one of two N-terminal NESs. Secondary structure predictions of NEP suggest that the NESs reside on separate alpha-helices that are bisected by an unstructured loop that contains the serine-rich phosphorylation motif (Akarsu et al. 2003). To investigate the role of NEP 24S phosphorylation in NEP nuclear export, NEP phosphomutants were tested using a luciferase-based HIV Rev-dependent nuclear export assay (O'Neill et al. 1998). This assay is based on the cytoplasmic translation of mRNA containing a reporter gene and a Rev response element (RRE) that can be bound by the N-terminal RNA-binding domain of the HIV Rev protein and exported from the nucleus by interacting with Crm1 through a C-terminal NES. By fusing the Rev RNA-binding domain to the N-terminus of NEP, the efficiency of NEP nuclear export can be measured as a function of luciferase expression.

As has been described previously (O'Neill et al. 1998), wild-type NEP was able to mediate nuclear export of the reporter mRNA (Fig 4.3). The NEP 24A mutation

resulted in similar levels of NEP nuclear export. In contrast, the phosphomimetic NEP 24E mutation resulted in a significant increase in NEP nuclear export, thereby implicating NEP 24S phosphorylation in the regulation of this process. To determine if the observed increase in the nuclear export of NEP 24E was dependent on Crm1, the experiment was repeated in the presence of leptomycin B, a potent inhibitor of the Crm1:NES interaction (Sun et al. 2013). Addition of leptomycin B abolished nuclear export of all NEP variants, indicating that the increase in nuclear export observed for NEP 24E remains Crm1-dependent. Accordingly, the addition of a negative charge to NEP 24, broadly consistent with that expected for phosphoserine, appears to up-regulate the nuclear export of NEP in a manner that remains dependent on Crm1.

4.2.4 Increased nuclear export of phosphomimetic NEP is conserved in influenza B viruses

The NEP proteins of influenza A and B viruses are largely similar (Paragas et al. 2001). Both contain at least one nuclear export signal on their N-termini that is responsible for mediating the nuclear export of viral vRNPs (O'Neill et al. 1998; Paragas et al. 2001). In addition, NEP proteins from both genera are capable of stimulating viral RNA replication (Robb et al. 2009) and contain a homologous serine-rich motif proximal to their N-terminal NES (Fig. 4.4A). There are, however, no descriptions of influenza B NEP being phosphorylated (Hutchinson et al. 2012). Nevertheless, to test whether introduction of a phosphomimetic

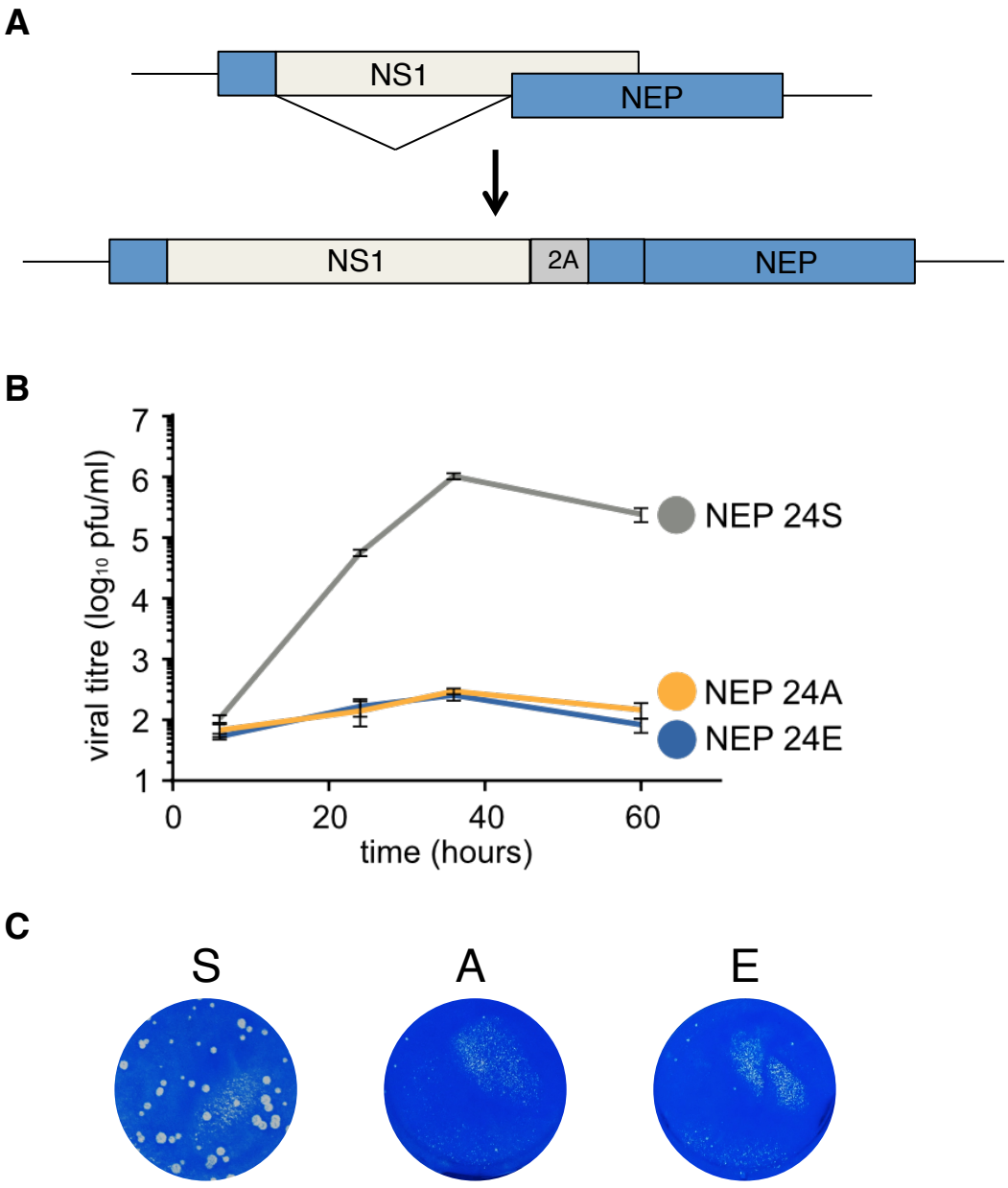

Figure 4.1. Effect of NEP phosphorylation on viral growth. (A) To introduce mutations into NEP for the generation of mutant viruses, a segment 8 reverse genetic construct that separated the NS1 and NEP ORFs was used. This construct contained both NS1 and NEP in the same ORF separated by a picornaviral 2A sequence. Translation of this sequence results in NS1 and NEP protein derived from independent nucleotide sequences without the requirement for splicing. (B) Viruses with mutations mimicking constitutively phosphorylated (24E) or non-phosphorylatable (24A) versions of NEP were generated and their replication in MDBK cells was measured over the course of 60h and quantified by plaque assay. Viral titres represent the mean of three independent repeats with standard errors indicated. (C) Representative plaque assays showing differences in plaque size between NEP mutant and wildtype viruses

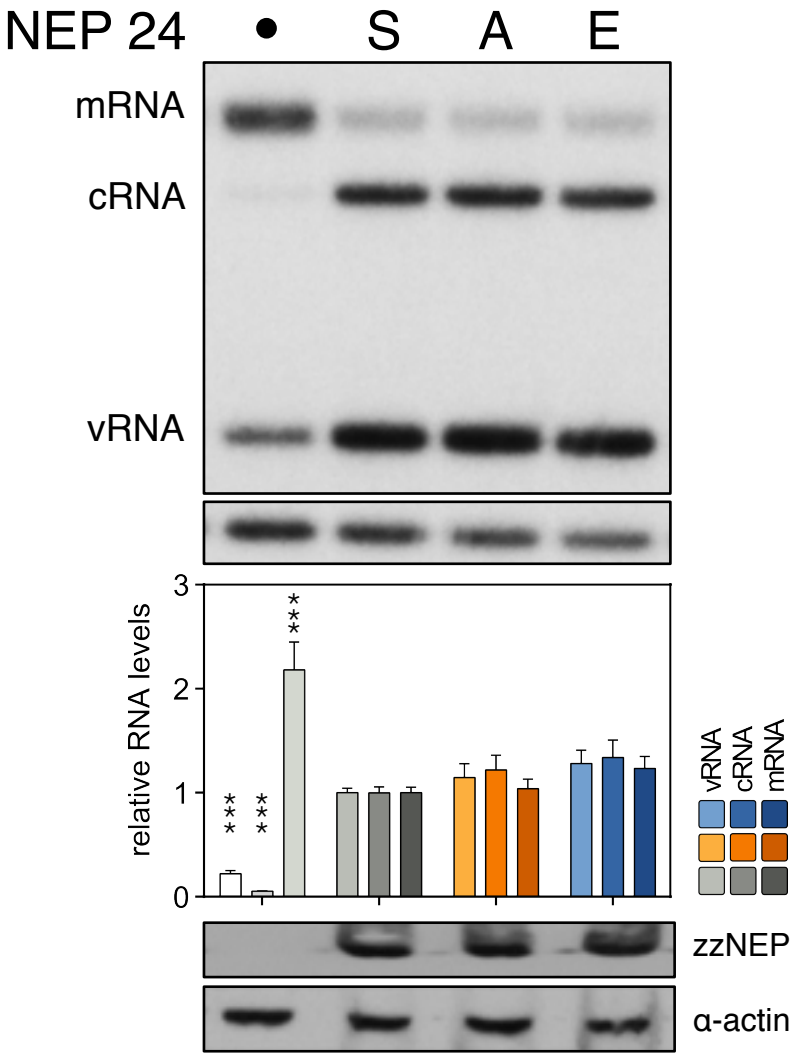

Figure 4.2. Effect of mutations to NEP 24S on replication and transcription of viral RNA. HEK 293T cells were co-transfected with plasmids expressing PA, PB1, PB2, NP and a segment 6 vRNA, as well as wild-type or mutated forms of NEP, or without NEP (●). Accumulation of mRNA, cRNA or vRNA was assessed by primer extension 48 hours post-transfection. RNA levels were compared to those measured with the addition of wild-type NEP and set to 1. Error bars indicate standard error margins of three individual replicates. Asterisks represent significant difference from NEP 24S RNA levels (Students t-test; ***: $p < 0.001$). Expression of NEP mutants was analysed by immunoblotting with alpha-actin serving as a loading control

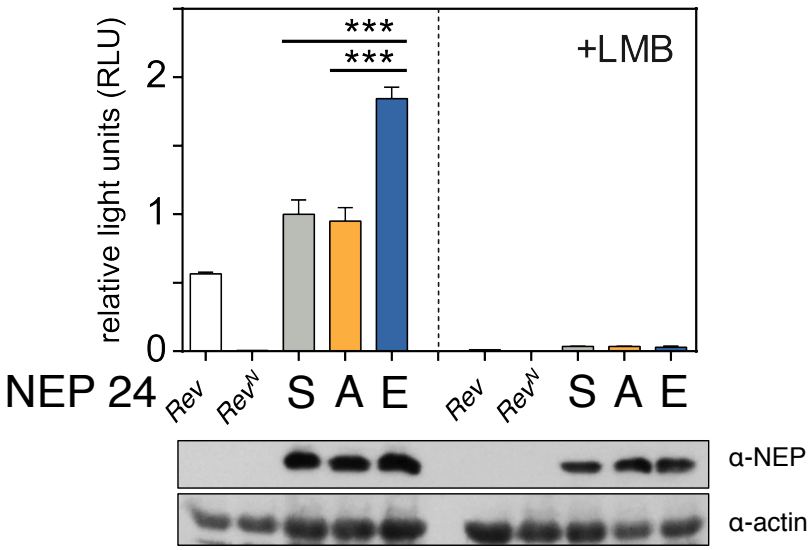

Figure 4.3. Nuclear export activity of influenza A virus NEP mutants was assayed using an HIV–1 Rev-based luciferase assay. Rev-NEP fusion proteins and a Rev-response element (RRE) containing mRNA encoding luciferase were transiently expressed in HEK 293T cells for 24h with or without the addition of the Crm1 inhibitor leptomycin B (LMB). Wildtype Rev was used as a positive control and the N-terminal domain of Rev that contains the RRE but no NES (Rev^N) was used as a negative control. Luminescence values represent the mean of 3 independent experimental repeats with standard error indicated. Asterisks indicate a significant difference from wildtype NEP (one sample t test; *P<0.05, **P<0.01, ***P<0.001). Expression of the NEP nuclear export constructs was analysed by immunoblotting, with actin as a loading control.

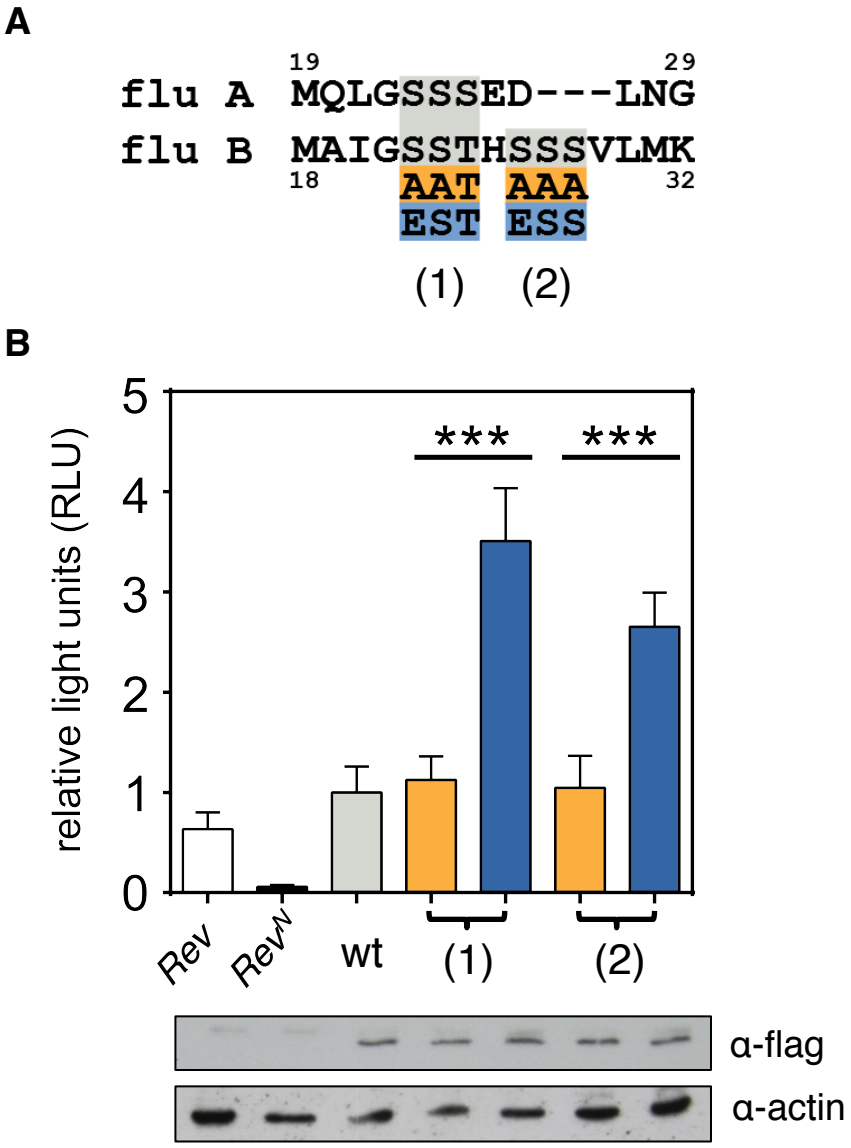

Figure 4.4. Nuclear export activity of influenza B virus NEP mutants. (A) Influenza A and B virus NEP sequences from A/WSN/33 and B/Beijing/1/87 were aligned using Clustal. Mutations introduced to test the conservation of nuclear export regulation are indicated. (B) Rev-flag-NEP fusion proteins containing the mutations shown in (A) were transiently expressed, along with a Rev-response element (RRE) containing mRNA encoding luciferase, in HEK 293T cells for 24h. Rev was used as a positive control and the N-terminal domain of Rev that contains the RRE but no NES (Rev^N) was used as a negative control. Luminescence values represent the mean of 3 independent experimental repeats with standard error indicated. Asterisks indicate a significant difference from wildtype (one sample t test; ***P<0.001). Expression of the influenza B virus NEP nuclear export constructs was analysed by immunoblotting, with actin as a loading control.

residue into the influenza B NEP serine-rich motif similarly caused an increase in its nuclear export, two different serine positions were mutated to glutamic acid and subjected to the same nuclear export assay as described for influenza A NEP. Intriguingly, the introduction of a phosphomimetic mutation at either position increased nuclear export of influenza B NEP (Fig 4.4B). This finding suggests that regulation of NEP nuclear export by phosphorylation is conserved in both influenza A and B viruses, further suggesting that this mechanism may represent a fundamental part of influenza virus biology.

4.3 Discussion

Although a large number of phosphorylation sites have now been catalogued for influenza viruses (Hutchinson et al. 2012), comparatively few of these modifications have been ascribed a function during viral infection. To this end, the role of NEP 24S phosphorylation in viral replication was investigated. As a coarse test of the importance of NEP 24S phosphorylation during viral infection, influenza A viruses with NEP 24 mutations that either mimic phosphorylation or are non-phosphorylatable were generated using a specifically adapted segment 8 construct. Introduction of either glutamic acid or alanine at NEP 24, representing constitutively phosphorylated and non-phosphorylated NEP variants, severely attenuated viral replication. Accordingly, this result suggests that both phosphorylated and non-phosphorylated forms of NEP are required during viral infection. This is unsurprising given that NEP is known to play multiple roles during infection and therefore the potential exists that one or more of these roles

is performed by a modified form of NEP. To test this possibility the effect of NEP 24S mutations was tested with regard to stimulation of viral RNA replication and nuclear export. Whilst mutations to NEP 24 did not affect the accumulation of viral RNA products in vRNP reconstitution assays, a mutation mimicking NEP 24S phosphorylation increased nuclear export of NEP. Indeed, it may appear counter intuitive that an increase in NEP nuclear export may not affect the stimulation of viral RNA replication, particularly as this activity has been demonstrated to be dependent on NEP expression levels (Mänz et al. 2012; Reuther et al. 2014). However, it is likely that in these assays the amount of NEP expressed was more than adequate to overcome the reduction in intranuclear NEP concentration due to increased nuclear export.

A role for phosphorylation in the regulation of NEP nuclear export is perhaps not surprising, given the location of the phosphorylation site between two NESs. In addition, the proteomic screen that identified phosphorylation of NEP 24S was conducted on purified virions, suggesting that any NEP present after purification would already have been successfully exported from the nucleus (Hutchinson et al. 2012). In this regard, the nuclear export of several cellular proteins has been demonstrated to be regulated by a phosphorylation site proximal to an NES (Engel et al. 1998; Alt et al. 2000; Sasaki et al. 2006). However, these studies show that regulation of nuclear export by phosphorylation does not appear to share a specific mechanism, suggesting that this process has evolved independently on several occasions. Nevertheless, influenza B virus NEP does appear to utilise the

same mechanism for vRNP nuclear export as influenza A virus, a finding which is consistent with vRNP export representing a conserved mechanism that evolved before these genera diverged. Interestingly, influenza C virus NEP shares very little sequence homology with influenza A and B virus NEPs, likely indicating that it mediates vRNP nuclear export by a distinct mechanism (Paragas et al. 2001).

Whatever the method, vRNP nuclear export is likely to be stringently controlled during viral infection. Uncontrolled nuclear export of vRNPs has the potential to severely disrupt influenza virus infection by depleting the templates necessary for viral RNA replication and transcription. Likewise, early export of vRNPs may expose the virus to recognition by the innate immune system, specifically RIG-I which is known to be stimulated by vRNA (Rehwinkel et al. 2010). To counter this, the virus has been demonstrated to use suboptimal splicing of the NS segment to coordinate NEP expression with vRNP accumulation and subsequent export (Chua et al. 2013). Our results suggest that influenza viruses may further fine-tune vRNP nuclear export by making use of phosphorylation. Indeed, phosphorylation has long been implicated in the control of this process. The mitogen activated protein kinase (MAPK) signalling cascade has been implicated in vRNP nuclear export, with MAPK inhibition leading to the nuclear accumulation of vRNPs (Pleschka et al. 2001). It has further been demonstrated that MAPK signalling requires activation by protein kinase Cα (PKCα), which is activated by the accumulation of viral glycoproteins on the cell surface (Marjuki et al. 2006), suggesting an elegant mechanism by which vRNPs are only exported

from the nucleus once the other virion components are present to encapsidate them into mature virions.

Nuclear export of vRNPs represents an important waypoint during influenza virus infection. Accordingly, it should be expected that this process would be regulated to some degree. To this end, phosphorylation of NEP 24S represents an interesting method whereby the virus can control the multiple functions of NEP during infection, ultimately leading to the coordinated nuclear export of vRNPs for packaging into the next generation of virions.

5. NEP structural and biophysical studies

5.1 Introduction

The NEP protein of influenza A viruses was traditionally thought to play a minor role during influenza virus infection. More recently however, NEP has been ascribed multiple functions during the viral replication cycle. Not only does NEP mediate the nuclear export of vRNPs for packaging into nascent virions, but it is also proposed to orchestrate the transition from viral RNA transcription to replication. In addition, NEP has been demonstrated to recruit an ATPase that is essential for efficient virus budding (Gorai et al. 2012), as well as interact with several other cellular proteins the functions of which are currently unclear (Eisfeld et al. 2011; Chen et al. 2010; de Chassey et al. 2013). Even with these diverse functions ascribed to it, very little is known about the structure of NEP and how this relates to functional regulation.

What is known about the structure of NEP is that the C-terminal half of the protein forms a highly structured α-helical hairpin that has been elucidated by crystallography (Akarsu et al. 2003). This region of NEP is proposed to be responsible for binding to M1 during vRNP nuclear export, by way of interaction with the residue NEP 78W (Akarsu et al. 2003). Very little is known about the structure of the NEP N-terminal domain. It has been proposed that the N-terminal domain of NEP is highly unstructured (Lommer & Luo 2002), an observation reinforced by experiments demonstrating that this region of the protein is highly sensitive to digestion by proteases (Akarsu et al. 2003). Furthermore, the entire NEP molecule has been described as a "near molten globule" on account of structural disorder associated with the N-terminus (Lommer & Luo 2002). The N-terminal domain of NEP is known to harbour two NESs (Huang et al. 2013; O'Neill et al. 1998) that bind to the cellular nuclear export protein Crm1 to mediate the nuclear export of vRNPs. Cellular NESs generally occur in diverse protein contexts but the signals themselves are usually present on solvent exposed α-helices (Güttler et al. 2010). As such, it is expected that the NESs of NEP also reside on α-helical regions on the N-terminal domain. Between the two NESs is a serine-rich motif that has been demonstrated to be phosphorylated during influenza virus infection (Hutchinson et al. 2012). Introduction of mutations mimicking phosphorylation of this region results in increased nuclear export activity of NEP (Chapter 4).

The N-terminal domain of NEP is also proposed to play a role in the regulation of viral RNA replication. In this regard, the C-terminal domain of NEP has been shown to interact with the viral polymerase, however, the predicted N-terminal α-helices appear to modulate NEP regulation of RNA synthesis. This modulation is proposed to stem from dynamic interaction between the N- and C-terminal domains of NEP by a mechanism that has yet to be determined (Reuther et al. 2014).

Cumulatively, little is known about the structure of NEP, especially with regard to its N-terminal domain. To gain a better understanding of how it fulfils its functions during viral infection, NEP was studied by nuclear magnetic resonance (NMR) and other biophysical methods.

5.2 Results

5.2.1 Expression, purification and characterisation of NEP

Analysis of proteins by NMR has traditionally required millimolar concentrations of highly pure protein. Although the advent of non-uniform sampling strategies has allowed NMR analysis of samples of lower concentrations, the requirement for high protein concentration still represents a limiting factor for NMR analysis. To this end, multiple attempts were made to express large quantities of soluble NEP in *E. coli*. However, despite strong expression, NEP was predominantly found in the insoluble fraction of cell lysates. Accordingly, a purification strategy based on refolding NEP from insoluble inclusion bodies was developed. Insoluble

material was isolated after homogenisation of the *E. coli* cell pellet and solubilised by resuspension in a solution that contained 6M guanidine hydrochloride. Once solubilised, NEP was bound to a nickel sepharose column and refolded by slowly decreasing the concentration of denaturant running through the column. This method produced milligram quantities of a single high purity protein species that corresponded to the molecular weight expected for NEP (Fig 5.1A). Soluble NEP is known to exist as a monomer (Akarsu et al. 2003; Lommer & Luo 2002). To determine if the refolding protocol produced a monomeric form of NEP, the refolded product was analysed by gel-filtration chromatography on a Superdex 75 column. The resultant elution profile confirmed that NEP produced by the on-column refolding protocol was a single protein species corresponding to the expected molecular weight of an NEP monomer (Fig 5.1B).

NEP is predicted to have a secondary structure composed of four α-helices (Fig 5.2), with the existence of two C-terminal α-helices having been confirmed by crystallography (Akarsu et al. 2003). However, even if the refolding strategy produced a monomeric form of NEP, the possibility still exists that eluted protein remained in an unfolded form. To ascertain whether the refolded NEP protein was indeed composed predominantly of α-helices, the peak fractions from gel filtration were concentrated and analysed by circular dichroism (CD) spectroscopy. The resultant spectra were consistent with a predominantly α-helical protein, indicating that NEP purified in this manner had discernible secondary structure (Fig. 5.1C). To further determine its suitability for NMR

spectroscopic analysis, NEP was expressed in media containing $^{15}NH_4Cl$, purified and subjected to ^{1}H, ^{15}N homonuclear single quantum coherence (HSQC) spectroscopy (Fig 5.3B). The resultant HSQC spectra of NEP displayed well distributed peaks consistent with a predominantly α-helical protein.

5.2.2 NEP backbone assignment

For sequential assignment of NEP by NMR, ^{1}H, ^{15}N, ^{13}C-labelled protein samples were produced using the on-column refolding method. Triple resonance experiments including HNCA, HN(CO)CA, HNCACB, CBCA(CO)NH, HNCO and HN(CA)CO were acquired on a 600Mhz spectrometer equipped with a cryo-probe. Sequential amino acid residues were initially assigned by establishing the connectivity of α-carbon (CA) resonances for *i* and *i–1* residues using HNCA and HN(CO)CA spectra. These connections were then validated using resonance information from the carbonyl (CO) and beta (CB) carbon experiments. In addition to triple resonance experiments, the connectivity of NEP backbone resonances was confirmed using sequential NOEs in ^{15}N NOESY-HSQC spectra. Unique CA and CB resonances characteristic of certain residue types (e.g. alanine, glycine, serine and threonine) were subsequently used to map the connected resonances onto the amino acid sequence. This strategy led to the unambiguous assignment of 115 of the 121 amino acids in NEP (Fig 5.3A, B). Residues that could not be unambiguously assigned predominantly clustered to regions that had previously been predicted to form loops between α-helices in the crystal structure of the C-terminal domain of NEP (Fig 5.3C). The inability to assign some

of these residues is likely to result from spectral overlap of unstructured residues in looped regions as well as spectral broadening due to conformational exchange. Intriguingly, several NEP residues exhibited peak doubling, specifically in a region predicted to form a loop in the central region of the protein (Fig 5.3B, 5.3A). Peak doubling for these residues is consistent with multiple conformations present in this region, potentially suggesting that this loop undergoes slow conformational exchange.

5.2.3 Chemical shift-based prediction of NEP secondary structure

Although NEP has been predicted *in silico* to form four α-helices (Fig 5.2), only the existence of two C-terminal α-helices have been confirmed (Akarsu et al. 2003). A more robust method of predicting secondary structure involves the calculation of the *phi* and *psi* dihedral angles from chemical shifts of atoms assigned to specific protein residues. Accordingly, TALOS-N was used to predict the α-helical propensity for residues in NEP (Fig 5.4A), using chemical shifts for CA, CB, CO and NH resonances from ^{1}H, ^{15}N HSQC and triple resonance experiments, as well as HA chemical shifts obtained from a 3D ^{15}N TOCSY experiment. TALOS-N prediction of NEP secondary structure indicated that NEP is indeed composed of four major α-helices. The first helix is preceded by a short disordered N-terminal region that gives way to an α-helix containing the first NES. Between α1 and α2 is a short loop that contains the highly conserved serine-rich motif which has been demonstrated to be phosphorylated during infection (Hutchinson et al. 2012).

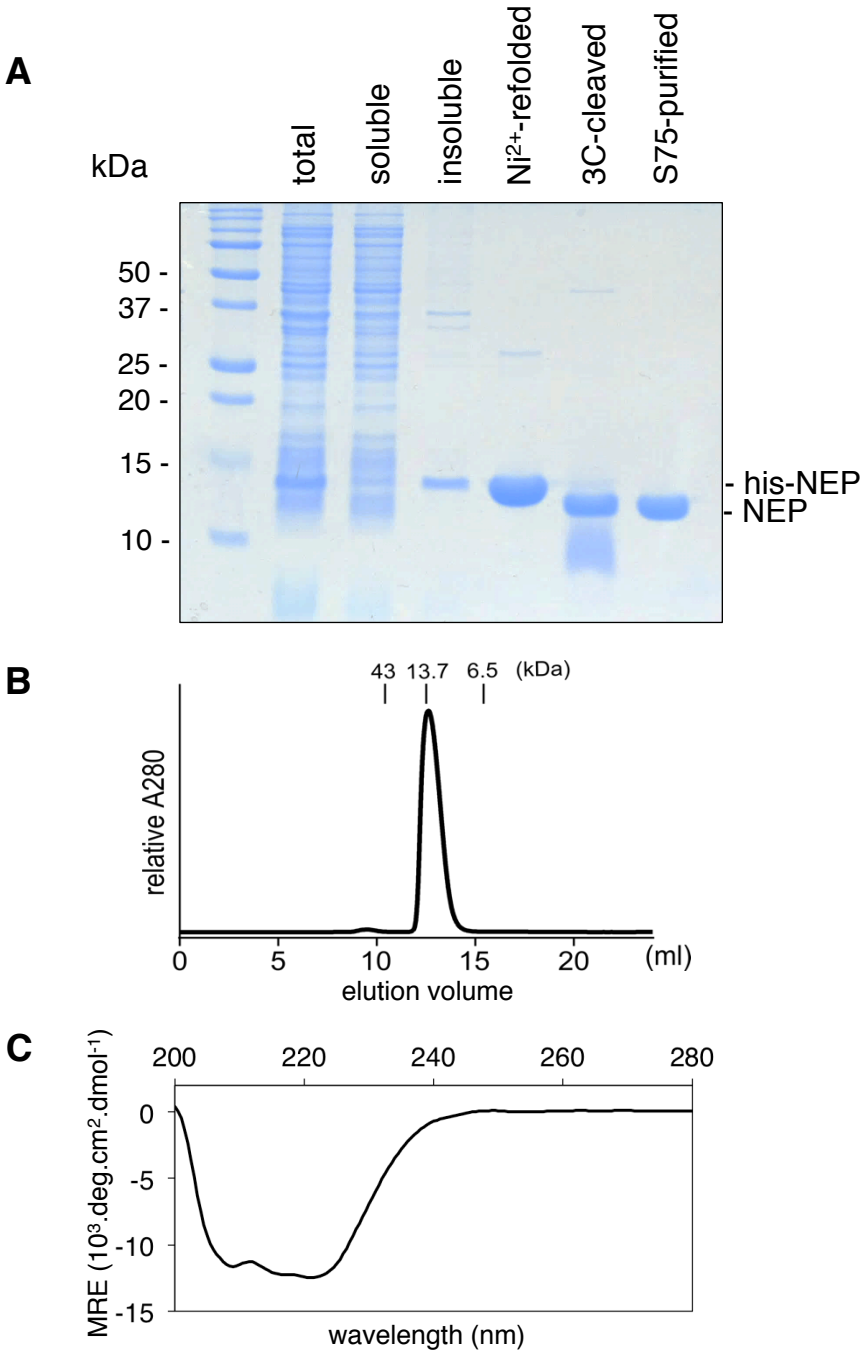

Figure 5.1. Expression, purification and characterisation of NEP. (A) NEP was expressed in *E.coli* BL21(DE3) as a polyHistidine-tagged construct that formed insoluble inclusion bodies within cells. The insoluble fraction of cell lysate was solubilised in guanidine-HCl and refolded in a gradient of urea whilst bound to a Ni-NTA column. The polyHistidine-tag was removed from eluted protein by cleavage with 3C protease and the resultant product purified on a Superdex 75 column. (B) Superdex 75 elution profile of bacterially expressed NEP. Elution profile of molecular weight markers is indicated above plot. (C) CD spectrum of purified NEP expressed as Mean Residue Ellipticity (MRE)

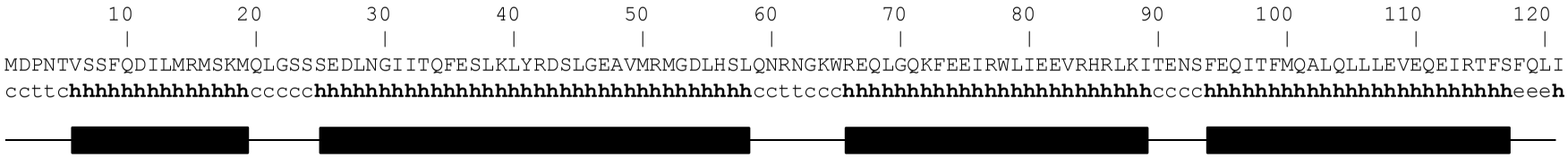

Figure 5.2. Predicted secondary structure of NEP. The sequence of A/WSN/1933 NEP with the predicted secondary structure beneath each residue. Secondary structure was predicted using the APSSP webserver, which forms part of the ExPASy tools database. h: α-helix, c: coil, t: turn, e: extended. A schematic diagram showing NEP secondary structure prediction is below with each black box representing an α-helix.

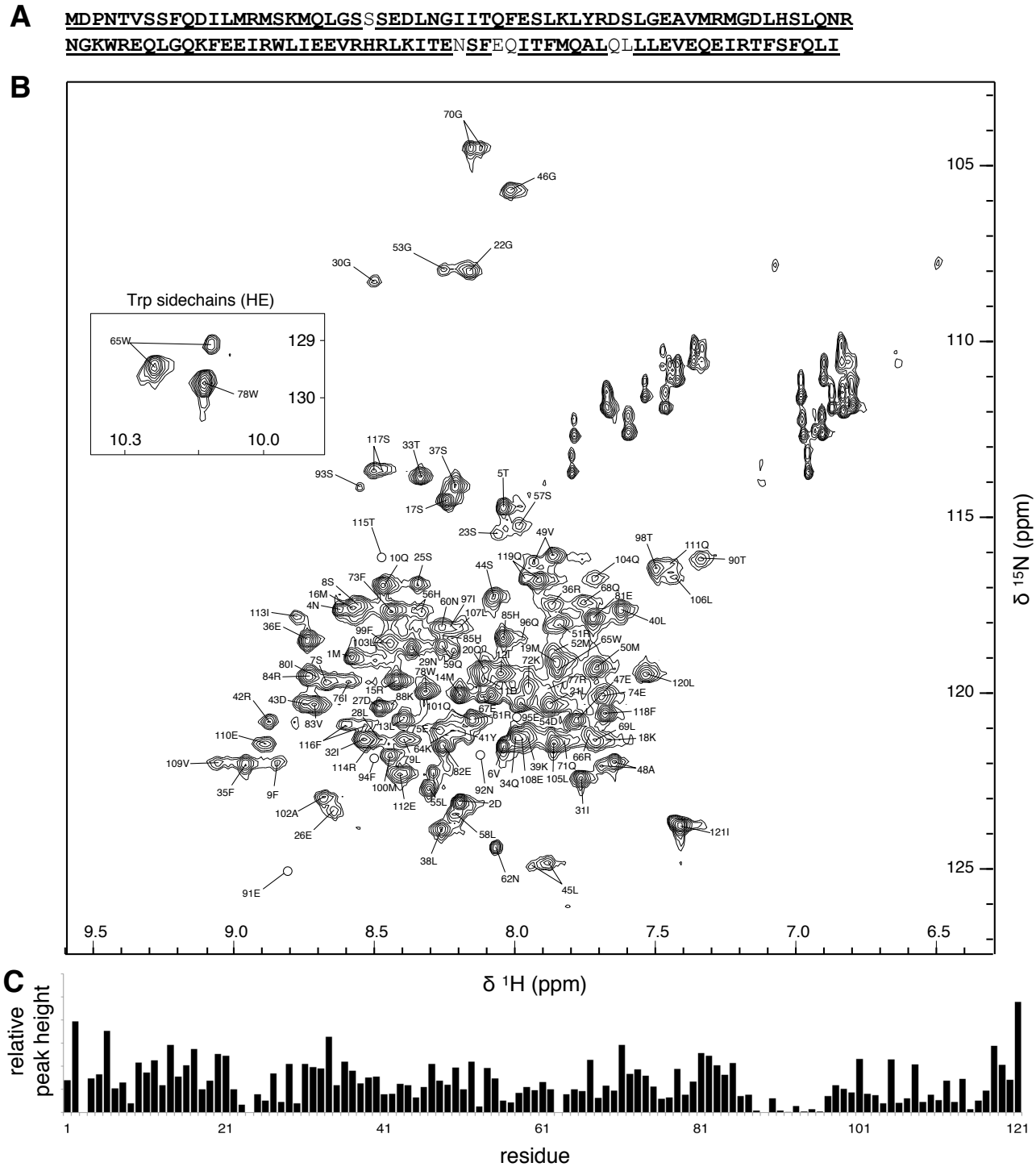

Figure 5.3. Assignment of NEP backbone resonances. (A) NEP residues successfully assigned to backbone resonances on the ^{1}H, ^{15}N HSQC spectrum are bold and underlined. (B) Fully assigned ^{1}H, ^{15}N HSQC spectrum of NEP. Resonances for some residues show doubling and are indicated as such e.g. 70G, 48A and 65W(HE) among others. (C) NEP ^{1}H, ^{15}N HSQC spectral height plotted as a function of residue number identifies protein regions of low peak signal intensity.

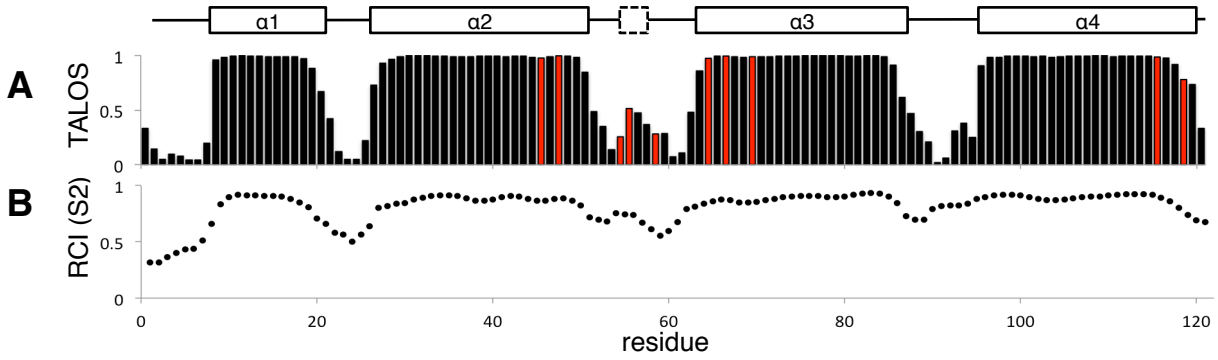

Figure 5.4. NEP secondary structure and molecular model. (A) Secondary structure and (B) random coil index (RCI) calculated from NEP CA, CB, CO, NH and HA chemical shifts. A schematic diagram above indicates the four α-helical regions predicted for NEP (α1–4), as well as a low confidence fifth α-helix between α2 and α3. Residues corresponding to peaks that show spectral doubling are denoted in red.

The second α-helix contains the second NES and is linked to α3 by an interesting loop that appears to harbour a single α-helical turn within it. Helices α3 and α4 appear to form secondary structure consistent with that seen in the previously published crystal structure of this region (Akarsu et al. 2003). The random coil index (RCI) parameter, which is an approximate measure of protein order, appears to correlate strongly with helical propensity, suggesting that less ordered regions of NEP reside in the looped regions between α-helices (Fig 5.4B).

5.3 Discussion

NEP has been ascribed several functions during influenza virus infection, however little structural data is available to elucidate the mechanics of NEP function. Accordingly, bacterially expressed NEP was studied using biophysical approaches to better understand its structural composition. Before these experiments could be carried out, a protocol for the production of large quantities of NEP had to be developed. To this end, NEP was expressed in bacterial cells as inclusion bodies and the protein refolded whilst attached to the chromatagraphic substrate. This technique produced large amounts of NEP that existed as a monomer in solution, consistent with previous studies (Akarsu et al. 2003; Lommer & Luo 2002). In addition to being monomeric, NEP was found to be largely α-helical, as has been described previously (Akarsu et al. 2003; Lommer & Luo 2002). Indeed, *in silico* prediction of NEP secondary structure suggests that the protein is composed of four α-helices, two of which make up the N-terminal domain that harbours the two NESs required for vRNP export (Huang et al. 2013;

O'Neill et al. 1998). This analysis was at odds with other reports that the N-terminal domain is largely unstructured (Akarsu et al. 2003; Lommer & Luo 2002). To address this disparity, NEP was analysed by NMR spectroscopy.

An initial ^{1}H, ^{15}N HSQC experiment suggested that NEP was folded, producing spectra largely consistent with those expected for an α-helical protein. The backbone resonances of NEP were subsequently assigned to specific NEP residues. Several residues that could not be assigned to backbone resonances clustered specifically to the region of NEP that has previously been demonstrated to fall on a loop between the two α-helices of the crystallised C-terminal domain (Fig 5.3C) (Akarsu et al. 2003). Consequently, it is likely that spectral broadening of peaks associated with these residues results from conformational exchange in this region. Indeed, the NEP C-terminal domain crystal structure was solved as a dimer of two NEP C-terminal domain fragments that interacted in a manner that appears to stabilise this interhelical loop (Akarsu et al. 2003).

Using the assigned backbone resonances, the secondary structure of NEP was predicted using TALOS-N. The resultant secondary structure prediction was similar to that predicted *in silico*, with the N-terminal domain being composed of two α-helices, each of which contained an NES. A phosphomimetic mutation at the serine-rich motif on a loop between the two NES-containing α-helices has been demonstrated to play a role in NEP nuclear export (Chapter 4). This suggests that modification of this loop by phosphorylation could affect the two α-helices adjacent to it in a manner that increases their accessibility by the cellular nuclear

export protein Crm1. This method of regulating nuclear export would not be entirely novel. In this respect, FRET-based assays have previously implicated phosphorylation in a structural rearrangement that unmasks the NES of the MAPK-signalling target MK2, allowing recognition by Crm1 (Neininger et al. 2001).

The looped region between α2 and α3 is predicted by TALOS-N analysis to contain a single α-helical turn, albeit with low confidence. Intriguingly, resonances assigned to residues in this region of NEP show considerable doubling (Fig 5.2B). Accordingly, it is possible that this loop may be undergoing slow conformational exchange that is resolvable by HSQC-based experiments. This region of NEP has previously been proposed to be somewhat flexible and govern the association between N- and C-terminal domains in a manner that affects the role of NEP during viral RNA synthesis (Reuther et al. 2014). In addition, it has been demonstrated that this region of NEP is highly sensitive to proteolytic cleavage (Akarsu et al. 2003), suggesting that the loop is sufficiently large and unstructured to allow a protease access. The C-terminal domain of NEP displays secondary structure consistent with that determined by previous structural studies (Akarsu et al. 2003).

Structural information on NEP has the potential to deliver insights into the mechanism by which NEP fulfils it diverse roles during viral infection. Here, we demonstrate the first experimental evidence that the functionally important N-terminal domain of NEP is composed of two NES-containing α-helices that are

joined by a loop containing a phosphorylation site. In addition, the loop between α2 and α3 appears to show conformational heterogeneity, consistent with previous suggestions that this loop acts as a hinge between the N- and C-terminal domains. Finally, these initial NMR analyses provide a platform with which to investigate various aspects of NEP biology.

6. A Phosphomimetic mutation alters NEP conformational dynamics leading to increased nuclear export

6.1 Introduction

In contrast to most negative strand viruses, influenza viruses replicate and transcribe their genomes within the nucleus of infected cells. This allows viral RNA synthesis to proceed in an environment flush with raw materials and unhindered by cellular innate immune sensors. However, once synthesised, the progeny vRNPs must be transported across the nuclear membrane to be packaged into new viral particles at the cellular periphery. NEP is responsible for mediating this process by way of N-terminal interactions with the cellular nuclear export protein Crm1 (Huang et al. 2013; O'Neill et al. 1998) and C-terminal interactions with the viral M1 protein (Akarsu et al. 2003) that is in turn bound to vRNPs. Accordingly, NEP could be said to form the interpretable interface through which influenza viruses interact with cellular machinery to export newly synthesised vRNPs from the host cell nucleus.

NEP is a small, 121 amino acid, protein that is translated from the spliced transcription product of the shortest viral genome segment. Commensurate with its function, the N-terminus of NEP is known to contain two NESs which mimic the sequences found on cellular Crm1 cargo proteins (O'Neill et al. 1998; Huang et al. 2013; Güttler et al. 2010). A highly conserved serine-rich motif resides between these two NESs (Hutchinson et al. 2012), the phosphorylation of which has been demonstrated to increase NEP nuclear export (Chapter 4). In addition to its nuclear export function, NEP stimulates viral RNA replication via a C-terminal interaction with the viral polymerase (Robb et al. 2009; Mänz et al. 2012); a process implicated in the adaptation of avian influenza viruses to replicate in human hosts (Mänz et al. 2012).

Although many viral and cellular proteins have been proposed to play a role in vRNP nuclear export, very little is known about the mechanisms underlying this process. Nevertheless, the nuclear export of vRNPs — which are both the templates for, and the products of viral RNA replication — is likely to be tightly controlled. In this respect, phosphorylation has long been known to play an important but undefined role in vRNP nuclear export (Whittaker et al. 1995; Whittaker et al. 1996; Pleschka et al. 2001). Accordingly, it is conceivable that phosphorylation of NEP, which has been suggested to increase nuclear export (Chapter 4), represents a method by which the virus can exert temporal control over vRNP nuclear export. However, this still begs the fundamental question of how phosphorylation actually acts to increase NEP nuclear export. Accordingly,

NMR spectroscopy and other biophysical methods were used to study the effect of a phosphomimetic mutation on NEP with the goal of establishing the mechanism by which NEP nuclear export is governed.

6.2 Results

6.2.1 A phosphomimetic mutation alters NEP conformation and stability

Previous studies have indicated that the introduction of a mutation at NEP 24S that mimics phosphorylation at that residue resulted in increased nuclear export of NEP (Chapter 4). To study the physical implications of NEP 24S phosphomimetic mutation, NEP 24S and NEP 24E were expressed, refolded and purified as described previously (Chapter 5). Initial experiments to ascertain broad physical differences between NEP 24S and 24E were then conducted on the purified proteins. Firstly, CD spectroscopy was used to determine whether there was a change in secondary structure associated with the phosphomimetic residue NEP 24E. Overlaid CD spectra indicated that although both proteins displayed spectra characteristic of α-helical proteins, introduction of NEP 24E resulted in subtle differences to the CD spectra (Fig 6.1A). In addition to conventional CD spectroscopy, the melting profile of NEP 24S and NEP 24E was measured by CD spectroscopy (Fig 6.1B). Intriguingly, the NEP phosphomimetic mutant maintained its secondary structure at far higher temperatures than observed for NEP 24S (T_m NEP 24S: 52.53°C , T_m NEP 24E: 56.79°C). This likely indicates that

NEP 24E represents a more stable form of the protein, resulting in an increased ability to withstand thermal denaturation.

To ascertain whether the introduction of a mutation that mimics phosphorylation at NEP 24 results in any conformational changes that increase the hydrodynamic radius of the molecule, NEP 24S and 24E were subjected to size exclusion chromatography (Fig 6.1C). NEP 24E eluted earlier than NEP 24S (13.19 ± 0.13 ml and 13.85 ± 0.24 ml respectively), which is indicative of an increased hydrodynamic radius and usually correlates with a larger molecular mass. However, this shift in mobility on a size exclusion column is fairly subtle and is less than would be expected for dimerisation of NEP. Consequently, the larger hydrodynamic radius could be accounted for by NEP 24E existing in less of a tightly packed conformation than NEP 24S.

6.2.2 A phosphomimetic mutation has a localised effect on NEP structure

The results of CD spectroscopy and size-exclusion chromatography experiments indicate that there are certain physical differences between NEP 24S and NEP 24E, however these methods are not capable of defining the specific effect of NEP phosphomimetic mutations on the protein structure. Consequently, utilising the previously assigned NEP ^{1}H, ^{15}N HSQC spectra (Chapter 5), the chemical shift perturbation (CSP) associated with the introduction of an NEP phosphomimetic mutation were determined (Fig 6.2A). To this end, an ^{1}H, ^{15}N HSQC experiment was conducted on NEP 24E followed by confirmation of individual backbone

resonances using an HNCA experiment. The resultant CSPs were relatively small and localised around the site of the phosphomimetic mutation (Fig 6.2B). NEP 25S and 26E showed the largest changes in chemical shift, suggesting that NEP 24E may affect the junction between the α1–2 loop and α2. However, these results clearly demonstrate that the introduction of a phosphomimetic mutation at NEP 24 does not result in drastic changes to the NEP backbone structure.

6.2.3 NEP 24E displays significantly increased protein dynamics

Mutation of NEP 24S to a residue mimicking phosphoserine appeared to result in only localised changes to the NEP backbone, in contrast to the relatively large changes observed between NEP variants in preliminary biophysical experiments. These observations lead to the hypothesis that the differences between NEP 24S and 24E may be due to changes in the backbone dynamics upon the addition of a negatively charged residue at NEP 24. Accordingly, both NEP variants were subjected to ^{15}N T_1 and T_2 relaxation experiments capable of measuring protein dynamics on a pico-nanosecond timescale.

Results of T_1 relaxation experiments showed large differences between NEP 24S and NEP 24E (Fig 6.3A). Specifically, NEP 24E showed a dramatically increased rate of T_1 relaxation ($1/R_1$) that is usually indicative of decreased motional anisotropy. A reduction in motional anisotropy stems from an increase in the rotational correlation time (τc), indicating that NEP 24E has the characteristics of

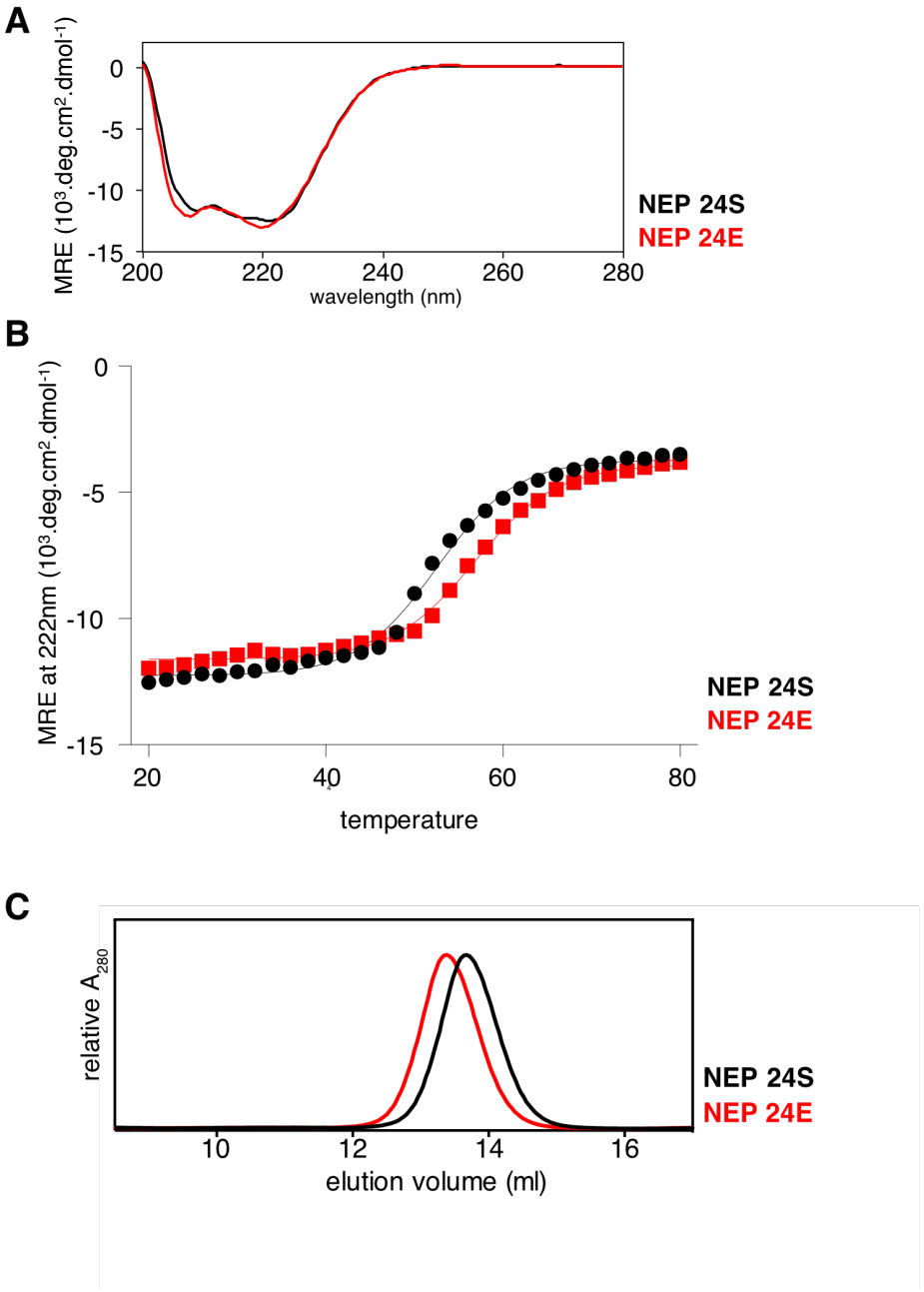

Figure 6.1. Biophysical implications of the NEP 24E phosphomimetic mutation. (A) The overall sencondary structure characteristics of NEP 24S and NEP 24E were analysed by CD spectroscopy. (B) Thermal stability of the NEP variants was measured by multiple CD spectroscopy experiments, each at successively higher temperatures. Melting curves were plotted from Mean Residue Ellipticity (MRE) values at 222 nm and fitted to a Boltzmann sigmoid curve. (C) Relative migration of NEP 24S and NEP 24E was analysed by size exclusion chromatography on a Superdex 75 column. Elution volume is indirectly proportional to molecular weight. This figure is a representative example of 5 independent experiments.

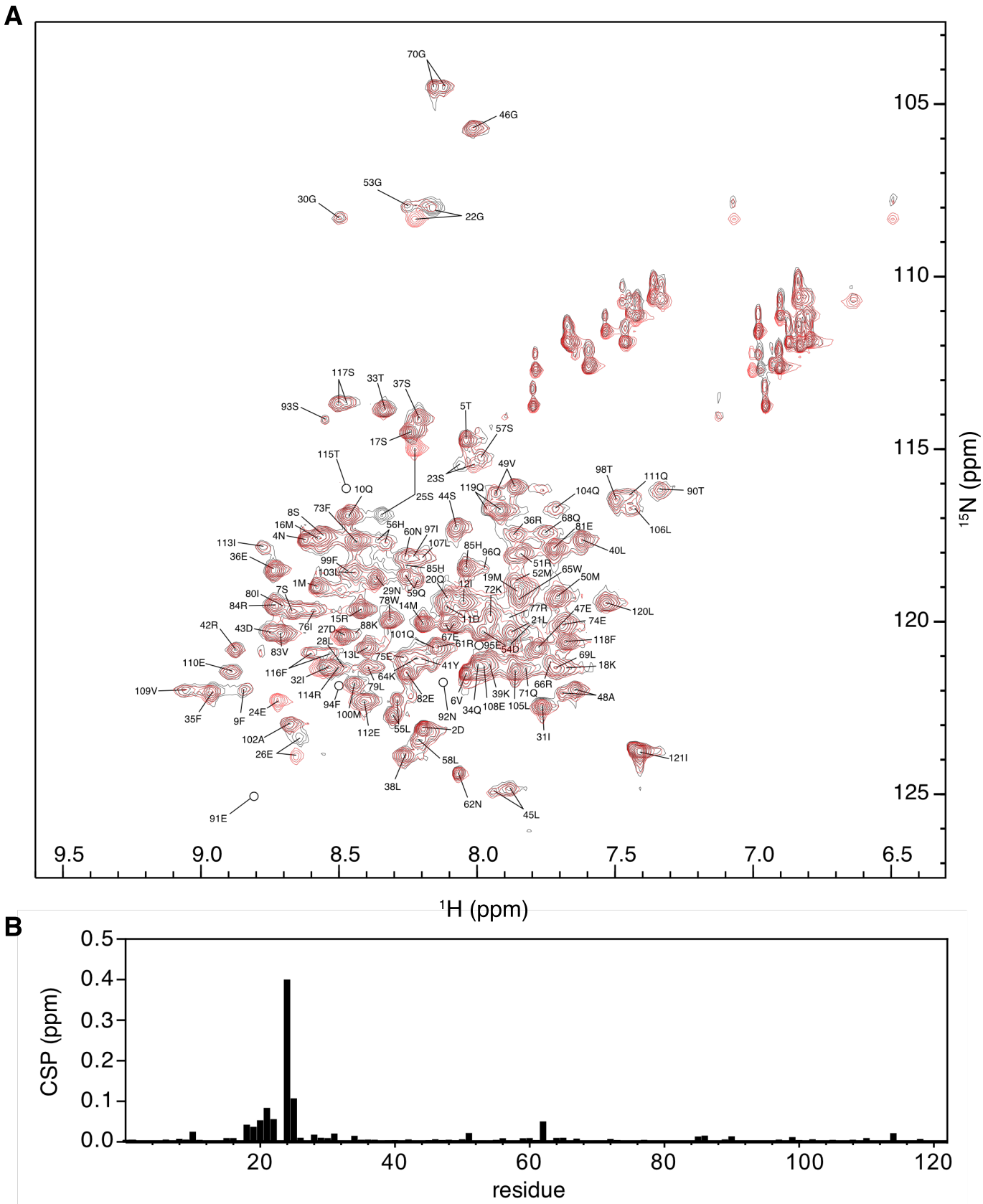

Figure 6.2. Introduction of NEP 24E has a limited effect on NEP backbone structure. (A) 1H, 15N HSQC spectra corresponding to NEP 24S (black) and NEP 24E (red) were collected at 30C and overlayed. (B) Graphical representation of the scale of chemical shift perturbations (CSPs) that result from the NEP 24E mutation.

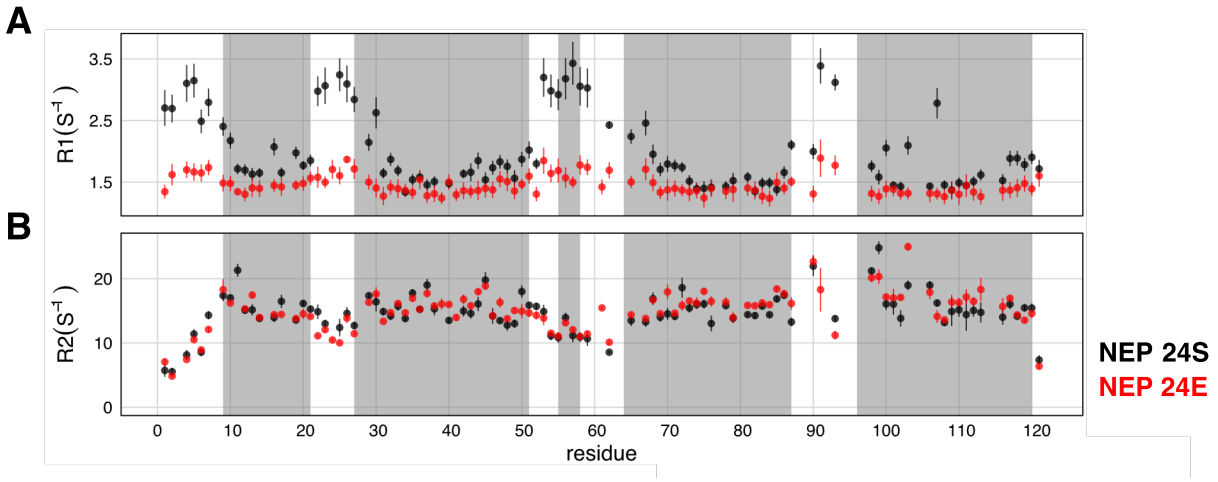

Figure 6.3. Introduction of the NEP 24E phosphomimetic mutation alters NEP backbone dynamics. (A) 15N longitudinal (R1) and (B) transverse (R2) relaxation rates of NEP 24S and NEP 24E collected at 600 MHz are plotted as a function of residue number. The positions of secondary structure elements are indicated in grey. Error bars are representative of duplicate experiments. Values for some residues were excluded from analysis due to extreme peak-broadening or spectral overlap.

a molecule with a larger hydrodynamic radius than NEP 24S. Indeed, τc for NEP 24S and NEP 24E were calculated from the 30% trimmed mean of T_1 and T_2 values to be 9.12 ns and 9.99 ns respectively. The rates of T_2 relaxation ($1/R_2$) appeared to be fairly similar for both NEP variants across the length of the molecule (Fig 6.3B), with decreased R_2 values for residues on looped regions. This result suggests that intramolecular motions responsible for the changes observed in NEP 24E were unlikely to occur on a pico-nanosecond timescale.

6.3 Discussion

Several mechanisms have been proposed for the regulation of influenza virus vRNP nuclear export. One of these relies on post-translational modification of NEP, which in turn may lead to increased nuclear export (Chapter 4). Accordingly, the mechanism of increased nuclear export was investigated using NMR and other biophysical techniques. The previous observation that introduction of a negatively charged residue onto the α1–2 loop increases NEP nuclear export suggests that phosphorylation of this serine-rich sequence may shift NEP toward a conformational state that leads to better accessibility of the NESs on α-helices flanking this region. Increased accessibility of the NESs could in turn enhance their recognition by Crm1, thereby increasing nuclear export. To test this possibility NMR-based experiments were conducted on bacterially expressed NEP 24S and NEP 24E to determine whether introduction of a negatively charged residue at position 24 altered the relaxation dynamics of NEP. NEP 24E displayed markedly increased ^{15}N T_1 relaxation rates, indicating an increase in τc. An

increase in τc due to larger anisotropy of NEP 24E suggests that the phosphomimetic mutant preferentially inhabits a more open conformation, thereby increasing its hydrodynamic radius. This finding was confirmed by size exclusion chromatography experiments that indicated that NEP 24E eluted earlier than NEP 24S (Fig 6.1C), as would be expected for a molecule with a larger hydrodynamic radius.

A more open conformation of NEP could conceivably result from two mechanisms. Firstly, a phosphomimetic mutation could have localised effects within the α1–2 loop, thereby altering its flexibility and any movement of α-helix 1. Alternatively, a phosphomimetic mutation could have an impact on long-range interactions, resulting in global alterations to NEP structure. Consistent with the former prediction, the 24E mutation resulted only in localised chemical shift perturbations. These observations suggest that NEP 24E decreases the flexibility of the α1–2 loop, stabilising the N-terminal helices in a conformation that appears to increase the relative surface area of NEP whilst also increasing thermostability of the protein. Consequently, these results predict that phosphomimetic mutation of NEP 24S would shift the energy landscape of NEP towards the predominance of an conformation that would increase NES accessibility and enhance the efficiency of vRNP nuclear export. However, the specifics of this conformation remain unclear, although it is conceivable that introduction of a negative charge at NEP 24S could orient α-helix 1and 2 in a manner that unmasks the NESs and

contribute to protein stability. Nevertheless, further experiments need to be conducted to confirm this possibility.

Due to influenza virus RNA replication and transcription occurring solely in the nucleus, the nuclear export of vRNPs is likely to be tightly controlled. It is already known that influenza virus uses suboptimal splicing of the NS segment to coordinate NEP expression with vRNP accumulation and subsequent export (Chua et al. 2013). Our data suggests that influenza viruses further fine-tune vRNP nuclear export by making use of phosphorylation. Indeed, cellular phosphorylation cascades have long been implicated in the control of this process. The mitogen activated protein kinase (MAPK) signalling cascade has been implicated in vRNP nuclear export, with MAPK inhibition leading to the nuclear accumulation of vRNPS (Pleschka et al. 2001). It has further been demonstrated that MAPK signalling requires activation by protein kinase Cα (PKCα), which is activated by the accumulation of viral glycoproteins on the cell surface (Marjuki et al. 2006), suggesting an elegant mechanism by which vRNPs are only exported from the nucleus once the other virion components are present to encapsidate them.

Nuclear export by Crm1 relies on recognition of a conserved hydrophobic NES, the identity and conformations of which have been well characterised using short NES-containing peptides (Güttler et al. 2010; Xu et al. 2012). Nevertheless, it is unclear how Crm1 gains access to an NES in the context of a globular protein where the packing of structural features may preclude NES recognition by Crm1.

NEP appears to overcome this problem by using phosphorylation to modulate the plasticity of its N-terminal domain, thereby shifting its conformational ensemble towards a more stable state that can be better recognised by Crm1. As such, our data suggest that Crm1 cargo can undergo conformational selection not only within the NES-binding pocket (Güttler et al. 2010) but also with respect to NES accessibility. NEP is not alone in regulating nuclear export by post translational modification. FRET-based assays have previously implicated phosphorylation in unmasking the NES of the MAPK-signalling target MK2, allowing recognition by Crm1 (Neininger et al. 2001; Engel et al. 1998). Likewise, nuclear export of cyclin D1 is dependent on phosphorylation proximal to a Crm1-dependent NES, although the mechanics of this process are unknown (Alt et al. 2000). In contrast, phosphorylation of a residue within the NES of the c-Fos oncoprotein has been demonstrated to disrupt Crm1 binding and consequent nuclear export (Sasaki et al. 2006).

In conclusion, this work has sought to elucidate the structural implications of NEP phosphorylation and thereby its role in the regulation of influenza virus vRNP export. Accordingly, this represents the first experimental indication of a structural basis for phosphorylation-dependent protein dynamics in Crm1 cargo recognition and subsequent nuclear export.

7. References

Aggarwal, S. et al., 2011. Biochemical impact of the host adaptation-associated PB2 E627K mutation on the temperature-dependent RNA synthesis kinetics of influenza A virus polymerase complex. *The Journal of biological chemistry*, 286(40), pp.34504–34513.

Air, G.M. & Laver, W.G., 1989. The neuraminidase of influenza virus. *Proteins*, 6(4), pp.341–356.

Akarsu, H. et al., 2003. Crystal structure of the M1 protein-binding domain of the influenza A virus nuclear export protein (NEP/NS2). *The EMBO journal*, 22(18), pp.4646–4655.

Ali, A. et al., 2000. Influenza virus assembly: effect of influenza virus glycoproteins on the membrane association of M1 protein. *Journal of virology*, 74(18), pp.8709–8719.

Almond, J.W., 1977. A single gene determines the host range of influenza virus. *Nature*, 270(5638), pp.617–618.

Amorim, M.J. et al., 2011. A Rab11- and microtubule-dependent mechanism for cytoplasmic transport of influenza A virus viral RNA. *Journal of virology*, 85(9), pp.4143–4156.

Area, E. et al., 2004. 3D structure of the influenza virus polymerase complex: localization of subunit domains. *Proceedings of the National Academy of Sciences of the United States of America*, 101(1), pp.308–313.

Arranz, R. et al., 2012. The structure of native influenza virion ribonucleoproteins. *Science*, 338(6114), pp.1634–1637.

Askjaer, P. et al., 1998. The specificity of the CRM1-Rev nuclear export signal interaction is mediated by RanGTP. *The Journal of biological chemistry*, 273(50), pp.33414–33422.

Atreya, P.L., Peeples, M.E. & Collins, P.L., 1998. The NS1 protein of human respiratory syncytial virus is a potent inhibitor of minigenome transcription and RNA replication. *Journal of virology*, 72(2), pp.1452–1461.

Ayora-Talavera, G. et al., 2009. Mutations in H5N1 influenza virus hemagglutinin that confer binding to human tracheal airway epithelium. *PloS one*, 4(11), p.e7836.

Azzeh, M., Flick, R. & Hobom, G., 2001. Functional analysis of the influenza A virus cRNA promoter and construction of an ambisense transcription system. *Virology*, 289(2), pp.400–410.

Basler, C.F. et al., 2001. Sequence of the 1918 pandemic influenza virus nonstructural gene (NS) segment and characterization of recombinant viruses bearing the 1918 NS genes. *Proceedings of the National Academy of Sciences of the United States of America*, 98(5), pp.2746–2751.

Bae, S.H. et al., 2001. Structural features of an influenza virus promoter and their implications for viral RNA synthesis. *Proceedings of the National Academy of Sciences of the United States of America*, 98(19), pp.10602–10607.

Baudin, F. et al., 2001. In vitro dissection of the membrane and RNP binding activities of influenza virus M1 protein. *Virology*, 281(1), pp.102–108.

Bean, W.J. et al., 1985. Characterization of virulent and avirulent A/chicken/Pennsylvania/83 influenza A viruses: potential role of defective interfering RNAs in nature. *Journal of virology*, 54(1), pp.151–160.

Beaton, A.R. & Krug, R.M., 1981. Selected host cell capped RNA fragments prime influenza viral RNA transcription in vivo. *Nucleic acids research*, 9(17), pp.4423–4436.

Bergmann, M. & Muster, T., 1995. The relative amount of an influenza A virus segment present in the viral particle is not affected by a reduction in replication of that segment. *The Journal of general virology*, 76 (Pt 12), pp.3211–3215.

Bier, K., York, A. & Fodor, E., 2011. Cellular cap-binding proteins associate with influenza virus mRNAs. *The Journal of general virology*, 92(Pt 7), pp.1627–1634.

Biswas, S.K., Boutz, P.L. & Nayak, D.P., 1998. Influenza virus nucleoprotein interacts with influenza virus polymerase proteins. *Journal of virology*, 72(7), pp.5493–5501.

Biswas, S.K. & Nayak, D.P., 1994. Mutational analysis of the conserved motifs of influenza A virus polymerase basic protein 1. *Journal of virology*, 68(3), pp.1819–1826.

Blaas, D., Patzelt, E. & Kuechler, E., 1982. Identification of the cap binding protein of influenza virus. *Nucleic acids research*, 10(15), pp.4803–4812.

Bogs, J. et al., 2011. Reversion of PB2-627E to -627K during replication of an H5N1 Clade 2.2 virus in mammalian hosts depends on the origin of the nucleoprotein. *Journal of virology*, 85(20), pp.10691–10698.

Bortz, E. et al., 2011. Host- and Strain-Specific Regulation of Influenza Virus Polymerase Activity by Interacting Cellular Proteins. *mBio*, 2(4). Available at: http://mbio.asm.org/content/2/4/e00151-11 [Accessed October 31, 2012].

Boulay, F. et al., 1987. The influenza hemagglutinin precursor as an acid-sensitive probe of the biosynthetic pathway. *The EMBO journal*, 6(9), pp.2643–2650.

Braam, J., Ulmanen, I. & Krug, R.M., 1983. Molecular model of a eucaryotic transcription complex: functions and movements of influenza P proteins during capped RNA-primed transcription. *Cell*, 34(2), pp.609–618.

Brown, D.A. & Rose, J.K., 1992. Sorting of GPI-anchored proteins to glycolipid-enriched membrane subdomains during transport to the apical cell surface. *Cell*, 68(3), pp.533–544.

Brownlee, G.G. & Sharps, J.L., 2002. The RNA Polymerase of Influenza A Virus Is Stabilized by Interaction with Its Viral RNA Promoter. *Journal of virology*, 76(14), pp.7103–7113.

Bruce, E.A., Digard, P. & Stuart, A.D., 2010. The Rab11 pathway is required for influenza A virus budding and filament formation. *Journal of virology*, 84(12), pp.5848–5859.

Bui, M. et al., 2000. Role of the influenza virus M1 protein in nuclear export of viral ribonucleoproteins. *Journal of virology*, 74(4), pp.1781–1786.

Bullido, R. et al., 2001. Influenza A virus NEP (NS2 protein) downregulates RNA synthesis of model template RNAs. *Journal of virology*, 75(10), pp.4912–4917.

Bullough, P.A. et al., 1994. Structure of influenza haemagglutinin at the pH of membrane fusion. *Nature*, 371(6492), pp.37–43.

Bussey, K.A. et al., 2011. PA residues in the 2009 H1N1 pandemic influenza virus enhance avian influenza virus polymerase activity in mammalian cells. *Journal of virology*, 85(14), pp.7020–7028.

Cadd, T. et al., 1996. The Sendai paramyxovirus accessory C proteins inhibit viral genome amplification in a promoter-specific fashion. *Journal of virology*, 70(8), pp.5067–5074.

Cao, S. et al., 2012. A Nuclear Export Signal in the Matrix Protein of Influenza A Virus Is Required for the Efficient Virus Replication. *Journal of virology*, 86(9), pp.4883–4891.

Carrasco, M., Amorim, M.J. & Digard, P., 2004. Lipid raft-dependent targeting of the influenza A virus nucleoprotein to the apical plasma membrane. *Traffic* , 5(12), pp.979–992.

Cauldwell, A.V. et al., 2014. Viral determinants of influenza A virus host range. *The Journal of general virology*, 95(Pt 6), pp.1193–1210.

Cauldwell, A.V., Moncorgé, O. & Barclay, W.S., 2012. Unstable Polymerase-Nucleoprotein Interaction Is Not Responsible for Avian Influenza Virus Polymerase Restriction in Human Cells. *Journal of virology*, 87(2), pp.1278–1284.

Chambers, T.M. & Webster, R.G., 1991. Protection of chickens from lethal influenza virus infection by influenza A/chicken/Pennsylvania/1/83 virus: characterization of the protective effect. *Virology*, 183(1), pp.427–432.

Chase, G.P. et al., 2011. Influenza virus ribonucleoprotein complexes gain preferential access to cellular export machinery through chromatin targeting. *PLoS pathogens*, 7(9), p.e1002187.

De Chassey, B. et al., 2013. The Interactomes of Influenza Virus NS1 and NS2 Proteins Identify New Host Factors and Provide Insights for ADAR1 Playing a Supportive Role in Virus Replication. *PLoS pathogens*, 9(7), p.e1003440.

Chen, B.J. et al., 2007. Influenza virus hemagglutinin and neuraminidase, but not the matrix protein, are required for assembly and budding of plasmid-derived virus-like particles. *Journal of virology*, 81(13), pp.7111–7123.

Chen, B.J. et al., 2008. The influenza virus M2 protein cytoplasmic tail interacts with the M1 protein and influences virus assembly at the site of virus budding. *Journal of virology*, 82(20), pp.10059–10070.

Chen, G.-W. et al., 2006. Genomic Signatures of Human versus Avian Influenza A Viruses. *Emerging infectious diseases*, 12(7), pp.1353–1360.

Cheng, X. et al., 2005. Overexpression of the M2-2 protein of respiratory syncytial virus inhibits viral replication. *Journal of virology*, 79(22), pp.13943–13952.

Chen, J., Huang, S. & Chen, Z., 2010. Human cellular protein nucleoporin hNup98 interacts with influenza A virus NS2/nuclear export protein and overexpression of its GLFG repeat domain can inhibit virus propagation. *The Journal of general virology*, 91(10), pp.2474–2484.

Chen, J., Skehel, J.J. & Wiley, D.C., 1998. A polar octapeptide fused to the N-terminal fusion peptide solubilizes the influenza virus HA2 subunit ectodomain. *Biochemistry*, 37(39), pp.13643–13649.

Chen, W. et al., 2001. A novel influenza A virus mitochondrial protein that induces cell death. *Nature medicine*, 7(12), pp.1306–1312.

Chua, M.A. et al., 2013. Influenza A Virus Utilizes Suboptimal Splicing to Coordinate the Timing of Infection. *Cell reports*, 3(1), pp.23–29.

Cianci, C., Tiley, L. & Krystal, M., 1995. Differential activation of the influenza virus polymerase via template RNA binding. *Journal of virology*, 69(7), pp.3995–3999.

Collins, P.L. et al., 1995. Production of infectious human respiratory syncytial virus from cloned cDNA confirms an essential role for the transcription elongation factor from the 5' proximal open reading frame of the M2 mRNA in gene expression and provides a capability for vaccine. *Proceedings of the National Academy of Sciences of the United States of America*, 92(25), pp.11563–11567.

Coloma, R. et al., 2009. The structure of a biologically active influenza virus ribonucleoprotein complex. *PLoS pathogens*, 5(6), p.e1000491.

Compans, R.W., Content, J. & Duesberg, P.H., 1972. Structure of the ribonucleoprotein of influenza virus. *Journal of virology*, 10(4), pp.795–800.

Connor, R.J. et al., 1994. Receptor specificity in human, avian, and equine H2 and H3 influenza virus isolates. *Virology*, 205(1), pp.17–23.

Couceiro, J.N., Paulson, J.C. & Baum, L.G., 1993. Influenza virus strains selectively recognize sialyloligosaccharides on human respiratory epithelium; the role of the host cell in selection of hemagglutinin receptor specificity. *Virus research*, 29(2), pp.155–165.

Crow, M. et al., 2004. Mutational analysis of the influenza virus cRNA promoter and identification of nucleotides critical for replication. *Journal of virology*, 78(12), pp.6263–6270.

Delaglio, F. et al., 1995. NMRPipe: a multidimensional spectral processing system based on UNIX pipes. *Journal of biomolecular NMR*, 6(3), pp.277–293.

Deng, T., Vreede, F.T. & Brownlee, G.G., 2006. Different de novo initiation strategies are used by influenza virus RNA polymerase on its cRNA and viral RNA promoters during viral RNA replication. *Journal of virology*, 80(5), pp.2337–2348.

Desselberger, U. et al., 1980. The 3'and 5'-terminal sequences of influenza A, B and C virus RNA segments are highly conserved and show partial inverted complementarity. *Gene*, 8(3), pp.315–328.

Dias, A. et al., 2009. The cap-snatching endonuclease of influenza virus polymerase resides in the PA subunit. *Nature*, 458(7240), pp.914–918.

Dong, X. et al., 2009. Structural basis for leucine-rich nuclear export signal recognition by CRM1. *Nature*, 458(7242), pp.1136–1141.

Edinger, T.O., Pohl, M.O. & Stertz, S., 2014. Entry of influenza A virus: host factors and antiviral targets. *The Journal of general virology*, 95(Pt 2), pp.263–277.

Eisfeld, A.J., Neumann, G. & Kawaoka, Y., 2011. Human immunodeficiency virus rev-binding protein is essential for influenza a virus replication and promotes genome trafficking in late-stage infection. *Journal of virology*, 85(18), pp.9588–9598.

Elton, D. et al., 2001. Interaction of the influenza virus nucleoprotein with the cellular CRM1-mediated nuclear export pathway. *Journal of virology*, 75(1), pp.408–419.

Enami, M., Fukuda, R. & Ishihama, A., 1985. Transcription and replication of eight RNA segments of influenza virus. *Virology*, 142(1), pp.68–77.

Engel, K., Kotlyarov, A. & Gaestel, M., 1998. Leptomycin B-sensitive nuclear export of MAPKAP kinase 2 is regulated by phosphorylation. *The EMBO journal*, 17(12), pp.3363–3371.

Engelhardt, O.G. & Fodor, E., 2006. Functional association between viral and cellular transcription during influenza virus infection. *Reviews in medical virology*, 16(5), pp.329–345.

Farrow, N.A. et al., 1995. Comparison of the Backbone Dynamics of a Folded and an Unfolded SH3 Domain Existing in Equilibrium in Aqueous Buffer. *Biochemistry*, 34(3), pp.868–878.

Fields, S. & Winter, G., 1982. Nucleotide sequences of influenza virus segments 1 and 3 reveal mosaic structure of a small viral RNA segment. *Cell*, 28(2), pp.303–313.

Fields, S., Winter, G. & Brownlee, G.G., 1981. Structure of the neuraminidase gene in human influenza virus A/PR/8/34. *Nature*, 290(5803), pp.213–217.

Fischer, U. et al., 1995. The HIV-1 Rev activation domain is a nuclear export signal that accesses an export pathway used by specific cellular RNAs. *Cell*, 82(3), pp.475–483.

Flick, R. et al., 1996. Promoter elements in the influenza vRNA terminal structure. *RNA* , 2(10), pp.1046–1057.

Flick, R. & Hobom, G., 1999. Interaction of influenza virus polymerase with viral RNA in the "corkscrew"conformation. *The Journal of general virology*, 80(10), pp.2565–2572.

Fodor, E., 2013. The RNA polymerase of influenza A virus: mechanisms of viral transcription and replication. *Acta virologica*, 57(02), pp.113–122.

Fodor, E. et al., 1999. Rescue of influenza A virus from recombinant DNA. *Journal of virology*, 73(11), pp.9679–9682

Fodor, E., Pritlove, D.C. & Brownlee, G.G., 1995. Characterization of the RNA-fork model of virion RNA in the initiation of transcription in influenza A virus. *Journal of virology*, 69(7), pp.4012–4019.

Fodor, E., Pritlove, D.C. & Brownlee, G.G., 1994. The influenza virus panhandle is involved in the initiation of transcription. *Journal of virology*, 68(6), pp.4092–4096.

Fodor, E., Seong, B.L. & Brownlee, G.G., 1993. Photochemical cross-linking of influenza A polymerase to its virion RNA promoter defines a polymerase binding site at residues 9 to 12 of the promoter. *The Journal of general virology*, 74 (Pt 7)(7), pp.1327–1333.

Foeglein, Á. et al., 2011. Influence of PB2 host-range determinants on the intranuclear mobility of the influenza A virus polymerase. *The Journal of general virology*, 92(7), pp.1650–1661.

Fouchier, R.A.M. et al., 2004. Avian influenza A virus (H7N7) associated with human conjunctivitis and a fatal case of acute respiratory distress syndrome. *Proceedings of the National Academy of Sciences of the United States of America*, 101(5), pp.1356–1361.

Fournier, E., Moules, V., Essere, B., Paillart, J.-C., Sirbat, J.-D., Isel, C., et al., 2012. A supramolecular assembly formed by influenza A virus genomic RNA segments. *Nucleic acids research*, 40(5), pp.2197–2209.

Fournier, E., Moules, V., Essere, B., Paillart, J.-C., Sirbat, J.-D., Cavalier, A., et al., 2012. Interaction network linking the human H3N2 influenza A virus genomic RNA segments. *Vaccine*, 30(51), pp.7359–7367.

Gabriel, G. et al., 2011. Differential use of importin-alpha isoforms governs cell tropism and host adaptation of influenza virus. Nat. Commun. 2: 156. *Nat. Commun.*, 2(1), p.156.

Gabriel, G. et al., 2005. The viral polymerase mediates adaptation of an avian influenza virus to a mammalian host. *Proceedings of the National Academy of Sciences of the United States of America*, 102(51), pp.18590–18595.

Gabriel, G., Herwig, A. & Klenk, H.-D., 2008. Interaction of polymerase subunit PB2 and NP with importin alpha1 is a determinant of host range of influenza A virus. *PLoS pathogens*, 4(2), p.e11.

Gao, P. et al., 1999. Biological Heterogeneity, Including Systemic Replication in Mice, of H5N1 Influenza A Virus Isolates from Humans in Hong Kong. *Journal of virology*, 73(4), pp.3184–3189.

Gao, Q. et al., 2012. The influenza A virus PB2, PA, NP, and M segments play a pivotal role during genome packaging. *Journal of virology*, 86(13), pp.7043–7051.

Garaigorta, U. & Ortín, J., 2007. Mutation analysis of a recombinant NS replicon shows that influenza virus NS1 protein blocks the splicing and nucleo-cytoplasmic transport of its own viral mRNA. *Nucleic acids research*, 35(14), pp.4573–4582.

Gastaminza, P. et al., 2003. Mutations in the N-terminal region of influenza virus PB2 protein affect virus RNA replication but not transcription. *Journal of virology*, 77(9), pp.5098–5108.

Gavazzi, C. et al., 2013. An in vitro network of intermolecular interactions between viral RNA segments of an avian H5N2 influenza A virus: comparison with a human H3N2 virus. *Nucleic acids research*, 41(2), pp.1241–1254.

González, S. & Ortín, J., 1999a. Characterization of influenza virus PB1 protein binding to viral RNA: two separate regions of the protein contribute to the interaction domain. *Journal of virology*, 73(1), pp.631–637.

González, S. & Ortín, J., 1999b. Distinct regions of influenza virus PB1 polymerase subunit recognize vRNA and cRNA templates. *The EMBO journal*, 18(13), pp.3767–3775.

Gorai, T. et al., 2012. F1Fo-ATPase, F-type proton-translocating ATPase, at the plasma membrane is critical for efficient influenza virus budding. *Proceedings of the National Academy of Sciences of the United States of America*, 109(12), pp.4615–4620.

Görler, A. & Kalbitzer, H.R., 1997. Relax, a flexible program for the back calculation of NOESY spectra based on complete-relaxation-matrix formalism. *Journal of magnetic resonance* , 124(1), pp.177–188.

Guilligay, D. et al., 2008. The structural basis for cap binding by influenza virus polymerase subunit PB2. *Nature structural & molecular biology*, 15(5), pp.500–506.

Güttler, T. et al., 2010. NES consensus redefined by structures of PKI-type and Rev-type nuclear export signals bound to CRM1. *Nature structural & molecular biology*, 17(11), pp.1367–1376.

Hamilton, B.S., Whittaker, G.R. & Daniel, S., 2012. Influenza virus-mediated membrane fusion: determinants of hemagglutinin fusogenic activity and experimental approaches for assessing virus fusion. *Viruses*, 4(7), pp.1144–1168.

Hao, L. et al., 2008. Drosophila RNAi screen identifies host genes important for influenza virus replication. *Nature*, 454(7206), pp.890–893.

Hatada, E. et al., 1989. Control of influenza virus gene expression: quantitative analysis of each viral RNA species in infected cells. *Journal of biochemistry*, 105(4), pp.537–546.

Hatta, M. et al., 2007. Growth of H5N1 influenza A viruses in the upper respiratory tracts of mice. *PLoS pathogens*, 3(10), pp.1374–1379.

Hatta, M. et al., 2001. Molecular Basis for High Virulence of Hong Kong H5N1 Influenza A Viruses. *Science*, 293(5536), pp.1840–1842.

Heggeness, M.H. et al., 1982. Studies on the helical nucleocapsid of influenza virus. *Virology*, 118(2), pp.466–470.

Herfst, S. et al., 2012. Airborne Transmission of Influenza A/H5N1 Virus Between Ferrets. *Science*, 336(6088), pp.1534–1541.

Herfst, S. et al., 2010. Introduction of virulence markers in PB2 of pandemic swine-origin influenza virus does not result in enhanced virulence or transmission. *Journal of virology*, 84(8), pp.3752–3758.

He, X. et al., 2008. Crystal structure of the polymerase PA(C)-PB1(N) complex from an avian influenza H5N1 virus. *Nature*, 454(7208), pp.1123–1126.

Hoffmann, E. et al., 2000. A DNA transfection system for generation of influenza A virus from eight plasmids. *Proceedings of the National Academy of Sciences of the United States of America*, 97(11), pp.6108–6113.

Honda, A., Mizumoto, K. & Ishihama, A., 1998. Identification of the 5' terminal structure of influenza virus genome RNA by a newly developed enzymatic method. *Virus research*, 55(2), pp.199–206.

Hsu, M.T. et al., 1987. Genomic RNAs of influenza viruses are held in a circular conformation in virions and in infected cells by a terminal panhandle. *Proceedings of the National Academy of Sciences of the United States of America*, 84(22), pp.8140–8144.

Huang, I.-C. et al., 2008. Influenza A virus neuraminidase limits viral superinfection. *Journal of virology*, 82(10), pp.4834–4843.

Huang, S. et al., 2013. A Second CRM1-Dependent Nuclear Export Signal in the Influenza A Virus NS2 Protein Contributes to the Nuclear Export of Viral Ribonucleoproteins. *Journal of virology*, 87(2), pp.767–778.

Huang, T.S., Palese, P. & Krystal, M., 1990. Determination of influenza virus proteins required for genome replication. *Journal of virology*, 64(11), pp.5669–5673.

Hudjetz, B. & Gabriel, G., 2012. Human-like PB2 627K influenza virus polymerase activity is regulated by importin-alpha1 and-alpha7. *PLoS pathogens*, 8(1), p.e1002488.

Hutchinson, E.C. et al., 2010. Genome packaging in influenza A virus. *The Journal of general virology*, 91(Pt 2), pp.313–328.

Hutchinson, E.C. et al., 2012. Mapping the Phosphoproteome of Influenza A and B Viruses by Mass Spectrometry. *PLoS pathogens*, In Press(11), p.e1002993.

Hutchinson, E.C. & Fodor, E., 2012. Nuclear import of the influenza A virus transcriptional machinery. *Vaccine*, 30(51), pp.7353–7358.

Hyberts, S.G. et al., 2012. Application of iterative soft thresholding for fast reconstruction of NMR data non-uniformly sampled with multidimensional Poisson Gap scheduling. *Journal of biomolecular NMR*, 52(4), pp.315–327.

Hyberts, S.G., Takeuchi, K. & Wagner, G., 2010. Poisson-gap sampling and forward maximum entropy reconstruction for enhancing the resolution and sensitivity of protein NMR data. *Journal of the American Chemical Society*, 132(7), pp.2145–2147.

Inglis, S.C. et al., 1979. The smallest genome RNA segment of influenza virus contains two genes that may overlap. *Proceedings of the National Academy of Sciences of the United States of America*, 76(8), pp.3790–3794.

Ito, T. et al., 1998. Molecular basis for the generation in pigs of influenza A viruses with pandemic potential. *Journal of virology*, 72(9), pp.7367–7373.

Iwatsuki-Horimoto, K. et al., 2004. Generation of influenza A virus NS2 (NEP) mutants with an altered nuclear export signal sequence. *Journal of virology*, 78(18), pp.10149–10155.

Jagger, B.W. et al., 2012. An Overlapping Protein-Coding Region in Influenza A Virus Segment 3 Modulates the Host Response. *Science*, 337(6091), pp.199–204.

Jagger, B.W. et al., 2010. The PB2-E627K mutation attenuates viruses containing the 2009 H1N1 influenza pandemic polymerase. *mBio*, 1(1). Available at: http://dx.doi.org/10.1128/mBio.00067-10.

Johnson, L.N., 2009. The regulation of protein phosphorylation. *Biochemical Society transactions*, 37(Pt 4), pp.627–641.

De Jong, M.D. et al., 2006. Fatal outcome of human influenza A (H5N1) is associated with high viral load and hypercytokinemia. *Nature medicine*, 12(10), pp.1203–1207.

Jorba, N., Coloma, R. & Ortín, J., 2009. Genetic trans-Complementation Establishes a New Model for Influenza Virus RNA Transcription and Replication. *PLoS pathogens*, 5(5), p.e1000462.

Jung, T.E. & Brownlee, G.G., 2006. A new promoter-binding site in the PB1 subunit of the influenza A virus polymerase. *The Journal of general virology*, 87(Pt 3), pp.679–688.

Kageyama, T. et al., 2013. Genetic analysis of novel avian A(H7N9) influenza viruses isolated from patients in China, February to April 2013. *Euro surveillance: bulletin Europeen sur les maladies transmissibles = European communicable disease bulletin*, 18(15), p.20453.

Kawaoka, Y., Krauss, S. & Webster, R.G., 1989. Avian-to-human transmission of the PB1 gene of influenza A viruses in the 1957 and 1968 pandemics. *Journal of virology*, 63(11), pp.4603–4608.

Kim, H.J. et al., 1997. Mutational analysis of the RNA-fork model of the influenza A virus vRNA promoter in vivo. *The Journal of general virology*, 78 (Pt 2), pp.353–357.

Kuzuhara, T. et al., 2009. Structural Basis of the Influenza A Virus RNA Polymerase PB2 RNA-binding Domain Containing the Pathogenicity-determinant Lysine 627 Residue. *The Journal of biological chemistry*, 284(11), pp.6855–6860.

Labadie, K. et al., 2007. Host-range determinants on the PB2 protein of influenza A viruses control the interaction between the viral polymerase and nucleoprotein in human cells. *Virology*, 362(2), pp.271–282.

Laemmli, U.K., 1970. Cleavage of structural proteins during the assembly of the head of bacteriophage T4. *Nature*, 227(5259), pp.680–685.

Lakdawala, S.S. et al., 2014. Influenza a virus assembly intermediates fuse in the cytoplasm. *PLoS pathogens*, 10(3), p.e1003971.

Lamb, R.A. & Choppin, P.W., 1981. Identification of a second protein (M2) encoded by RNA segment 7 of influenza virus. *Virology*, 112(2), pp.729–737.

Lamb, R.A. & Horvath, C.M., 1991. Diversity of coding strategies in influenza viruses. *Trends in genetics: TIG*, 7(8), pp.261–266.

Lamb, R.A. & Krug, R.M., 2001. Orthomyxoviridae: the viruses and their replication. Fields virology: p. 1487--1531. *Fields virology, 4th ed. Philadelphia: Lippincott Williams & Wilkins*.

Lamb, R.A. & Lai, C.J., 1980. Sequence of interrupted and uninterrupted mRNAs and cloned DNA coding for the two overlapping nonstructural proteins of influenza virus. *Cell*, 21(2), pp.475–485.

Lamb, R.A., Lai, C.J. & Choppin, P.W., 1981. Sequences of mRNAs derived from genome RNA segment 7 of influenza virus: colinear and interrupted mRNAs code for overlapping proteins. *Proceedings of the National Academy of Sciences of the United States of America*, 78(7), pp.4170–4174.

Leahy, M.B. et al., 2001. Mutagenic Analysis of the 5′ Arm of the Influenza A Virus Virion RNA Promoter Defines the Sequence Requirements for Endonuclease Activity. *Journal of virology*, 75(1), pp.134–142.

Leahy, M.B., Dobbyn, H.C. & Brownlee, G.G., 2001. Hairpin loop structure in the 3' arm of the influenza A virus virion RNA promoter is required for endonuclease activity. *Journal of virology*, 75(15), pp.7042–7049.

Lee, K.-H. & Seong, B.L., 1998. The position 4 nucleotide at the 3'end of the influenza virus neuraminidase vRNA is involved in temporal regulation of transcription and replication of neuraminidase RNAs and affects the repertoire of influenza virus surface antigens. *The Journal of general virology*, 79(8), pp.1923–1934.

Lee, M.-T.M. et al., 2003. Activation of influenza virus RNA polymerase by the 5' and 3' terminal duplex of genomic RNA. *Nucleic acids research*, 31(6), pp.1624–1632.

Lee, M.T.M. et al., 2002. Definition of the minimal viral components required for the initiation of unprimed RNA synthesis by influenza virus RNA polymerase. *Nucleic acids research*, 30(2), pp.429–438.

Leser, G.P. & Lamb, R.A., 2005. Influenza virus assembly and budding in raft-derived microdomains: a quantitative analysis of the surface distribution of HA, NA and M2 proteins. *Virology*, 342(2), pp.215–227.

Li, C. et al., 2005. Evolution of H9N2 influenza viruses from domestic poultry in Mainland China. *Virology*, 340(1), pp.70–83.

Li, M.L., Ramirez, B.C. & Krug, R.M., 1998. RNA-dependent activation of primer RNA production by influenza virus polymerase: different regions of the same protein subunit constitute the two required RNA-binding sites. *The EMBO journal*, 17(19), pp.5844–5852.

Lim, K. et al., 2014. Biophysical characterization of sites of host adaptive mutation in the influenza A virus RNA polymerase PB2 RNA-binding domain. *The international journal of biochemistry & cell biology*, 53, pp.237–245.

Luke, G.A. et al., 2008. Occurrence, function and evolutionary origins of "2A-like" sequences in virus genomes. *The Journal of general virology*, 89(Pt 4), pp.1036–1042.

Ma, K., Roy, A.M. & Whittaker, G.R., 2001. Nuclear export of influenza virus ribonucleoproteins: identification of an export intermediate at the nuclear periphery. *Virology*, 282(2), pp.215–220.

Mänz, B. et al., 2012. Adaptive mutations in NEP compensate for defective H5N1 RNA replication in cultured human cells. *Nature communications*, 3, p.802.

Marjuki, H. et al., 2006. Membrane accumulation of influenza A virus hemagglutinin triggers nuclear export of the viral genome via protein kinase Calpha-mediated activation of ERK signaling. *The Journal of biological chemistry*, 281(24), pp.16707–16715.

Marley, J., Lu, M. & Bracken, C., 2001. A method for efficient isotopic labeling of recombinant proteins. *Journal of biomolecular NMR*, 20(1), pp.71–75.

Martin, K. & Helenius, A., 1991. Nuclear transport of influenza virus ribonucleoproteins: the viral matrix protein (M1) promotes export and inhibits import. *Cell*, 67(1), pp.117–130.

Massin, P., van der Werf, S. & Naffakh, N., 2001. Residue 627 of PB2 Is a Determinant of Cold Sensitivity in RNA Replication of Avian Influenza Viruses. *Journal of virology*, 75(11), pp.5398–5404.

McCown, M.F. & Pekosz, A., 2006. Distinct domains of the influenza a virus M2 protein cytoplasmic tail mediate binding to the M1 protein and facilitate infectious virus production. *Journal of virology*, 80(16), pp.8178–8189.

Mehle, A. et al., 2012. Reassortment and Mutation of the Avian Influenza Virus Polymerase PA Subunit Overcome Species Barriers. *Journal of virology*, 86(3), pp.1750–1757.

Mehle, A. & Doudna, J.A., 2009. Adaptive strategies of the influenza virus polymerase for replication in humans. *Proceedings of the National Academy of Sciences of the United States of America*, 106(50), pp.21312–21316.

Mehle, A. & Doudna, J.A., 2008. An Inhibitory Activity in Human Cells Restricts the Function of an Avian-like Influenza Virus Polymerase. *Cell host & microbe*, 4(2), pp.111–122.

Mercer, J., Schelhaas, M. & Helenius, A., 2010. Virus entry by endocytosis. *Annual review of biochemistry*, 79, pp.803–833.

Meyer, B.E. & Malim, M.H., 1994. The HIV-1 Rev trans-activator shuttles between the nucleus and the cytoplasm. *Genes & development*, 8(13), pp.1538–1547.

Miotto, O. et al., 2010. Complete-Proteome Mapping of Human Influenza A Adaptive Mutations: Implications for Human Transmissibility of Zoonotic Strains. *PloS one*, 5(2), p.e9025.

Moeller, A. et al., 2012. Organization of the influenza virus replication machinery. *Science*, 338(6114), pp.1631–1634.

Momose, F. et al., 2011. Apical transport of influenza A virus ribonucleoprotein requires Rab11-positive recycling endosome. *PloS one*, 6(6), p.e21123.

Momose, F. et al., 2001. Cellular splicing factor RAF-2p48/NPI-5/BAT1/UAP56 interacts with the influenza virus nucleoprotein and enhances viral RNA synthesis. *Journal of virology*, 75(4), pp.1899–1908.

Moncorgé, O., Mura, M. & Barclay, W.S., 2010. Evidence for Avian and Human Host Cell Factors That Affect the Activity of Influenza Virus Polymerase. *Journal of virology*, 84(19), pp.9978–9986.

Muramoto, Y. et al., 2013. Identification of novel influenza A virus proteins translated from PA mRNA. *Journal of virology*, 87(5), pp.2455–2462.

Naito, T. et al., 2007. An influenza virus replicon system in yeast identified Tat-SF1 as a stimulatory host factor for viral RNA synthesis. *Proceedings of the National Academy of Sciences of the United States of America*, 104(46), pp.18235–18240.

Neininger, A., Thielemann, H. & Gaestel, M., 2001. FRET-based detection of different conformations of MK2. *EMBO reports*, 2(8), pp.703–708.

Neumann, G., Hughes, M.T. & Kawaoka, Y., 2000. Influenza A virus NS2 protein mediates vRNP nuclear export through NES-independent interaction with hCRM1. *The EMBO journal*, 19(24), pp.6751–6758.

Neumann, G. & Kawaoka, Y., 2015. Transmission of influenza A viruses. *Virology*, 479-480, pp.234–246.

Neumann, G., Noda, T. & Kawaoka, Y., 2009. Emergence and pandemic potential of swine-origin H1N1 influenza virus. *Nature*, 459(7249), pp.931–939.

Ng, A.K.-L. et al., 2012. Influenza polymerase activity correlates with the strength of interaction between nucleoprotein and PB2 through the host-specific residue K/E627. *PloS one*, 7(5), p.e36415.

Ng, A.K.-L. et al., 2008. Structure of the influenza virus A H5N1 nucleoprotein: implications for RNA binding, oligomerization, and vaccine design. *FASEB journal: official publication of the Federation of American Societies for Experimental Biology*, 22(10), pp.3638–3647.

Noda, T. et al., 2012. Three-dimensional analysis of ribonucleoprotein complexes in influenza A virus. *Nature communications*, 3, p.639.

Noton, S.L. et al., 2007. Identification of the domains of the influenza A virus M1 matrix protein required for NP binding, oligomerization and incorporation into virions. *The Journal of general virology*, 88(Pt 8), pp.2280–2290.

Obayashi, E. et al., 2008. The structural basis for an essential subunit interaction in influenza virus RNA polymerase. *Nature*, 454(7208), pp.1127–1131.

Odagiri, T. et al., 1994. An amino acid change in the non-structural NS2 protein of an influenza A virus mutant is responsible for the generation of defective interfering (DI) particles by amplifying DI RNAs and suppressing complementary RNA synthesis. *The Journal of general virology*, 75 (Pt 1), pp.43–53.

Odagiri, T. & Tobita, K., 1990. Mutation in NS2, a nonstructural protein of influenza A virus, extragenically causes aberrant replication and expression of the PA gene and leads to generation of defective interfering particles. *Proceedings of the National Academy of Sciences of the United States of America*, 87(15), pp.5988–5992.

O'Neill, R.E., Talon, J. & Palese, P., 1998. The influenza virus NEP (NS2 protein) mediates the nuclear export of viral ribonucleoproteins. *The EMBO journal*, 17(1), pp.288–296.

Ortega, J. et al., 2000. Ultrastructural and functional analyses of recombinant influenza virus ribonucleoproteins suggest dimerization of nucleoprotein during virus amplification. *Journal of virology*, 74(1), pp.156–163.

Paragas, J. et al., 2001. Influenza B and C virus NEP (NS2) proteins possess nuclear export activities. *Journal of virology*, 75(16), pp.7375–7383.

Pal, S. et al., 2011. Influenza A virus interacts extensively with the cellular SUMOylation system during infection. *Virus research*, 158(1-2), pp.12–27.

Papantonis, A. & Cook, P.R., 2013. Transcription factories: genome organization and gene regulation. *Chemical reviews*, 113(11), pp.8683–8705.

Perales, B. et al., 1996. Mutational analysis identifies functional domains in the influenza A virus PB2 polymerase subunit. *Journal of virology*, 70(3), pp.1678–1686.

Perez, J.T. et al., 2010. Influenza A virus-generated small RNAs regulate the switch from transcription to replication. *Proceedings of the National Academy of Sciences of the United States of America*, 107(25), pp.11525–11530.

Pflug, A. et al., 2014. Structure of influenza A polymerase bound to the viral RNA promoter. *Nature*, 516(7531), pp.355–360.

Pinto, L.H., Holsinger, L.J. & Lamb, R.A., 1992. Influenza virus M2 protein has ion channel activity. *Cell*, 69(3), pp.517–528.

Pleschka, S. et al., 2001. Influenza virus propagation is impaired by inhibition of the Raf/MEK/ERK signalling cascade. *Nature cell biology*, 3(3), pp.301–305.

Plotch, S.J. et al., 1981. A unique cap (m 7 GpppXm)-dependent influenza virion endonuclease cleaves capped RNAs to generate the primers that initiate viral RNA transcription. *Cell*, 23(3), pp.847–858.

Pons, M. & Hirst, G.K., 1969. The single- and double-stranded RNA's and the proteins of incomplete influenza virus. *Virology*, 38(1), pp.68–72.

Poole, E. et al., 2004. Functional domains of the influenza A virus PB2 protein: identification of NP- and PB1-binding sites. *Virology*, 321(1), pp.120–133.

Poon, L.L. et al., 1999. Direct evidence that the poly(A) tail of influenza A virus mRNA is synthesized by reiterative copying of a U track in the virion RNA template. *Journal of virology*, 73(4), pp.3473–3476.

Poon, L.L.M., Fodor, E. & Brownlee, G.G., 2000. Polyuridylated mRNA Synthesized by a Recombinant Influenza Virus Is Defective in Nuclear Export. *Journal of virology*, 74(1), pp.418–427.

Pritlove, D.C. et al., 1998. Polyadenylation of influenza virus mRNA transcribed in vitro from model virion RNA templates: requirement for 5' conserved sequences. *Journal of virology*, 72(2), pp.1280–1286.

Rameix-Welti, M.-A. et al., 2009. Avian Influenza A Virus Polymerase Association with Nucleoprotein, but Not Polymerase Assembly, Is Impaired in Human Cells during the Course of Infection. *Journal of virology*, 83(3), pp.1320–1331.

Read, E.K.C. & Digard, P., 2010. Individual influenza A virus mRNAs show differential dependence on cellular NXF1/TAP for their nuclear export. *The Journal of general virology*, 91(Pt 5), pp.1290–1301.

Rehwinkel, J. et al., 2010. RIG-I detects viral genomic RNA during negative-strand RNA virus infection. *Cell*, 140(3), pp.397–408.

Reich, S. et al., 2014. Structural insight into cap-snatching and RNA synthesis by influenza polymerase. *Nature*, 516(7531), pp.361–366.

Reperant, L.A., Kuiken, T. & Osterhaus, A.D.M.E., 2012. Adaptive pathways of zoonotic influenza viruses: From exposure to establishment in humans. *Vaccine*, 30(30), pp.4434–4419.

Resa-Infante, P. et al., 2010. Structural and Functional Characterization of an Influenza Virus RNA Polymerase-Genomic RNA Complex. *Journal of virology*, 84(20), pp.10477–10487.

Resa-Infante, P. et al., 2008. The host-dependent interaction of alpha-importins with influenza PB2 polymerase subunit is required for virus RNA replication. *PloS one*, 3(12), p.e3904.

Reuther, P. et al., 2014. Adaptive mutations in the nuclear export protein of human-derived H5N1 strains facilitate a polymerase activity-enhancing conformation. *Journal of virology*, 88(1), pp.263–271.

Richardson, J.C. & Akkina, R.K., 1991. NS2 protein of influenza virus is found in purified virus and phosphorylated in infected cells. *Archives of virology*, 116(1-4), pp.69–80.

Robb, N.C. et al., 2009. NS2/NEP protein regulates transcription and replication of the influenza virus RNA genome. *The Journal of general virology*, 90(Pt 6), pp.1398–1407.

Robb, N.C. et al., 2010. Splicing of influenza A virus NS1 mRNA is independent of the viral NS1 protein. *The Journal of general virology*, 91(Pt 9), pp.2331–2340.

Robertson, J.S., 1979. 5′ and 3′ terminal nucleotide sequences of the RNA genome segments of influenza virus. *Nucleic acids research*, 6(12), pp.3745–3758.

Robertson, J.S., Schubert, M. & Lazzarini, R.A., 1981. Polyadenylation sites for influenza virus mRNA. *Journal of virology*, 38(1), pp.157–163.

Rodgers, B.C. & Mims, C.A., 1982. Influenza virus replication in human alveolar macrophages. *Journal of medical virology*, 9(3), pp.177–184.

Rodriguez Boulan, E. & Sabatini, D.D., 1978. Asymmetric budding of viruses in epithelial monlayers: a model system for study of epithelial polarity. *Proceedings of the National Academy of Sciences of the United States of America*, 75(10), pp.5071–5075.

Rossman, J.S. et al., 2010. Influenza virus M2 protein mediates ESCRT-independent membrane scission. *Cell*, 142(6), pp.902–913.

Rossman, J.S. & Lamb, R.A., 2011. Influenza virus assembly and budding. *Virology*, 411(2), pp.229–236.

Ruigrok, R.W.H. & Baudin, F., 1995. Structure of influenza virus ribonucleoprotein particles. II. Purified RNA-free influenza virus ribonucleoprotein forms structures that are indistinguishable from the intact influenza virus ribonucleoprotein particles. *The Journal of general virology*, 76(4), pp.1009–1014.

Sasaki, T. et al., 2006. Spatiotemporal regulation of c-Fos by ERK5 and the E3 ubiquitin ligase UBR1, and its biological role. *Molecular cell*, 24(1), pp.63–75.

Scheiffele, P. et al., 1999. Influenza viruses select ordered lipid domains during budding from the plasma membrane. *The Journal of biological chemistry*, 274(4), pp.2038–2044.

Scholtissek, C. et al., 1978. On the origin of the human influenza virus subtypes H2N2 and H3N2. *Virology*, 87(1), pp.13–20.

Sedano, C.D. & Sarnow, P., 2014. Hepatitis C virus subverts liver-specific miR-122 to protect the viral genome from exoribonuclease Xrn2. *Cell host & microbe*, 16(2), pp.257–264.

Selman, M. et al., 2012. Adaptive mutation in influenza A virus non-structural gene is linked to host switching and induces a novel protein by alternative splicing. *Emerging microbes & infections*, 1(11), p.e42.

Shapiro, G.I., Gurney, T., Jr & Krug, R.M., 1987. Influenza virus gene expression: control mechanisms at early and late times of infection and nuclear-cytoplasmic transport of virus-specific RNAs. *Journal of virology*, 61(3), pp.764–773.

Shimizu, T. et al., 2011. Crucial role of the influenza virus NS2 (NEP) C-terminal domain in M1 binding and nuclear export of vRNP. *FEBS letters*, 585(1), pp.41–46.

Simons, K. & Ikonen, E., 1997. Functional rafts in cell membranes. *Nature*, 387(6633), pp.569–572.

Skehel, J.J. & Hay, A.J., 1978. Nucleotide sequences at the 5' termini of influenza virus RNAs and their transcripts. *Nucleic acids research*, 5(4), pp.1207–1219.

Smith, G.L. & Hay, A.J., 1982. Replication of the influenza virus genome. *Virology*, 118(1), pp.96–108.

Steel, J. et al., 2009. Transmission of Influenza Virus in a Mammalian Host Is Increased by PB2 Amino Acids 627K or 627E/701N. *PLoS pathogens*, 5(1), p.e1000252.

Subbarao, E.K., London, W. & Murphy, B.R., 1993. A single amino acid in the PB2 gene of influenza A virus is a determinant of host range. *Journal of virology*, 67(4), pp.1761–1764.

Sugiyama, K. et al., 2009. Structural insight into the essential PB1-PB2 subunit contact of the influenza virus RNA polymerase. *The EMBO journal*, 28(12), pp.1803–1811.

Sun, D. et al., 2011. Identification of a phosphorylation site within the P protein important for mRNA transcription and growth of parainfluenza virus 5. *Journal of virology*, 85(16), pp.8376–8385.

Takeda, M. et al., 2003. Influenza virus hemagglutinin concentrates in lipid raft microdomains for efficient viral fusion. *Proceedings of the National Academy of Sciences of the United States of America*, 100(25), pp.14610–14617.

Tarendeau, F. et al., 2008. Host Determinant Residue Lysine 627 Lies on the Surface of a Discrete, Folded Domain of Influenza Virus Polymerase PB2 Subunit. *PLoS pathogens*, 4(8), p.e1000136.

Tarendeau, F. et al., 2007. Structure and nuclear import function of the C-terminal domain of influenza virus polymerase PB2 subunit. *Nature structural & molecular biology*, 14(3), pp.229–233.

Taubenberger, J.K. et al., 2005. Characterization of the 1918 influenza virus polymerase genes. *Nature*, 437(7060), pp.889–893.

Taubenberger, J.K. & Kash, J.C., 2010. Influenza Virus Evolution, Host Adaptation, and Pandemic Formation. *Cell host & microbe*, 7(6), pp.440–451.

Tiley, L.S. et al., 1994. Sequence-specific binding of the influenza virus RNA polymerase to sequences located at the 5'ends of the viral RNAs. *Journal of virology*, 68(8), pp.5108–5116.

Tomescu, A.I. et al., 2014. Single-molecule FRET reveals a corkscrew RNA structure for the polymerase-bound influenza virus promoter. *Proceedings of the National Academy of Sciences of the United States of America*, 111(32), pp.E3335–42.

Turrell, L. et al., 2013. The role and assembly mechanism of nucleoprotein in influenza A virus ribonucleoprotein complexes. *Nature communications*, 4, p.1591.

Umbach, J.L. et al., 2010. Influenza A virus expresses high levels of an unusual class of small viral leader RNAs in infected cells. *mBio*, 1(4). Available at: http://www.pubmedcentral.nih.gov/articlerender.fcgi?artid=2934610&tool=pmcentrez&rendertype=abstract.

Vranken, W.F. et al., 2005. The CCPN data model for NMR spectroscopy: development of a software pipeline. *Proteins*, 59(4), pp.687–696.

Vreede, F.T. & Brownlee, G.G., 2007. Influenza virion-derived viral ribonucleoproteins synthesize both mRNA and cRNA in vitro. *Journal of virology*, 81(5), pp.2196–2204.

Vreede, F.T., Gifford, H. & Brownlee, G.G., 2008. Role of Initiating Nucleoside Triphosphate Concentrations in the Regulation of Influenza Virus Replication and Transcription. *Journal of virology*, 82(14), pp.6902–6910.

Wang, W. et al., 2008. Imaging and characterizing influenza A virus mRNA transport in living cells. *Nucleic acids research*, 36(15), pp.4913–4928.

Ward, A.C. et al., 1995. Expression and analysis of the NS2 protein of influenza A virus. *Archives of virology*, 140(11), pp.2067–2073.

Watanabe, K. et al., 2001. Inhibition of nuclear export of ribonucleoprotein complexes of influenza virus by leptomycin B. *Virus research*, 77(1), pp.31–42.

Watanabe, T. et al., 2014. Influenza virus-host interactome screen as a platform for antiviral drug development. *Cell host & microbe*, 16(6), pp.795–805.

Whittaker, G., Bui, M. & Helenius, A., 1996. The role of nuclear import and export in influenza virus infection. *Trends in cell biology*, 6(2), pp.67–71.

Whittaker, G., Kemler, I. & Helenius, A., 1995. Hyperphosphorylation of mutant influenza virus matrix protein, M1, causes its retention in the nucleus. *Journal of virology*,

Williams, B.J.L. et al., 2005. The prototype gamma-2 herpesvirus nucleocytoplasmic shuttling protein, ORF 57, transports viral RNA through the cellular mRNA export pathway. *Biochemical Journal*, 387(Pt 2), pp.295–308.

Winter, G. et al., 1981. The use of synthetic oligodeoxynucleotide primers in cloning and sequencing segment 8 of influenza virus (A/PR/8/34). *Nucleic acids research*, 9(2), pp.237–246.

Winter, G. & Fields, S., 1980. Cloning of influenza cDNA ino M13: the sequence of the RNA segment encoding the A/PR/8/34 matrix protein. *Nucleic acids research*, 8(9), pp.1965–1974.

Winter, G. & Fields, S., 1982. Nucteotide sequence of human influenza A/PR/8/34 segment 2. *Nucleic acids research*, 10(6), pp.2135–2143.

Winter, G. & Fields, S., 1981. The structure of the gene encoding the nucleoprotein of human influenza virus A/PR/8/34. *Virology*, 114(2), pp.423–428.

Winter, G., Fields, S. & Brownlee, G.G., 1981. Nucleotide sequence of the haemagglutinin gene of a human influenza virus H1 subtype. *Nature*, 292(5818), pp.72–75.

Wise, H.M. et al., 2009. A complicated message: Identification of a novel PB1-related protein translated from influenza A virus segment 2 mRNA. *Journal of virology*, 83(16), pp.8021–8031.

Wise, H.M. et al., 2012. Identification of a novel splice variant form of the influenza A virus M2 ion channel with an antigenically distinct ectodomain. *PLoS pathogens*, 8(11), p.e1002998.

Wolstenholme, A.J. et al., 1980. Influenza virus-specific RNA and protein syntheses in cells infected with temperature-sensitive mutants defective in the genome segment encoding nonstructural proteins. *Journal of virology*, 35(1), pp.1–7.

Wurzer, W.J. et al., 2003. Caspase 3 activation is essential for efficient influenza virus propagation. *The EMBO journal*, 22(11), pp.2717–2728.

Xu, D. et al., 2012. Sequence and structural analyses of nuclear export signals in the NESdb database. *Molecular biology of the cell*, 23(18), pp.3677–3693.

Yamada, S. et al., 2010. Biological and Structural Characterization of a Host-Adapting Amino Acid in Influenza Virus. *PLoS pathogens*, 6(8), p.e1001034.

Yamanaka, K., Ishihama, A. & Nagata, K., 1990. Reconstitution of influenza virus RNA-nucleoprotein complexes structurally resembling native viral ribonucleoprotein cores. *The Journal of biological chemistry*, 265(19), pp.11151–11155.

Yángüez, E. & Nieto, A., 2011. So similar, yet so different: selective translation of capped and polyadenylated viral mRNAs in the influenza virus infected cell. *Virus research*, 156(1-2), pp.1–12.

Yasuda, J. et al., 1993. Molecular assembly of influenza virus: association of the NS2 protein with virion matrix. *Virology*, 196(1), pp.249–255.

Ye, Q., Krug, R.M. & Tao, Y.J., 2006. The mechanism by which influenza A virus nucleoprotein forms oligomers and binds RNA. *Nature*, 444(7122), pp.1078–1082.

Ye, Z. et al., 1999. Association of influenza virus matrix protein with ribonucleoproteins. *Journal of virology*, 73(9), pp.7467–7473.

York, A. et al., 2013. Isolation and characterization of the positive-sense replicative intermediate of a negative-strand RNA virus. *Proceedings of the National Academy of Sciences of the United States of America*, 110(45), pp.E4238–45.

York, A., Hutchinson, E.C. & Fodor, E., 2014. Interactome analysis of the influenza A virus transcription/replication machinery identifies protein phosphatase 6 as a cellular factor required for efficient virus replication. *Journal of virology*, 88(22), pp.13284–13299.

Yuan, P. et al., 2009. Crystal structure of an avian influenza polymerase PA(N) reveals an endonuclease active site. *Nature*, 458(7240), pp.909–913.

Yu, M. et al., 2012. Identification and characterization of three novel nuclear export signals in the influenza A virus nucleoprotein. *Journal of virology*, 86(9), pp.4970–4980.

Zhang, J., Pekosz, A. & Lamb, R.A., 2000. Influenza virus assembly and lipid raft microdomains: a role for the cytoplasmic tails of the spike glycoproteins. *Journal of virology*, 74(10), pp.4634–4644.

Zhang, S. et al., 2010. Internal initiation of influenza virus replication of viral RNA and complementary RNA in vitro. *The Journal of biological chemistry*, 285(52), pp.41194–41201.

Zhang, Y. et al., 2012. Key molecular factors in hemagglutinin and PB2 contribute to efficient transmission of the 2009 H1N1 pandemic influenza virus. *Journal of virology*, 86(18), pp.9666–9674.

Zhirnov, O.P., Ikizler, M.R. & Wright, P.F., 2002. Cleavage of influenza a virus hemagglutinin in human respiratory epithelium is cell associated and sensitive to exogenous antiproteases. *Journal of virology*, 76(17), pp.8682–8689.

Zhou, J. et al., 2013. Biological features of novel avian influenza A (H7N9) virus. *Nature*, 499(7459), pp.500–503.

Zhu, H. et al., 2010. Substitution of lysine at 627 position in PB2 protein does not change virulence of the 2009 pandemic H1N1 virus in mice. *Virology*, 401(1), pp.1–5.